In: Concrete Materials: Properties, Performance and Applications ISBN 978-1-60741-250-2
Editor: Jeffrey Thomas Sentowski, pp.

Chapter 1

PLASTERBOARD AND GYPSUM WASTE AS A NOVEL CEMENTITIOUS BINDER

E. Ganjian, H. Sadeghi-Pouya and P. Claisse
Department of Built Environment, Faculty of Engineering and Computing, Coventry University, Priory Street, Coventry CV1 5FB UK

ABSTRACT

Cements are substances which set and harden and can be used to bind other materials together. They are used throughout the construction industry, in a wide variety of applications, such as concrete. Gypsum is a key component in cementitious products and comes from a range of natural and synthetic sources as a by-product of industrial processes. Alternatively, recycled gypsum from waste plasterboard also has the potential to be used in cements. Interest in finding alternatives to landfill for plasterboard and other waste gypsum products has increased with the escalating costs of disposal and their reclassification as non-hazardous non-inert waste.

Coventry University in collaboration with Skanska and Lafarge Plasterboard recently undertook a WRAP (Waste and Resources Action Programme) funded research to develop a cost effective novel binder using recycled gypsum from waste plasterboard and a range of mineral wastes for construction of road foundations. This chapter gives details of this investigation on potential use of plasterboard gypsum in combination with a range of mineral wastes in road bases, sub-bases and stabilised sub-grades.

The use of plasterboard gypsum (PG) combined in mixtures with blast furnace slag, cement kiln dust (CKD), cement bypass dust (BPD) and power station run-of-station ash (ROSA) was investigated to form a novel blended binder with pozzolanic properties. This novel binder had potential use to stabilise soils and to produce semi-dry roller compacted paste and roller-compacted concrete (RCC) for road foundation construction.

The research consisted of five phases:

- characterisation of the materials used (particle size analysis, chemical composition);
- design and optimisation of the paste mix (mix proportions, water requirement, setting time, workability, compressive strength);
- design of the concrete mix (effect of different aggregates, workability, compressive strength);

- characterisation of mixes made with the novel blended powder (hydrogen sulphide release, long-term stability, potential for leaching, hydration mechanism, length change); and
- comparative trials at two construction sites:
    - a car park at Lowdham Grange prison in Nottingham, UK where the novel binder was used to prepare roller- compacted concrete (RCC) in a sub-base layer; and
    - part of an access road at the King's Mill Hospital site in Nottinghamshire where soil stabilised with the novel binder and a semi-dry paste (grout) containing the novel binder was used as the sub-base and base course respectively.

1. INTRODUCTION

The pressure to reutilise waste materials is increasing with the escalating cost of disposal to landfill. The majority of plasterboard waste has traditionally been landfilled, having been classified as a non-hazardous inert waste able to be co-disposed of with other wastes. But from July 2005, the EU Landfill Directive required plasterboard and other waste gypsum products to be reclassified as non-hazardous non-inert wastes [1, 2]. This has boosted demand for alternatives to disposal for these wastes. Detailed statistics on waste plasterboard arising are currently scarce, but it is estimated that some 300,000 tonnes of waste plasterboard are generated each year in the UK from new construction activity (largely as off-cuts). The amount of plasterboard waste arising from demolition projects is more difficult to quantify, but maybe in the range 500,000 tonnes to more than 1 million tonne annually in the UK (Mtpa) [2].

The application of cementitious materials with lower strength than Portland cement is not limited to backfills. They can be used in many application such structural fills, insulation and isolation fills, pavement bases, conduit bedding, erosion control, void filling, nuclear facilities and bridge reclamation [3].

1.1. Plasterboard Gypsum Waste Recycling

Plasterboard is made of a gypsum plaster core with a paper facing. It is a widely used construction material for applications such as forming partitions, lining walls and ceilings. Over 2.5 million tonnes of plasterboard are manufactured and used in the UK each year, and this is increasing.

From its use, plasterboard waste arises during installation through wasteful design, off-cuts, damaged boards, and over-ordering. Wastage of 10%-35% often occurs on sites, leading to around 300,000 tonnes of plasterboard waste being produced each year from this source. It also arises from its removal, such as from removing partitions, refurbishing wall and ceiling linings, repairing damaged linings, and from complete soft-strip before demolition of a building. It is estimated that in total more than one million tonnes of plasterboard waste is produced in the UK each year.

Although plasterboard waste from all these sources can be recycled, there are different barriers to fully recycle waste gypsum. These barriers are in general as follows [2]:

Educational barriers include:

- *Lack of knowledge amongst professionals.* Professionals within the industry may feel that they lack the knowledge on how to minimise waste arisings and increase materials recycling. For example, an architect may not have learnt techniques to design buildings in such a way as to optimise the use of whole sheets of plasterboard, so reducing waste off-cuts.
- *Site Training.* The construction industry includes thousands of skilled and unskilled workers, in many cases sub-contacted by the main contractor. Their time on the site could be relatively short and though an induction may be carried out on health and safety issues, it is rare for inductions to given on good site waste management, such as the importance of segregating waste into the correct skips.
- *Hassle factor.* With many sub contactors on sites it is difficult to ensure that everyone is carrying out their work as instructed. It is often not possible to ensure that the correct waste materials are placed in the correct skips, rather than 'the closer' skip, without overseeing them all day.

Market barriers include:

- Client specification. The construction industry is very competitive, with projects being priced and submitted in a closed tender process. Therefore, unless minimum levels of recycling are specified as a requirement by the client or other body, it is unlikely that a construction company will include it in their project.
- Contractual. There is generally no fiscal incentive within the standard contract for lesser amounts of material to be used than specified. In particular, dry lining is usually undertaken by specialist contractors who price jobs, and are paid, by the area installed. The time element of a contractor's costs are greater than the material costs for plasterboard, so standard practice is to work quickly by using whole sheets and cutting out window and door openings rather than fitting off-cuts to shape.
- Market uptake and public perception. Reducing the amount of construction waste on a new building has limited marketing value; however investing in a renewable technology or other more visible sustainable measures may bring attention to a project. Therefore a construction company may be more likely to invest in these areas rather than in recycling.
- Architects and Quantity Surveyors (QS) playing safe. The calculations done by Architects and QS provide the construction companies with a bill of quantities to price against. This will be based on measured amounts of products plus a factor to account for part pieces etc. Unless this is reduced then the contactor will provide a similar amount of the product to site, any un-used is normally wasted. Architects and QS will not reduce their safety factor as this could mean additional costs to the agreed price and delays in programme. This is exacerbated by the contractual arrangement with the dry lining contractor, as discussed above.

Financial barriers include:

- Economics. Many construction clients will have concerns about the environment and may specify some sustainable elements for their construction. Construction waste management costs are largely dependent on the size of the project. The recyclability depends on quantity, quality, and the inherent value of the waste material. The issues for builders centre on the relative cost and "bother" factor of recycling (collection, separation, and transportation), against landfill tipping fees, and transportation. For plasterboard, at present material costs are low and costs of disposal to landfill are low, so there is little economic incentive to segregate and recycle plasterboard waste.
- Economics. For high volume low cost materials such as plasterboard it is more economically viable to dispose of unused material at the end of the construction project, and re-order for the next project, than to store and carry unused materials over.
- Sub-contractors. A contactor brought onto site to carry out a specific job will want to complete their work in the minimum time, get paid and move on. Unless they are contractually obliged to recycle their waste they will not bother.
- Sector diversity. The construction sector includes many single-person operations as well as some very large operators. Commonly smaller operators work as sub-contractors for the larger organisations. While large organisations have sufficient economy of scale to incorporate and implement environmentally advantageous procedures in a cost effective manner, the burden upon small operators is generally disproportionately large. Therefore the larger organisations, and those letting contracts, hold the key to specifying recycling where it may result in added costs.

Legislative barriers include:

- *Lack of legislation.* Buildings are generally constructed to minimum requirements (such as to meet but not exceed the requirements of the Building Regulations), with few exceptions looking to higher aspiration levels. This provides an equal basis for the industry to price each job competitively. Therefore the current ethos within the much of the industry is to not react to anything unless clear mandatory legislation is in place.
- *Lack of legislation.* Although waste management legislation applies, there is currently no legislation to require main contractors to recycle the waste materials on their sites. However, The DTI are considering the introduction of mandatory Site Waste Management Plans (SWMPs) as part of the Clean Neighbourhoods and Environment Act 2005. SWMPs are an important tool for construction companies and their clients, of all sizes, to improve their environmental performance, meet regulatory controls and reduce rising costs of disposing of waste.
- *Lack of direct action.* There is no legislation currently in place to make each individual responsible for his or her actions on site, with respect to waste management. Individual control occurs at site level, and will depend on the attitude and degree of control by the site management.
- *Lack of clear policy.* Current guidance from the Environment Agency on the Landfill Regulations effectively allows a continuation of co-disposal of plasterboard with other wastes. There is therefore little incentive for construction companies to reduce

the production of plasterboard waste, or segregate plasterboard waste from other wastes.

In summary there are many barriers preventing the construction and demolition industry from adopting greater recycling of plasterboard and gypsum products. They are associated with cultural market and organisational barriers, economics and a lack of education. Whilst these barriers are real, change would be possible by introducing clear mandatory legislation or an agreed industry code of practice to require the construction and demolition industry to change its practises.

However, the vast majority of plasterboard gypsum waste is currently still disposed to landfill. It is increasingly necessary to find alternatives to this, due to factors such as:

- increases in landfill tax increasing the cost of disposal to landfill year on year;
- available space in landfill sites decreasing;
- the Landfill Regulations now requiring that quantities of gypsum-based materials being disposed of to landfill must be deposited in a specially engineered 'high-sulphate monocell in a non-hazardous landfill site, leading to increased disposal costs.

One alternative is to recycle any waste that is produced, and this investigation looks at its use in the production of cementitious products, that set and harden and can be used to bind other materials together.

1.2. Super-Sulphated Cement

Blast furnace slag is a by-product of steel manufacture and is formed when molten blast-furnace slag is rapidly cooled [4]. Blast furnace slag's major use is in the production of slag cement, primarily high slag blast furnace cement and Portland blast furnace cement.

Blast furnace slag cement in concrete is typically hydrated after mixing with Portland cement providing a source of alkalinity with which the slag reacts to form cement hydration products [5]. Cement made from granulated blast furnace slag activated by means of calcium sulphate and alkalis is known in the UK as "super-sulphated cement" [6]. The cement is made by grinding a mixture of 80-85 per cent granulated slag, 10-15 per cent anhydrite or hard-burned gypsum, and about 5 per cent Portland cement. To obtain the best mechanical properties, a high Calcium to Silica ratio greater than one of the slag is necessary. An Al_2O_3 content higher than 13 to 15 of percentage by weight is also recommended for optimised hydration behaviour. The main hydration products of super-sulphated cement are ettringite ($C_3A.3CaSO_4.32H_2O$) and C-S-H. Ettringite is precipitated from supersaturated pore solutions. This formation of ettringite is not associated with destructive swelling of the hydrating super-sulphated cement matrix. This behaviour was explained by the precipitation of ettringite crystals from a pore solution undersaturated in $Ca(OH)_2$, with low pH-values of approx. 11.5 – 11.8, particularly in larger pores. Owing to the high ratio of chemically bonded water in ettringite, the content of non-evaporable water of super-sulphated cement pastes is higher than that of OPC pastes assuming a similar degree of hydration for both cements. The

formation of ettringite benefits the development of early age strength of hydrating super-sulphated cement pastes [7].

Alternative sources of gypsum such as plasterboard waste and red gypsum can be used with slag and other sources of alkalis such as slaked lime or cement kiln dust to produce sulphate-alkali activated slag cement [8, 9].

Such waste ashes pose a major waste disposal problem. They can be used with slag, gypsum and alkalis to form a binder which can be used in blended cements or for various applications to:

- reduce greenhouse gas emissions;
- reduce the cost of concrete; and
- improve the strength, durability and other properties of construction materials [10].

In this project crushed plasterboard gypsum waste has been used successfully as an activator in slag-cement kiln dust mixture to develop a cost effective novel binder. Basic Oxygen Slag (BOS) was used in place of the more common Blast Furnace Slag because it is a waste.

2. LABORATORY RESEARCH

A series of laboratory trials were undertaken to determine the optimum proportions of recycled gypsum and mineral wastes required for a binder paste (i.e. a mixture of cementitious powder and water with no aggregate) to achieve the highest compressive strength.

2.1. Concrete and Paste Mix Development

2.1.1. Materials

The following materials have been used in the investigation:

- plasterboard gypsum (PG);
- two types of basic oxygen slag (BOS) and cement kiln dust (CKD);
- one source of run of station ash (ROSA);
- fine and coarse aggregates;
- superplasticiser.

Details of each material are given below.

2.1.1.1. Plasterboard Gypsum

The plasterboard gypsum used was obtained from Lafarge Plasterboard's recycling plant in Bristol. Because the waste plasterboard gypsum is collected from demolition sites, contaminants such as paper and glass can be found in the gypsum. At this stage, big pieces of paper and other contaminants were separated using a series of sieves before the gypsum was

crushed using a metal tamper. The crushed product was sieved through a 600 µm sieve and stored in a sealed bucket.

Another form of waste plasterboard gypsum from the Lafarge plasterboard recycling plant called 'processed PG' was also used. The processed PG contained lower levels of large particles of plasterboard but the size and amount of paper pieces were similar to the 'plasterboard gypsum' from the Lafarge plant. For the site trial, the plasterboard was dried, ground and passed through a 500 µm sieve[1] (see section 3).

Figure 1 shows the waste plasterboard before and after processing, together with other materials used in the project.

Particle size analysis of the gypsum was carried out using a Malvern Mastersize 2000 laser analyser with an accuracy of ±1%. As shown in Figure 2, the particles are between 1 µm and 1 mm in diameter, and mostly >300 µm.

The nature of this source of waste plasterboard means that some degree of impurities and contaminants is inevitable. Thermogravimetric analysis (TGA) of materials was carried out using a PerkinElmer Pyris 1 thermogravimetric analyser. The thermograph (Figure 3) confirms the presence of impurities in the PG. The loss of mass at ≥200° C implies the presence of a number of impurities and contaminants in the gypsum.

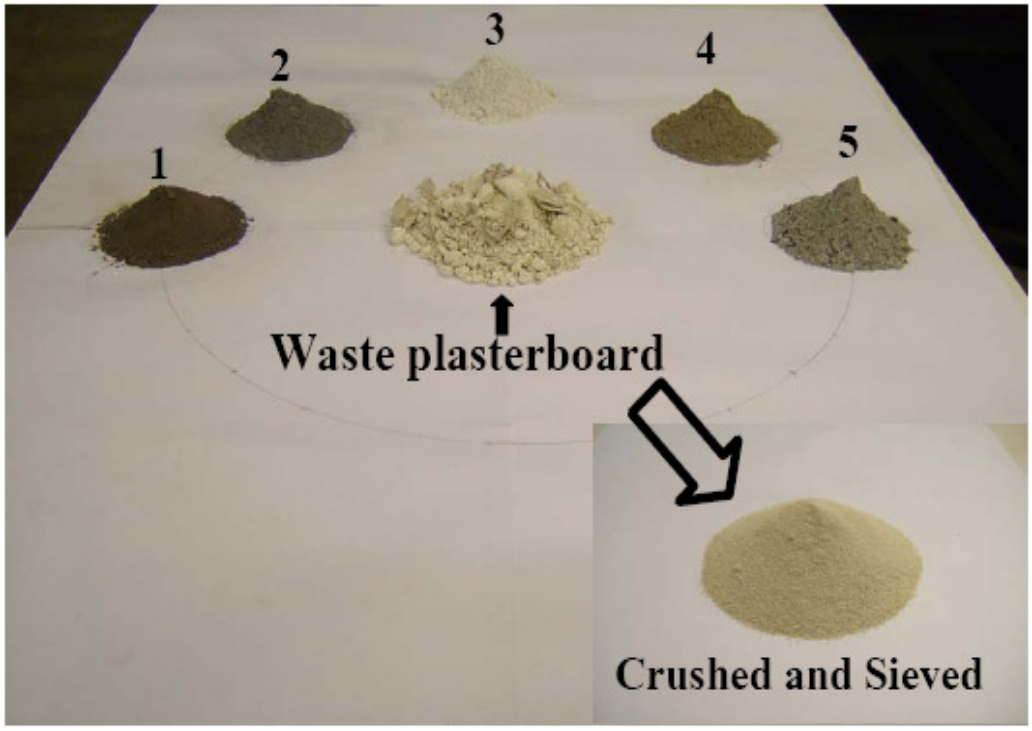

Figure 1. Waste plasterboard gypsum and various types of waste materials: (1) basin oxygen slag; (2) run of station ash; (3) lime; (4) cement kiln dust and (5) incinerated ash .

1 This was the only size of sieve available to the processing plant for preparation of the material for the site trials.

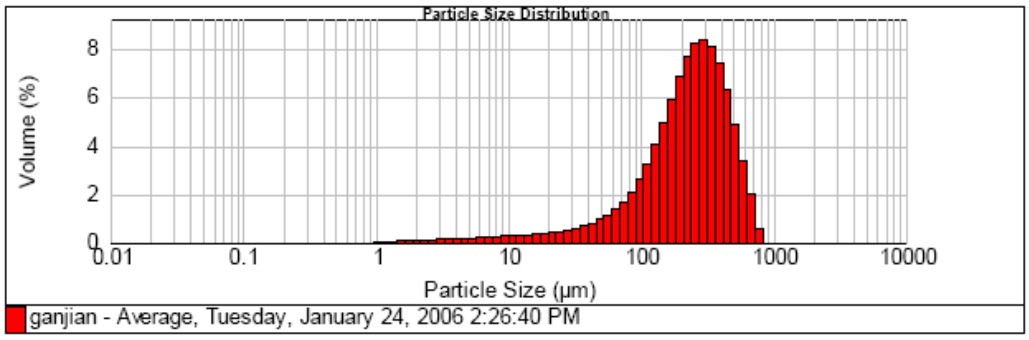

Figure 2. Particle size analysis of crushed and sieved PG.

The nature of this source of waste plasterboard means that some degree of impurities and contaminants is inevitable. Thermogravimetric analysis (TGA) of materials was carried out using a PerkinElmer Pyris 1 thermogravimetric analyser. The thermograph (Figure 3) confirms the presence of impurities in the PG. The loss of mass at ≥200° C implies the presence of a number of impurities and contaminants in the gypsum.

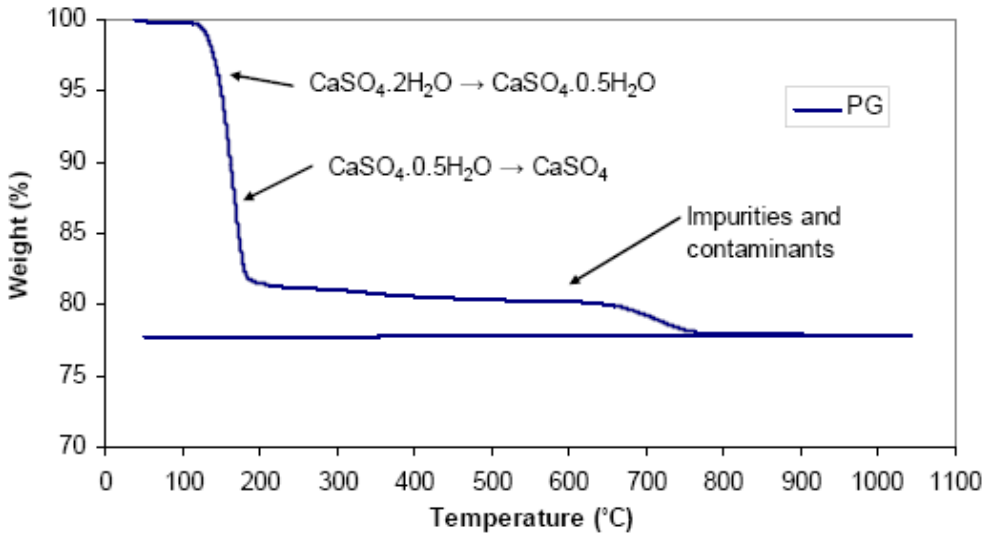

Figure 3. TGA results for plasterboard gypsum.

2.1.1.2. Basic Oxygen Slag

The blast furnace slag used was obtained from Tarmac UK (i.e. from the Corus plant at Scunthorpe). The slag was ground using a laboratory ball mill and passed through a 600 µm sieve before being added to the mixes. Figure 4 shows that the average particle size is 40–60 µm, indicating that the efficiency of the ball mill is acceptable.

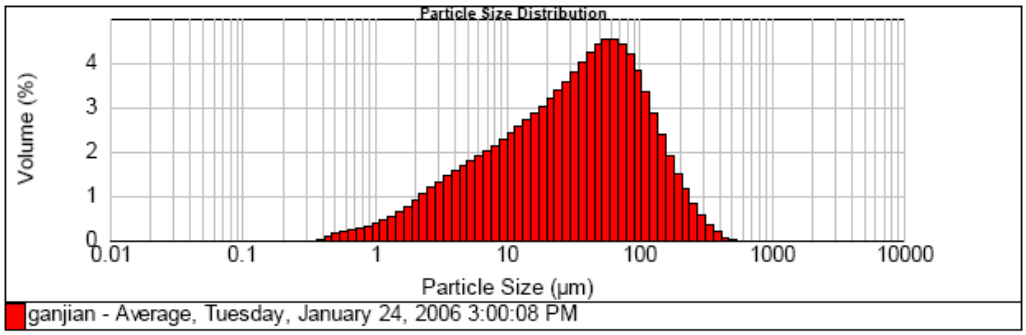

Figure 4. Particle size analysis of ground BOS.

Fresh slag left exposed to air for period of over one month is described as 'weathered' BOS (W-BOS). Further TGA studies confirmed a considerable difference between fresh slag (UW-BOS) and samples that had been affected by carbonation under atmospheric carbon dioxide (CO_2), i.e. weathered BOS (Figure 5.). The chemical composition of the unweathered and weathered BOS is given in Table 1 (section 2.1.3).

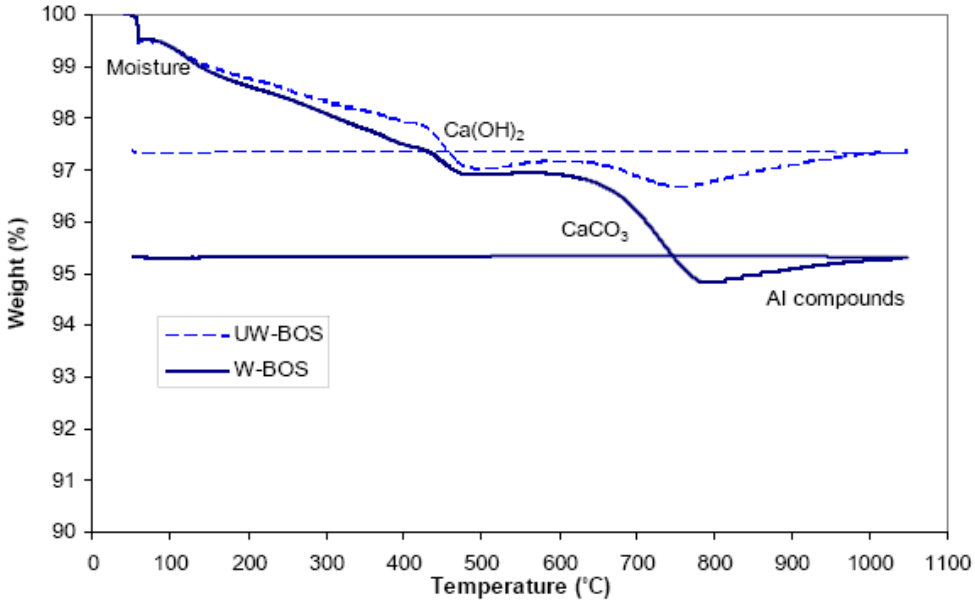

Figure 5. TGA results for unweathered and weathered BOS.

2.1.1.3. Cement Kiln Dust and Bypass Dust

Two different sources of cement kiln dust were used; one was obtained from Rugby Cement Barrington and the other from Castle Cement. As expected, the two dusts had a different composition (see Table 1 in section 2.1.3 for their relative oxide content).

The material supplied by Rugby Cement, called CKD, was obtained from electrostatic precipitators in the chimney stack. If the kiln has a bypass fitted, this material is usually recycled back into the kiln feed.

The material supplied by Castle Cement, called bypass dust (BPD), is obtained from the kiln bypass. The bypass is used to bleed off volatile materials that would otherwise recirculate around the kiln and pre-heater system (condensing in cooler parts of the kiln causing blockages) or eventually end up in the cement clinker.

The main difference between CKD and BPD is related to the temperature at which these materials are produced. CKD is taken out of the kiln during its initial length where the temperature is about 300° C, while BPD is from part of the kiln where the temperature is about 1000° C. As a result, BPD contains more cementitious phases compared with CKD, which contains a higher amount of calcium carbonate (limestone).

The CKD and BPD were supplied in powder form. The results of particle size analysis are shown in Figures 6 and 7 respectively. The CKD contains some type of coarser particles, which may be due to clustering and the moisture present in the sample. However, the average size of fine particles is nearly the same (about 10 μm) for the CKD and BPD.

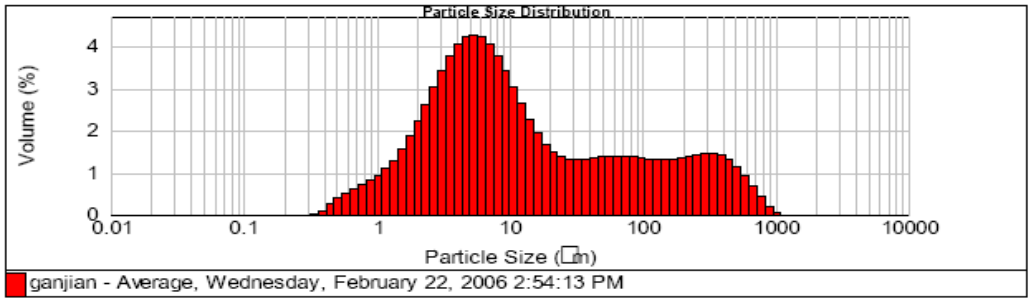

Figure 6. Particle size analysis of CKD.

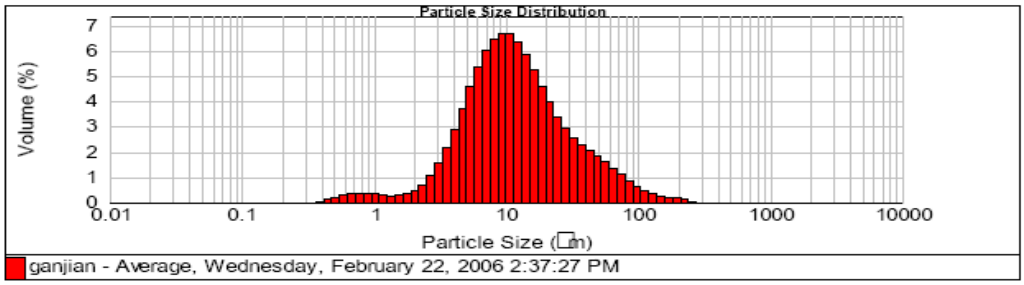

Figure 7. Particle size analysis of BPD.

The TGA results (Figure 8) confirmed there were significant differences between the CKD and BPD samples. TGA showed that the CKD contained about 25% $CaCO_3$, which might reduce the activity of the powder and pH of the pore solution in the mix. In addition, the chemical composition of these kinds of materials will differ with time and will not be consistent due to changes in the raw materials supplied to the kiln as well as variations in temperature and duration in the kiln.

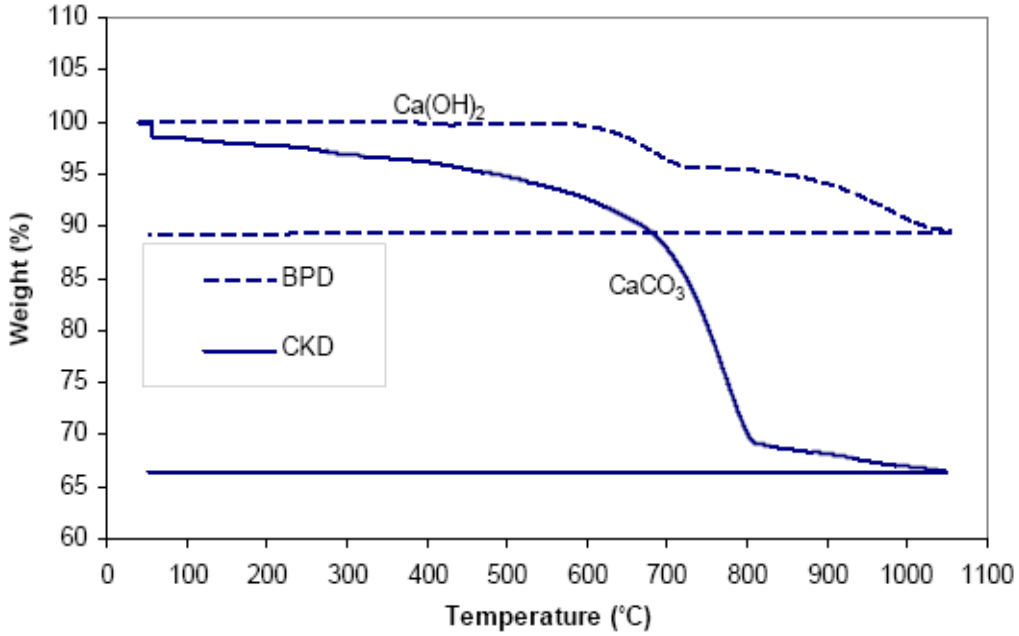

Figure 8. TGA results for BPD and CKD.

2.1.1.4. Run-of-Station Ash

Dry run-of-station ash (ROSA) supplied by Rugby Ash was also used in the concrete and paste mixes. ROSA is unclassified PFA (i.e. the rejects from PFA grading) and was supplied as a fine powder as shown by the particle size analysis (Figure 9). TGA indicated the presence of ~7% carbon content at around 600–800° C (Figure 10).

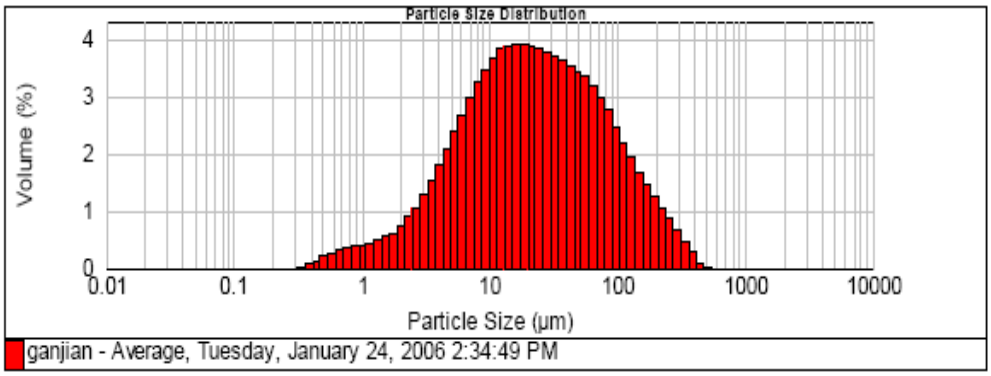

Figure 9. Particle size analysis of ROSA

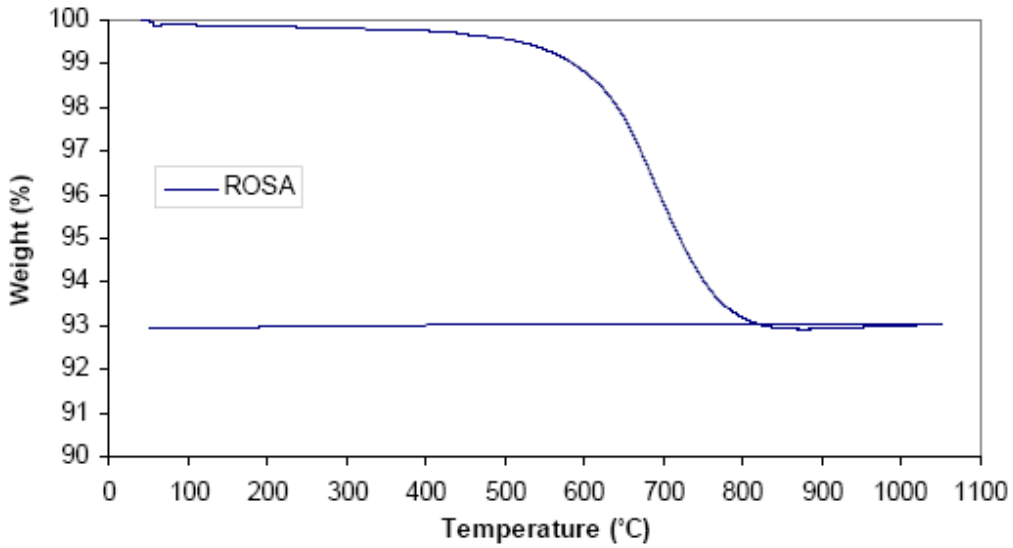

Figure 10. TGA results for ROSA.

2.1.1.5. Hydrated Lime and Maerz Kiln Dust

Lime used in construction works is made from limestone (calcium carbonate) burned in a lime kiln to form quicklime. The quicklime is added to water in a process known as slaking. The term 'hydrated' simply refers to any type of lime that has been slaked. After mixing with water, the mixture is hardened by a chemical process called carbonation as water evaporates and the lime reacts with carbon dioxide in the air. During each of these processes, the lime undergoes a chemical change but the final stage (carbonation) converts it back to calcium carbonate which is chemically and physically similar to the original limestone.

In this project, two sources of lime – commercial hydrated lime and Maerz kiln dust (MKD) lime – supplied by Buxton Lime Industries were used as a source of alkali in the paste mixtures.

The commercial hydrated lime was mainly calcium hydroxide complying with the requirements of BS EN 459-1: 2001 [11].

MKD is a by-product of lime manufacture and is collected from the chimney of lime kilns. It is a blend of calcium carbonate and calcium hydroxide. The MKD used in this project was supplied in a form of white powder. Its bulk density was 1000 kg/m^3 and the grading was 95% passing through 500 µm sieve. The typical chemical analysis of the MKD used is given in Table 1 (section 2.1.3).

2.1.1.6. Aggregates

Two sources of natural aggregates were used in the project:

- medium grade natural sand; and
- 10 mm uncrushed gravel complying with BS 882:1992 and BS EN 12620: 2002 [12].

The relative density of the sand and gravel was 2.6 g/cm^3.

A Type 1 recycled aggregate supplied by J.C. Balls and Sons (www.jcballs.co.uk /recycling.htm) was used to make concrete mixes. This recycled aggregate (Figure 11) contained crushed rocks, crushed concrete and masonry blocks, asphalt and fine materials such as silt and clay. The maximum size of recycled aggregates used was 75 mm and the average density was measured at about 2.5 g/cm^3.

Figure 12 shows the sieve analyses of the natural and recycled aggregates used in the project.

Figure 11. Recycled aggregate used.

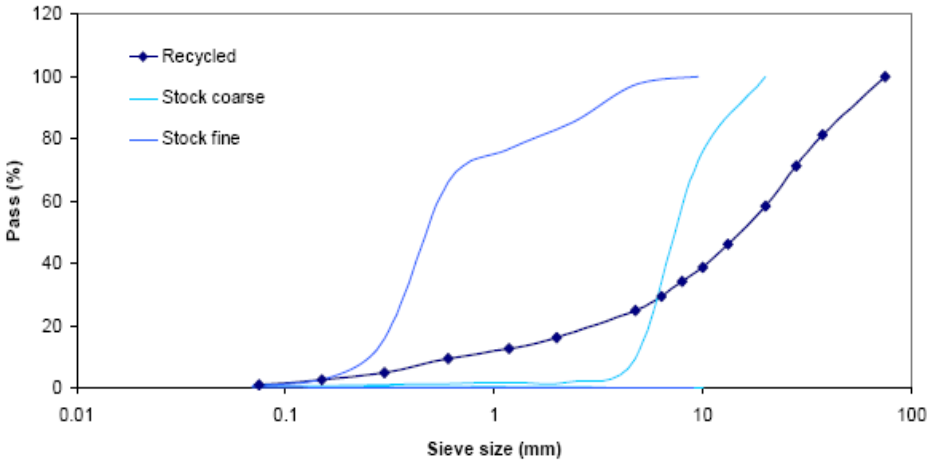

Figure 12. Sieve analysis of natural and recycled aggregates used in the project.

As shown in Figure 13, the calculated coarse and fine fractions of the recycled aggregate complied with the requirements of BS-EN 12620-2002.

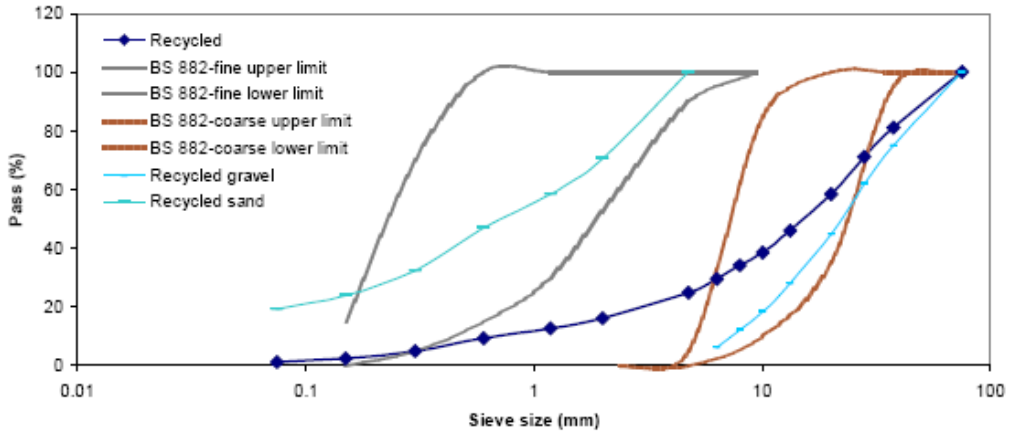

Figure 13. BS limits compared with coarse and fine fractions of recycled aggregates used.

2.1.1.7. Superplasticiser

Two types of high-range water-reducing agents, Sika ViscoCrete-10 and Sika ViscoCrete-premium, were used in the project to increase the workability of the paste and concrete mixtures. The former is sulphonate based and less effective compared with the latter, which is based on an acrylic polymer and has a high efficiency at low doses. It was used to complete the laboratory test series at the same liquid to binder (L/B) ratio.

2.1.1.8. Water

Potable tap water (i.e. drinking water quality) was used to make the paste and concrete mixes.

2.1.2. Particle size comparison of raw materials

Figure 14 shows the particle size distribution of the raw materials used in this project.

The crushed PG contains more particles in the range 200–400 μm compared with the other materials. The ground BOS has a maximum particle size of about 300 μm – an indication that the grinding process worked properly.

It is generally accepted that pozzolanic materials with a finer particle size results in faster hydration and reduced setting time of the binder. This is due to the higher surface area and electric charges induced on the surface of particles during the grinding process.

2.1.3. Chemical Analysis of Raw Materials

The chemical composition of the materials used was determined using X-ray fluorescence (XRF) techniques. The proportion of different oxides present is shown in Table 1. Although there are variations in the chemical composition of different batches of BPD supplied, it was concluded that the effect of these variations would not be detrimental when using a low proportion of BPD in the mixture.

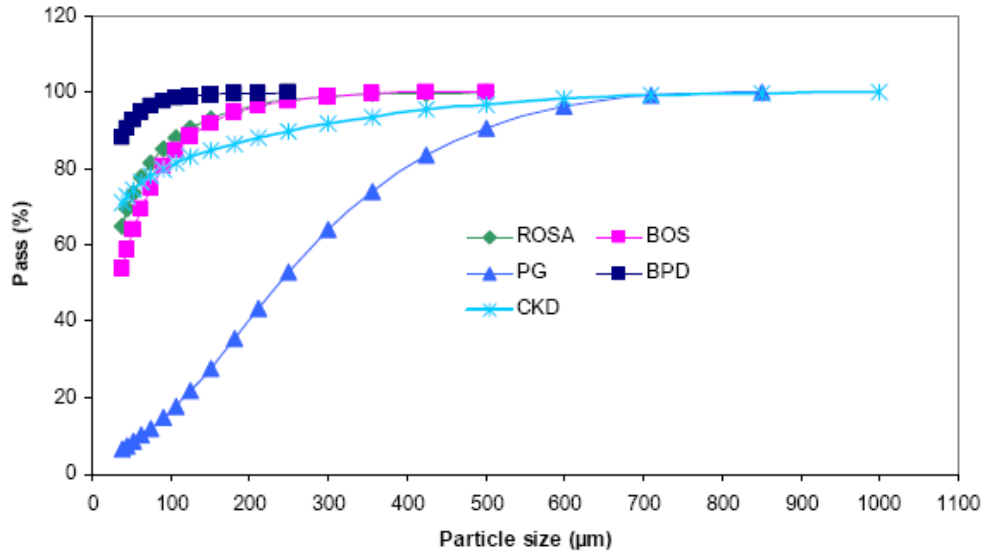

Figure 14. Particle size distribution of raw materials used in the project.

Table 1. Relative oxide content and loss on ignition (LOI) of the raw materials used in the project

Oxides	Percentage								
	PG	W-BOS	UW-BOS	ROSA	CKD	BPD I	BPD II	BPD (Coventry binder)*	MKD
SiO_2	2.43	11.45	11.43	45.91	9.89	12.86	21.86	13.9	2
TiO_2	0.03	0.37	0.39	1.41	0.14	0.12	0.29	0.12	–
Al_2O3	0.81	2.32	1.6	26.51	3.72	3.5	3.85	2.59	1
Fe_2O_3	0.36	27.32	28.24	5.23	1.24	2.12	2.57	1.51	0.4
MnO	0	3.65	4.35	0.08	0.02	0.02	0.02	0.01	–
MgO	0.4	9.32	8.27	2.13	0.94	2.46	1.13	0.69	0.3
CaO	37.3	37.44	41.29	6.88	40.42	58.28	53.4	51.61	10
Na_2O	0.03	0.03	0.02	0.61	0.43	0.29	0.41	0.74	–
K_2O	0.24	0.01	0.02	1.35	6.36	1.71	3.64	10.41	–
P_2O_5	0.02	1.26	1.48	0.98	0.08	0.06	0.08	0.05	–
SO_3	53.07	0.28	0.44	1.37	5.59	6.75	7.1	5.01	0.2
LOI	4.09	3.12	1.12	7.11	30.99	10.23	5.02	4.4	85

* See section 2.1.6.1.5.

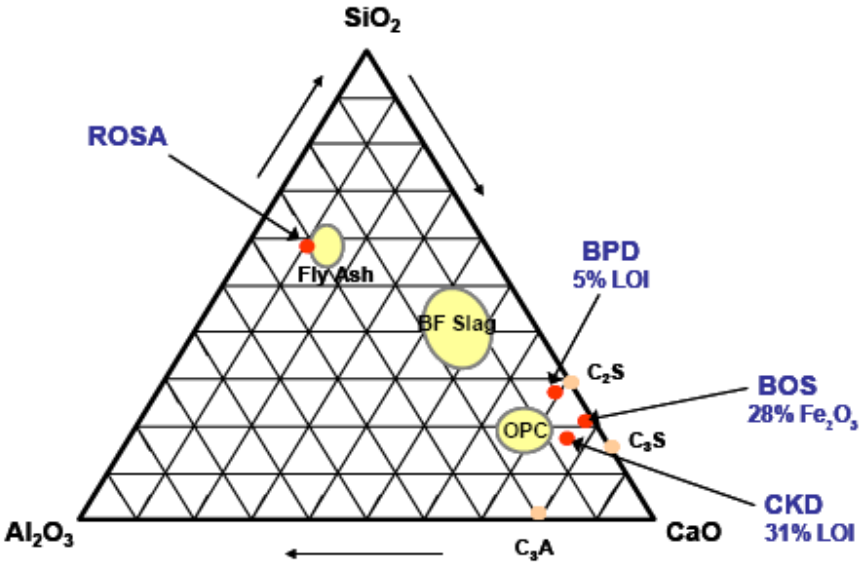

Figure 15. The comparative CaO-Al2O3-SiO2 content of conventional and waste pozzolanic materials.

The typical chemical composition of pozzolanic materials such as pulverised fuel ash (PFA) and ground granulated blast furnace slag (GGBS) is well understood and their use as cement replacements is well-established in construction and concrete technology. Figure 15 compares the chemical composition of the waste materials used in this project and commonly used cementitious materials (OPC, GGBS and PFA).

The composition of BOS is quite different from that of BF slag (GGBS). This is due to the nature of the process from which these materials are derived. GGBS is produced during the production of steel in the blast furnace while BOS is obtained from basic oxygen furnace process. Figure 16 presents a general schematic that depicts the blast furnace feedstocks and the production of blast furnace co-products (iron and slag).

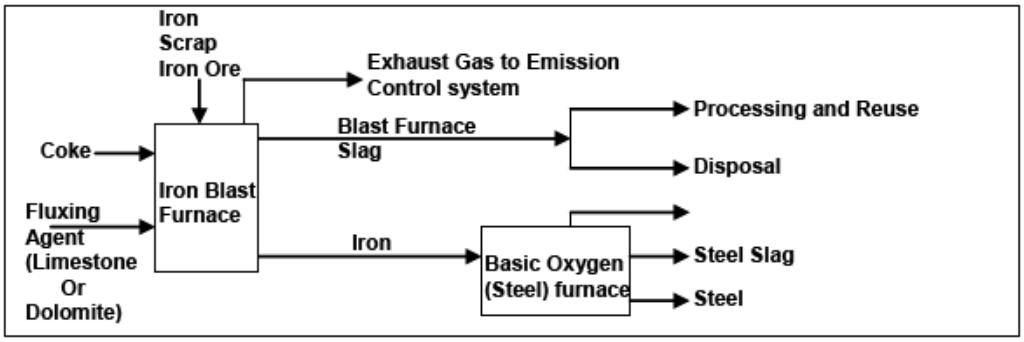

Figure 16. General schematic of blast furnace operation and blast furnace slag production.

2.1.4. Mix proportions

2.1.4.1. Paste And Concrete Mixtures

A large number of paste specimens were made during the investigation. This report uses the word 'paste' to mean a mixture of cementitious powder and water with no aggregate. 'Semi-dry' paste refers to a paste containing a low proportion of water.

The proportions used in the pastes in this study were designed to optimise the mixture ingredients to achieve the highest compressive strength. A considerable number of initial 'cup' mixes and trial mixes were made using various materials and proportions to identify suitable mix ingredients.

A systematic laboratory study was designed to determine the effects of:

- different replacement levels of PG, BOS, ROSA, CKD, BPD, hydrated lime and MKD;
- slag weathering; and
- water content.

Based on the optimum proportions obtained from the paste mixes, various concrete mixes were designed using 380 kg/m^3 binder and different L/B (liquid to binder) ratios. Tables 2–17 show the mixture proportions used to make pastes and concretes, their liquid-to-solid (L/S) ratios and flow as measured on a flow table (see section 2.1.6).

Table 2. Mix proportions for PG-CKD-BOS paste mixtures

Mix code	PG (%)	CKD (%)	UW-BOS (%)	L/S	Flow (mm)
PG 20/UW-BOS80	20	–	80	0.3	150
PG40/UW-BOS60	40	–	60	0.3	136
PG60/UW-BOS40	60	–	40	0.3	110
CKD60/PG8-UW-BOS32	8	60	32	0.3	161
CKD40/PG12-UW-BOS48	12	40	48	0.3	120
CKD20/PG16-UW-BOS64	16	20	64	0.3	92

Table 3. Mix proportions for PG-BPD-BOS paste mixtures

Mix code	PG (%)	BPD (%)	BOS (%)	L/S	Flow (mm)
BPD10/BOS90	–	10	90	0.3	146
BPD20/BOS80	–	20	80	0.3	104
BPD40/BOS60	–	40	60	0.3	108
BPD60/BOS40	–	60	40	0.3	91
BPD90/BOS10	–	90	10	0.3	88
PG5/BPD38-BOS57	5	38	57	0.3	178
PG10/BPD36-BOS54	10	36	54	0.3	176
PG15/BPD34-BOS51	15	34	51	0.3	158

Table 3. (Continued)

Mix code	PG (%)	BPD (%)	BOS (%)	L/S	Flow (mm)
PG20/BPD32-BOS48	20	32	48	0.3	157
PG30/BPD28-BOS42	30	28	42	0.3	115

Table 4. Mix proportions for BPD-PG-BOS paste mixtures

Mix code	PG (%)	BPD (%)	BOS (%)	L/S	Flow (mm)
PG10/BOS90	10	–	90	0.3	170
PG20/BOS80	20	–	80	0.3	158
PG40/BOS60	40	–	60	0.3	110
PG60/BOS40	60	–	40	0.3	90
BPD5/PG19/BOS76	19	5	76	0.3	175
BPD10/PG18/BOS72	18	10	72	0.3	177
BPD20/PG16/BOS64	16	20	64	0.3	160
BPD30/PG14/BOS56	14	30	56	0.3	185
BPD50/PG10/BOS40	10	50	40	0.3	171

Table 5. Mix proportions for PG-BPD paste mixtures

Mix code	PG (%)	BPD (%)	BOS (%)	L/S	Flow (mm)
PG10/BPD90	10	90	–	0.3	103
PG20/BPD80	20	80	–	0.3	105
PG40/BPD60	40	60	–	0.3	108
PG60/BPD40	60	40	–	0.3	109

Table 6. Mix proportions for fine tuning of BOS-PG-BPD paste mixtures*

Mix code	PG (%)	BPD (%)	BOS (%)	L/S	Flow (mm)
BOS80/PG15/BPD5	10	5	80	0.3	162
BOS85/PG10/BPD5	10	5	85	0.3	162
BOS77/PG20/BPD3	20	3	77	0.3	158
BOS80/PG5/BPD15	5	15	80	0.3	140
BOS80/PG10/BPD10	10	10	80	0.3	148
BOS80/PG12/BPD8	12	8	80	0.3	154
BOS80/PG2/BPD18	2	18	80	0.3	124

* Primary data prior to fine tuning are given in Tables 3–5#.

Table 7. Mix proportions for measuring the effect of ROSA on BOS-CKD-PG paste mixtures

Mix code	PG (%)	CKD (%)	W-BOS (%)	ROSA (%)	L/S	Flow (mm)
PG15/CKD5/BOS10/ROSA70	15	5	10	70	0.3	38.5
PG15/CKD5/BOS20/ROSA60	15	5	20	60	0.3	47.2
PG15/CKD5/BOS30/ROSA50	15	5	30	50	0.3	59.1
PG15/CKD5/BOS40/ROSA40	15	5	40	40	0.3	56.8
PG15/CKD5/BOS50/ROSA30	15	5	50	30	0.3	61.5
PG15/CKD5/BOS60/ROSA20	15	5	60	20	0.3	107.7
PG15/CKD5/BOS70/ROSA10	15	5	70	10	0.3	124

Table 8. Mix proportions for measuring the effect of L/S ratio and weathering on BOS-CKD-PG paste mixtures

Mix code	PG (%)	CKD (%)	UW-BOS (%)	W-BOS (%)	L/S	Flow (mm)
PG15/CKD5/W-BOS80-0.2	15	5	–	80	0.2	78
PG15/CKD5/W-BOS80-0.25	15	5	–	80	0.25	112
PG15/CKD5/W-BOS80-0.3	15	5	–	80	0.3	152
PG15/CKD5/W-BOS80-0.4	15	5	–	80	0.4	209
PG15/CKD5/UW-BOS80-0.2	15	5	80	–	0.2	78
PG15/CKD5/UW-BOS80-0.25	15	5	80	–	0.25	145
PG15/CKD5/UW-BOS80-0.3	15	5	80	–	0.3	191
PG15/CKD5/UW-BOS80-0.4	15	5	80	–	0.4	>250

Table 9. Mix proportions of semi-dry mixtures of BOS-BPD-PG and PG-BPD-BOS-ROSA

Mix code	PG (%)	BPD (%)	BOS (%)	ROSA (%)	L/S	Flow (mm)
PG15/BPD5/BOS80-0.3	15	5	80	–	0.3	175
PG15/BPD5/BOS80-0.2	15	5	80	–	0.2	0
PG15/BPD5/BOS80-.15	15	5	80	–	0.15	0
PG15/BPD5/BOS80-.13	15	5	80	–	0.13	0
PG15/BPD5/BOS30/ROSA50-0.3	15	5	30	50	0.3	125
PG15/BPD5/BOS30/ROSA50-0.25	15	5	30	50	0.25	0
PG15/BPD5/BOS30/ROSA50-0.23	15	5	30	50	0.23	0
PG15/BPD5/BOS30/ROSA50-0.19	15	5	30	50	0.19	0
PG15/BPD5/BOS30/ROSA50-0.15	15	5	30	50	0.15	0

Table 10. Mix proportions for BPD-BOS-ROSA mixtures

Mix code	BPD (%)	BOS (%)	ROSA (%)	L/S	Flow (mm)
BPD5/BOS76/ROSA19	5	76	19	0.3	>250
BPD5/BOS50/ROSA45	5	50	45	0.3	152
BPD5/BOS27/ROSA68	5	27	68	0.3	123
BPD5/BOS15/ROSA80	5	15	80	0.3	83
BPD10/BOS72/ROSA18	10	72	18	0.3	155
BPD10/BOS35/ROSA55	10	35	55	0.3	132
BPD20/BOS64/ROSA16	20	64	16	0.3	143
BPD40/BOS48/ROSA12	40	48	12	0.3	134
BPD40/BOS30/ROSA30	40	30	30	0.3	130
BPD60/BOS32/ROSA8	60	32	8	0.3	125

Table 11. Mix proportions for ROSA-BOS-BPD mixtures

Mix code	BPD (%)	BOS (%)	ROSA (%)	L/S	Flow (mm)
ROSA32/BOS8/BPD60	60	8	32	0.3	96
ROSA48/BOS12/BPD40	40	12	48	0.3	94
ROSA64/BOS16/BPD20	20	16	64	0.3	86
ROSA72/BOS18/BPD10	10	18	72	0.3	55

Table 12. Mix proportions for BPD-BOS-ROSA mixtures

Mix code	BPD (%)	BOS (%)	ROSA (%)	L/S	Flow (mm)
BOS20/ROSA48/BPD32	32	20	48	0.3	115
BOS40/ROSA36/BPD24	24	40	36	0.3	126
BOS60/ROSA24/BPD16	16	60	24	0.3	150

Table 13. Mix proportions for PG-BOS-ROSA mixtures

Mix code	PG (%)	BOS (%)	ROSA (%)	L/S	Flow (mm)
PG5/BOS15/ROSA80	5	15	80	0.3	90
PG5/BOS76/ROSA19	5	76	19	0.3	>250
PG5/BOS50/ROSA45	5	50	45	0.3	136
PG8/BOS20/ROSA72	8	20	72	0.3	85
PG10/BOS30/ROSA60	10	30	60	0.3	95
PG10/BOS75/ROSA15	10	75	15	0.3	>250
PG12/BOS48/ROSA40	12	48	40	0.3	153
PG16/BOS64/ROSA20	16	64	20	0.3	>250

Mix code	PG (%)	BOS (%)	ROSA (%)	L/S	Flow (mm)
PG20/BOS35/ROSA45	20	35	45	0.3	130
PG30/BOS40/ROSA30	30	40	30	0.3	119

Table 14. Mix proportions for BOS-Lime and BOS-MKD paste mixtures

Mix code	Hydrated lime (%)	MKD (%)	BOS (%)	L/S	Flow (mm)
Lime10/BOS90	10	–	90	0.3	>250
Lime30/BOS70	30	–	70	0.3	167
Lime50/BOS50	50	–	50	0.3	124
Lime70/BOS30	70	–	30	0.3	89
MKD10/BOS90	–	10	90	0.3	>250
MKD30/BOS70	–	30	70	0.3	172
MKD50/BOS50	–	50	50	0.3	132
MKD70/BOS30	–	70	30	0.3	93

Table 15. Mix proportions for BOS-Lime and BOS-MKD paste mixtures

Mix code	Hydrated lime (%)	MKD (%)	ROSA (%)	L/S	Flow (mm)
Lime10/ROSA90	10	–	90	0.3	130
Lime30/ROSA70	30	–	70	0.3	114
Lime50/ROSA50	50	–	50	0.3	95
Lime70/ROSA30	70	–	30	0.3	87
MKD10/ROSA90	–	10	90	0.3	142
MKD30/ROSA70	–	30	70	0.3	124
MKD50/ROSA50	–	50	50	0.3	98
MKD70/ROSA30	–	70	30	0.3	94

Table 16. Mix proportions for measuring the effect of hydrated lime and MKD on BOS-PG-ROSA paste mixtures

Mix code	Hydrated lime (%)	MKD (%)	PG (%)	BOS (%)	ROSA (%)	L/S	Flow (mm)
BOS80/PG15/Lime5	5	–	15	80	–	0.3	114
BOS80/PG15/MKD5	–	5	15	80	–	0.3	152
BOS50/ROSA30/PG15/Lime5	5	–	15	50	30	0.3	108
BOS50/ROSA30/PG15/MKD5	–	5	15	50	30	0.3	118
ROSA75/PG15/MKD10	–	10	15	–	75	0.3	110
ROSA65/PG15/MKD20	–	20	15	–	65	0.3	94

Table 17. Mix proportions of concrete mixtures

Mix code	Mix proportions (kg/m^3)											Slump (mm)
	PG	BPD	BOS	ROSA	Water	Water reducer		Sand	Coarse 10 mm	Recycled aggregate	L/B	
						Ordinary	Polymeric					
PG15/BPD5/BOS80 (SP)	57	19	304	–	152	7.6 (2%)	–	830	1050	–	0.4	10
PG15/BPD34/BOS51	57	129.2	193.8	–	152	–	–	795	1050	–	0.4	10
PG15/BPD5/BOS80 (PSP)	57	19	304	–	152	–	2.66 (0.7%)	830	1050	–	0.4	180
PG15/BPD5/BOS80 (RA-PSP)	57	19	304	–	152	–	1.9 (0.5%)	–	–	1545	0.4	20
PG15/BPD5/BOS80 (PPG-PSP)	57	19	304	–	152	–	2.66 (0.7%)	830	1050	–	0.4	160
PG15/BPD5/BOS80 (RA-PPG-PSP)	57	19	304	–	152	–	1.9 (0.5%)	–	–	1545	0.4	40
PG15/BPD5/BOS80 (RA-RCC)	57	19	304	–	95	–	–	–	–	1980	0.25	0
PG15/BPD5/BOS60/ROSA20	57	19	228	76	152	–	–	800	1050	–	0.4	0
PG10/BPD5/BOS32/ROSA53 (SP)	38	19	121.6	201.4	152	5.7 (1.5%)	–	770	1050	–	0.4	120
PG15/BPD5/BOS30/ROSA50 (RA-PSP)	57	19	114	190	152	–	2.66 (0.7%)	–	–	1808	0.4	30
PG15/BPD5/BOS30/ROSA50 (RA-RCC)	57	19	114	190	114	–	–	–	–	1910	0.3	0

PPG = processed plasterboard gypsum
PSP = polymer superplasticiser
RA = recycled aggregate
SP = superplasticiser

2.1.4.2. Soil Stabilisation Mixtures

Two types of soils – sandy clay (Figure 17) and silty sand (Figure 18) – were mixed with various amounts of two sele

The quantities of binder chosen were 20, 40, 50 and 60%; Table 18 shows the proportions of soil and binder used. The optimum moisture content (OMC) of each soil was determined according to BS 1377-4: 1990 [13]; the results are presented in Table 19 and Figure 19.

To compensate for the amount of water necessary for hydration of the binder, an extra 0.5% of water by weight was added to the mixture of soil and binder.

Figure 17. Sandy clay soil (Soil A).

Figure 18. Silty sand soil (Soil B).

Table 18. Mix proportions of stabilised soil mixtures

Mix code	Soil (%)	Binder (%)	Moisture content (%)
Soil-A 80/Binder-A 20	80	20	14.2
Soil-A 60/Binder-A 40	60	40	14.2
Soil-A 50/Binder-A 50	50	50	14.2
Soil-A 40/Binder-A 60	40	60	14.2
Soil-A 40/Binder-B 60	40	60	15.2
Soil-B 80/Binder-A 20	80	20	13.9
Soil-B 60/Binder-A 40	60	40	13.9
Soil-B 50/Binder-A 50	50	50	13.9

Table 19. Optimum moisture content of soils used (compatibility test)

Soil type	Optimum moisture content (%)	Peak dry density (g/cm3)
Soil-A	13.70	1.86
Soil-B	13.40	1.92

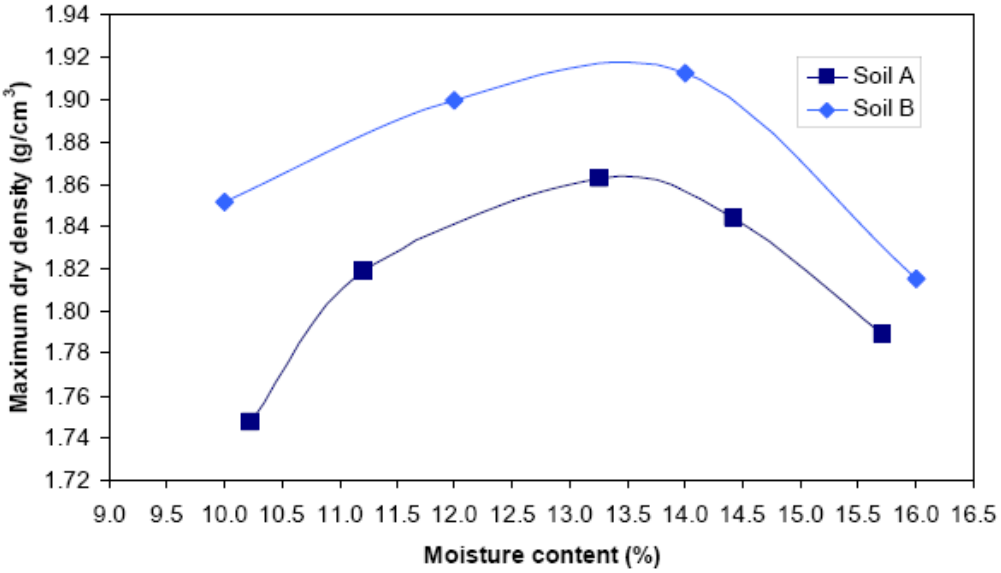

Figure 19. Compatibility and optimum moisture content of soils used.

2.1.5. Mixing and Casting

2.1.5.1. Paste mixtures

The mixing was carried out in a mixer of 2-litre capacity according to the following procedure:

- PG, BOS, BPD and ROSA (as applicable) were mixed dry for 1 minute.
- Half the mixing water (with superplasticiser if applicable) was added during the next 30 seconds of mixing.
- Mixing was continued for a further 30 seconds at medium speed.
- The mixer was stopped and the mixture scraped off the sides of the bowl and blades.
- The remainder of the mixing water was added and mixing was carried out for a further two minutes at high speed.

2.1.5.2. Concrete Mixtures

The fine and coarse aggregates were air-dried before mixing. The water content of the mix was adjusted based on natural moisture content and the measured saturated surface dry (SSD) moisture content of the aggregates. The mixing was performed according to the guidelines set out in BS 1881-125: 1986 [14].

A horizontal pan mixer of 10-litre capacity was used to make the concrete mixes. The mixing method was as follows:

- The fine and coarse aggregate were mixed with about one-third of the water to allow absorption to take place for 30 seconds.
- The PG, BOS and BPD were mixed dry by hand.
- Half the reminder of the water was added with PG, BOS, CKD, BPD and ROSA (as applicable) and mixed for 1 minute.
- The mixer was stopped and the mixture scraped off the sides of the pan and hand mixed.
- The remainder of mixing water was added and mixing continued for another 2 minutes.

2.1.5.3. Casting and Curing

The paste and concrete samples were cast in pre-oiled 50-mm and 100-mm cube moulds respectively. The moulds were covered after casting with wet fabric and a polyethylene sheet until demoulding the next day. After demoulding, specimens were stored in containers kept at 20±2˚ C and 98% relative humidity (RH).

2.1.6. Test Methods

The flow of the paste and concrete mixes was measured using a flow table (BS EN 12350-5: 2000 [15]) and a slump test.

A mix is considered to be flowable when the spread is 510–620 mm in diameter. This corresponds to 110–210 mm in diameter for the small modified flow table used in this study according BS 4551-1: 1998 [16] and ASTM C230 [17]. For high flowability, a spread of >190 mm in diameter is required.

Compressive strengths of cubes up to the age of 28 days were determined. Concrete specific compliance tests, including high pressure through-flow and hydrogen sulphide tests, were also carried out. The results of these tests are given in section 4.

2.1.6. Laboratory results

2.1.6.1. Paste Mixes

2.1.6.1.1. PG-BOS Mixture with and without CKD

The results of compressive strength tests on PG-BOS-CKD at two stages (i.e. initially without CKD) are presented in Table 20. Figure 20 shows the compressive strength development of PG-BOS paste mixes. The mix incorporating 20% PG and 80% BOS achieved the highest compressive strength compared to mixes with a lower slag content.

In the second stage, the ternary mixture of PG-CKD-BOS incorporating various amounts of CKD and the same BOS to PG ratio of 4 was tested for compressive strength as shown in Figure 21. The relationship between the compressive strength of the ternary system and the CKD content is depicted in Figure 22.

Table 20. Compressive strength of PG-BOS-CKD mixes

Mix code	Strength at days (MPa)*			Flow (mm)	Density (kg/m^3)
	3	7	28		
PG20/UW-BOS80	1.8	3.61	7.77	150	1910
PG40/UW-BOS60	1.65	3.37	4.18	136	1760
PG60/UW-BOS40	1.3	2.99	3.45	110	1580
CKD60/PG 8-UW-BOS32	1.23	2.1	6.97	161	1990
CKD40/PG12-UW-BOS48	0.91	1.6	7.22	120	1930
CKD20/PG16-UW-BOS64	1.35	2.9	13.1	92	2050

* Highlighted cells indicate the highest or optimum compressive strength achieved in each group.

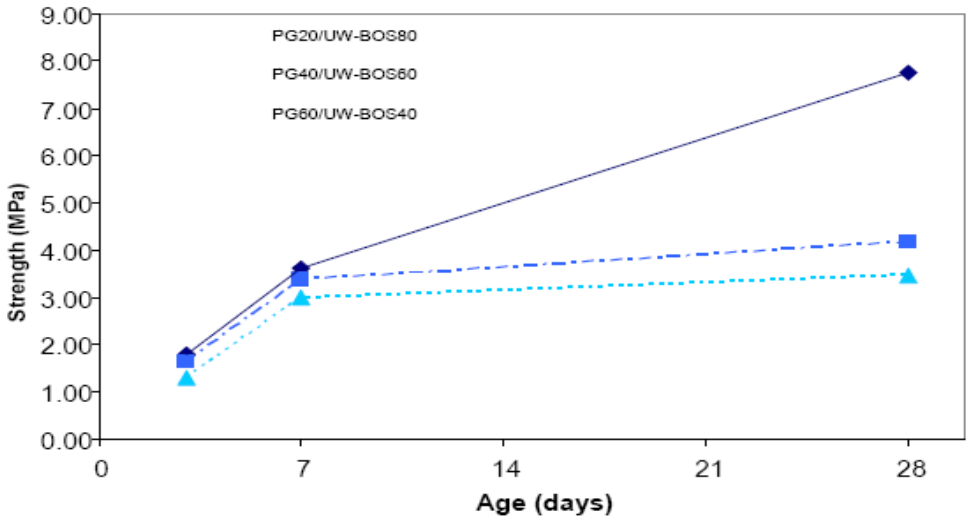

Figure 20. Compressive strength development of pastes containing PG and BOS.

Increasing the amount of CKD from 20 to 60% in the ternary system resulted in a reduction in the compressive strength of the mixes by nearly 50% at 28 days (Figure 21). The highest compressive strength (13.1 MPa) of the mixes tested was for the mix with 20% CKD, 16% PG and 64% BOS (Table 20). Because insufficient CKD was available, it was not possible to include other combinations of PG-CKD-BOS in these initial investigations. Therefore the mix optimisation focused on using BPD instead (see section 2.1.6.1.4).

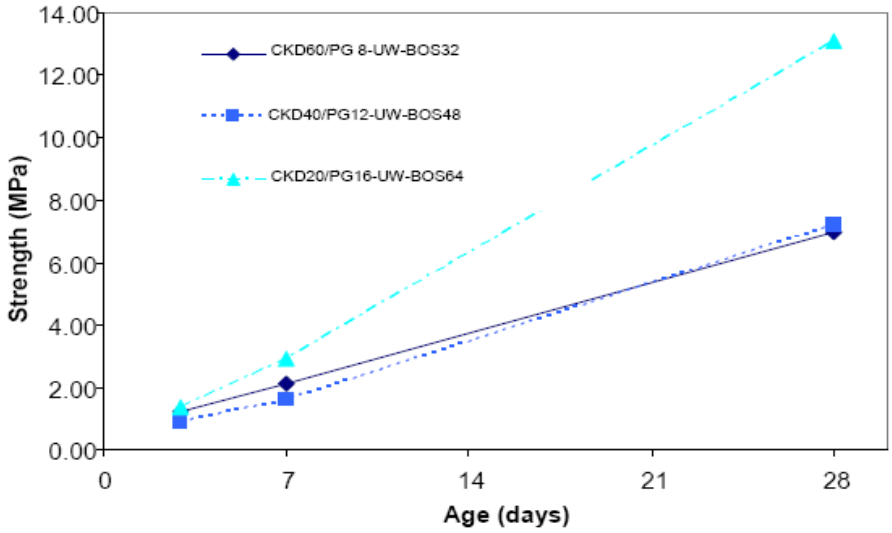

Figure 21. compressive strength development of pastes containing CKD, PG and BOS.

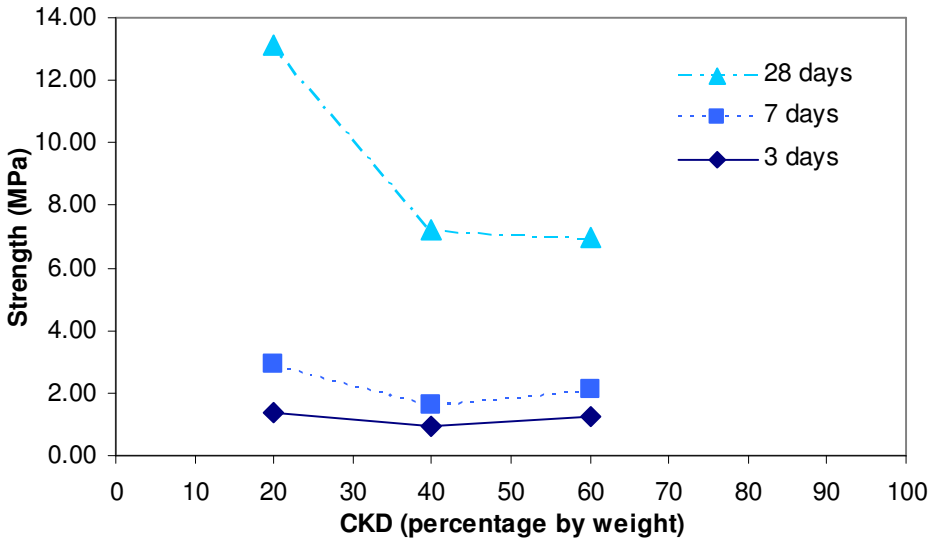

Figure 22. Compressive strength versus CKD content.

2.1.6.1.2. *Effect of ROSA on PG-CKD-BOS Mixture*

The results of compressive strength of mixes incorporating four components (PG, CKD, BOS and ROSA) are presented in Table 21. These tests were carried out using a mixture with 15% CKD rather than the one containing 20% CKD which had shown the highest compressive strength in earlier tests (see section 2.1.6.1.1) primarily due to the limited supplies of CKD.

Table 21. Compressive strength of PG, CKD, BOS and ROSA mixtures

Mix code	Strength at days (MPa)*			Flow (mm)	Density (kg/m^3)
	3	7	28		
PG15/CKD5/BOS10/ROSA70	0.46	1.41	10.6	108	1680
PG15/CKD5/BOS20/ROSA60	0.34	1.32	18.9	115	1760
PG15/CKD5/BOS30/ROSA50	0.31	1.33	19.1	124	1780
PG15/CKD5/BOS40/ROSA40	0.37	1.34	8.21	122	1860
PG15/CKD5/BOS50/ROSA30	0.98	1.48	11.45	126	1880
PG15/CKD5/BOS60/ROSA20	0.62	1.83	9.83	162	2080
PG15/CKD5/BOS70/ROSA10	0.5	1.73	6.32	175	2030

* Highlighted cell indicates the highest or optimum compressive strength achieved in the group.

Figure 23 shows the compressive strength development for the mixes containing a range of ROSA-BOS content and same amount of PG and CKD. It shows that the mix incorporating 50% ROSA and 30% BOS achieved the highest 28-day strength.

This result indicates that replacing part of the BOS content with ROSA had a beneficial effect on early and long-term compressive strength up to this stage. This could be due to the activating effect of ROSA on BOS or the intrinsic pozzolanic potential of ROSA. The L/S ratio for all mixes was kept constant at 0.3 (Table 3).

Figure 24 shows the changes in compressive strength with changes in ROSA content at different ages. Although change in ROSA content does not have a significant effect on strength at early ages, it becomes significant at the test age of 28 days. Two peaks of compressive strength at the testing age of 28 days can be observed. The highest strength belongs to the mix incorporating 50% ROSA, showing clearly the superior pozzolanic potential of this ash. At 7 days, the strength of the mix incorporating 20% ROSA is the highest but, in the long term, this trend changes.

The relative high strength of mixes incorporating ROSA is mainly because of the formation of aluminium-bearing products in the hydrated matrix of the paste.

In summary, use of a combination of BOS and ROSA is suggested for the trial mix, providing the four materials can be blended to form a final consistent powder.

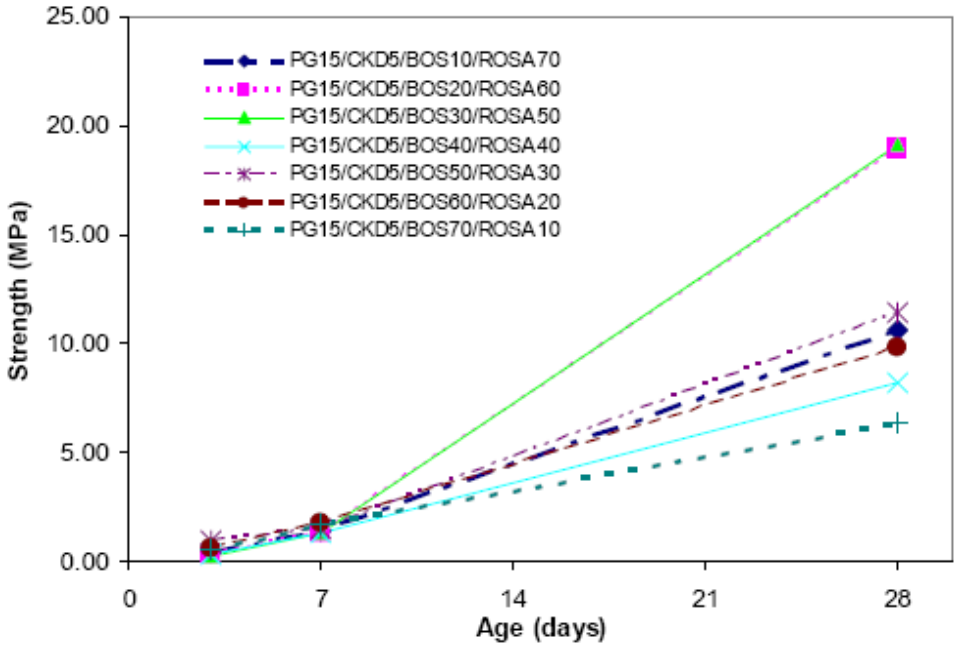

Figure 23. Compressive strength development of pastes containing PG, CKD, BOS and ROSA.

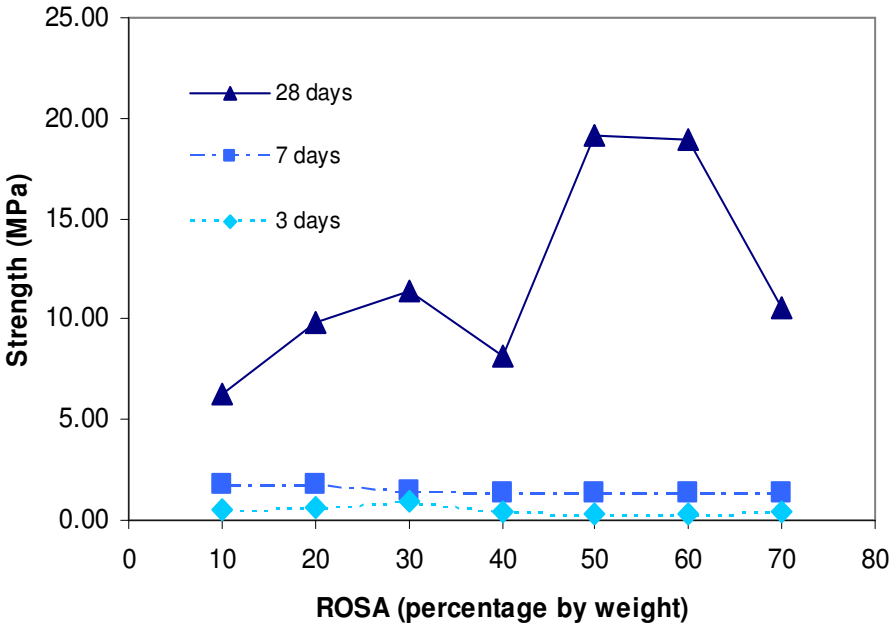

Figure 24. Compressive strength of PG-CKD-BOS-ROSA mixes versus ROSA content at different ages.

2.1.6.1.3. *Effect of Liquid to Solid Ratio, Superplasticisers and Weathering of BOS on PG-CKD-BOS Mixtures*

Table 22. presents the compressive strength results of PG-CKD-BOS mixtures with various liquid to binder ratios and workabilities.

Table 22. Compressive strength of mixtures of PG-CKD-BOS with various L/S ratios

Mix code	Strength at days (MPa)*			Flow (mm)	Density (kg/m^3)	L/S
	3	7	28			
PG15/CKD5/W-BOS80-0.2	0.26	2.23	6.44	78	2160	0.2
PG15/CKD5/W-BOS80-0.25	1.49	2.55	5.1	112	2090	0.25
PG15/CKD5/W-BOS80-0.3	1.14	1.9	4.7	152	1920	0.3
PG15/CKD5/W-BOS80-0.4	0.34	0.85	1.9	209	1790	0.4
PG15/CKD5/UW-BOS80-0.2	0.43	1.5	7.68	78	1970	0.2
PG15/CKD5/UW-BOS80-0.25	0.37	1.1	5.65	145	2060	0.25
PG15/CKD5/UW-BOS80-0.3	0.22	0.87	4.15	191	1890	0.3
PG15/CKD5/UW-BOS80-0.4	0.15	0.39	2.49	High	1790	0.4
PG15/CKD5/W-BOS80-0.2 superplasticiser	1.94	3.1	9.33	100	2340	nd

* Highlighted cells indicate the highest or optimum compressive strength achieved in each group. nd = not determined.

Figure 25 and 26 show that a lower water content of the mix results in a higher compressive strength. This is in accordance with general concepts of cement and concrete technology.

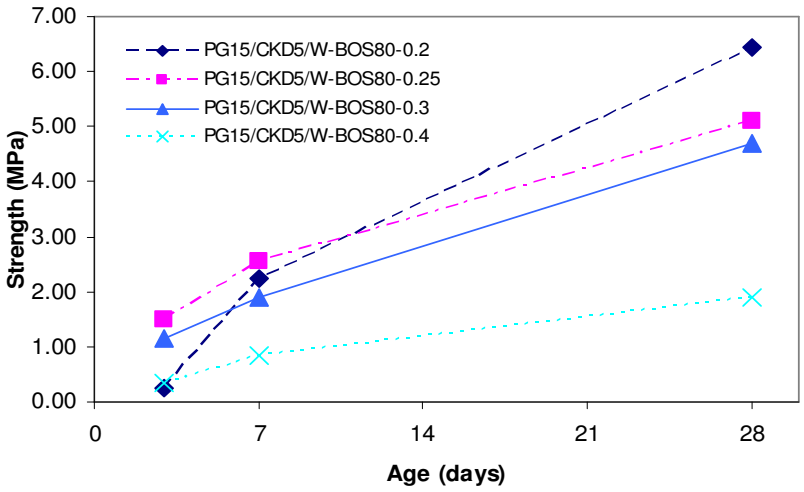

Figure 25. Compressive strength development of pastes containing PG, CKD, W-BOS with various L/S ratios.

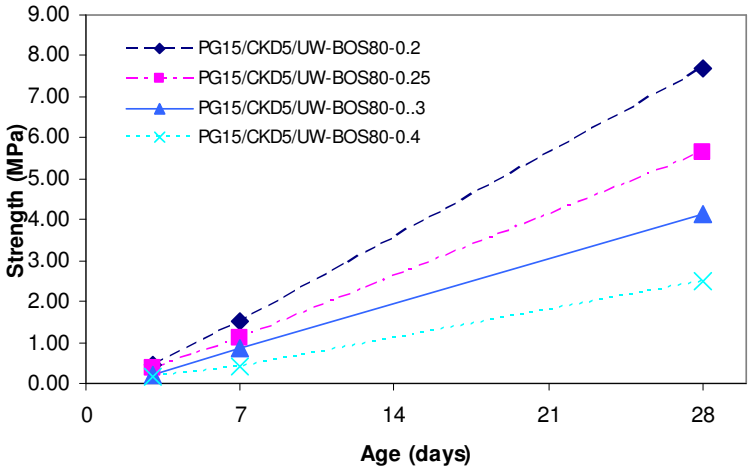

Figure 26. Compressive strength development of pastes containing PG, CKD, UW-BOS with various L/S ratios.

The mix with an L/S ratio of 0.2 achieved the highest strength at a test age of 28 days regardless of the weathering condition of the slag (Figures 25 and 26). The results also indicate that PG15/CKD5/BOS80-0.2 gains strength at a higher rate compared with other mixes.

These results indicate that reducing the water content will improve the long-term strength of the paste even though the flow of the mix might not be high enough to achieve appropriate compaction. A much greater improvement in strength might be achieved by using flow-improving agents and plasticisers, or different compaction methods instead of the vibrating table. Further results from studies on the effect of water content are discussed in section 2.1.6.1.6

Incorporating weathered slag resulted in an increase in compressive strength at early test ages of 3 and 7 days (Figure 27). As the weathered BOS contains more calcium carbonate than the unweathered BOS, the increase in strength could be due to presence of calcium carbonate improving the microstructure of the hardened paste. However, the lack of calcium hydroxide content in the weathered slag adversely affects the strength of these mixes at 28 days.

The mix PG15/CKD5/BOS80-0.2-P, which incorporates superplasticiser as a flow-improving agent, showed the highest gain in strength at 3, 7 and 28 days compared with the mix of the same L/S ratio (0.2) but without superplasticiser (Figure 28). Use of superplasticiser improved the flow from 78 to 100 mm (Table 22).

An increase in the flow of the mix will have a beneficial effect on compaction and, as a result, compressive strength will improve. The presence of the water-reducing agent may also improve the early strength by affecting the setting and hardening rate of such mixes.

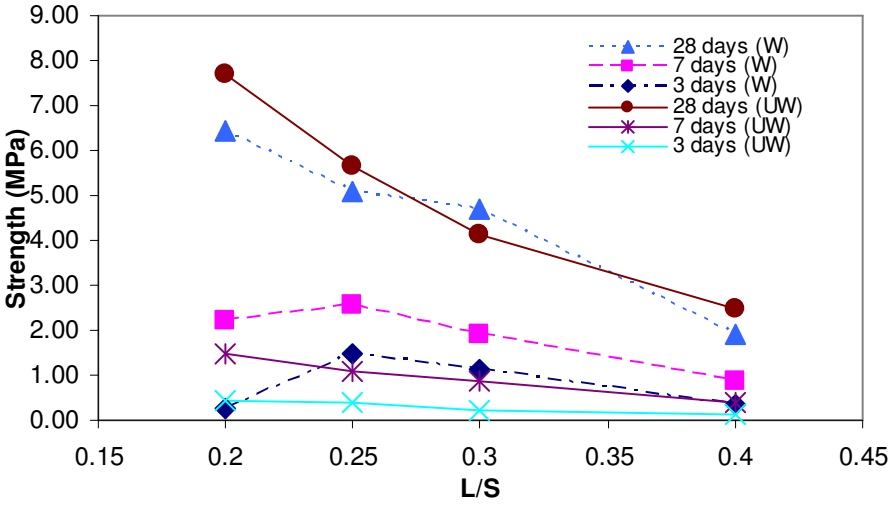

Figure 27. Compressive strength versus L/S ratio for weathered and unweathered BOS at different ages.

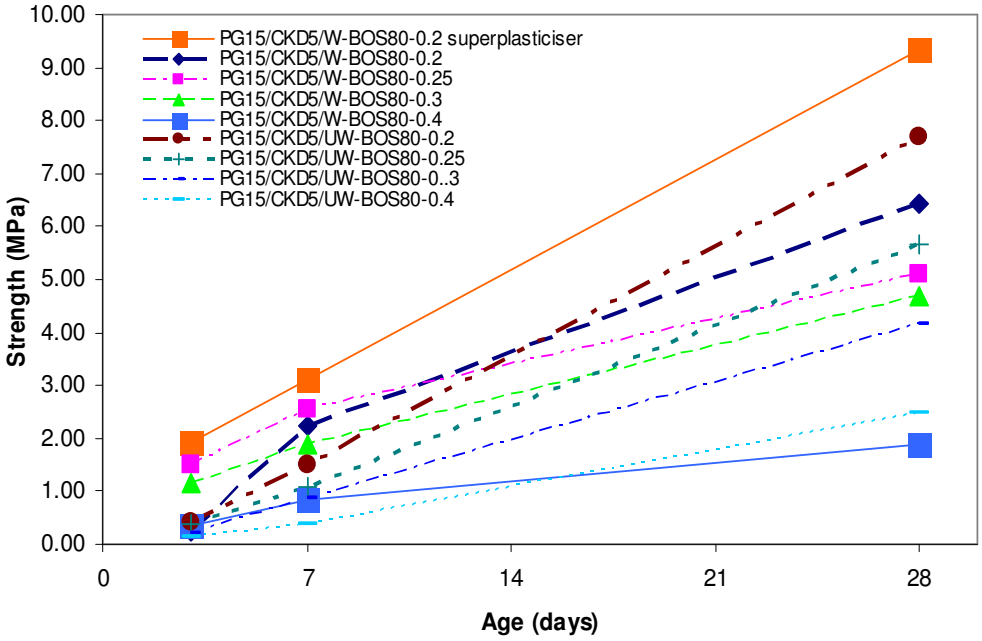

Figure 28. Comparison of the compressive strength development of PG-CKD-BOS pastes with superplasticiser and various L/S ratios.

2.1.6.1.4. *Optimisation of Mixture (PG, BPD, BOS)*

The combinations of PG, BPD and BOS were investigated with respect to compressive strength. In order to optimise the ternary mixture of PG, BPD and BOS, a two-stage method was adopted.

- In the first stage, the strength of binary mixtures of each ingredient was determined.
- In the second stage, the third ingredient was added to the binary mix with the highest strength.

To distinguish the order of the components in each mixture, the name of the last component added to the optimum binary mix is given first, e.g. PG-BOS-BPD means PG was added to the optimum binary mixture of BOS and BPD in the second stage.

(A) PG-BPD-BOS Mixture

The results for compressive strength of PG-BPD-BOS mixtures are shown in Table 23. The strength development of paste mixes using a range of BPD and BOS with same water content shows that the mix containing 40% BPD and 60% BOS had the highest strength at 7 days (Figure 29). Although Table 23 and Figure 30 show that the optimum amount of BPD for 3-day strength is 60%, this could be due to the rapidly reacting components of the BPD used. At 7 and 28 days, the highest compressive strength was achieved by the mix of BPD40/BOS60.

Table 23. Compressive strength of PG-BPD-BOS mixes*

Mix code	Strength at days (MPa)†			Flow (mm)	Density (kg/m^3)
	3	7	28		
BPD10/BOS90	0.22	0.5	3.58	146	2140
BPD20/BOS80	0.82	1.46	6.5	104	1940
BPD40/BOS60	1.34	2.8	9.5	108	1860
BPD60/BOS40	1.76	2.47	8.9	91	1700
BPD90/BOS10	0.27	0.89	6.4	88	1580
PG5/BPD38/BOS57	0.39	1.1	5.95	178	2030
PG10/BPD36/BOS54	0.73	1.81	8.04	176	1960
PG15/BPD34/BOS51	0.42	1.42	5.01	158	1970
PG20/BPD32/BOS48	0.67	1.19	3.68	157	1900
PG30/BPD28/BOS42	0.77	1.38	3.1	115	1760

* Figures 29-32 are derived from this table.

† Highlighted cells indicate the highest or optimum compressive strength achieved in each group.

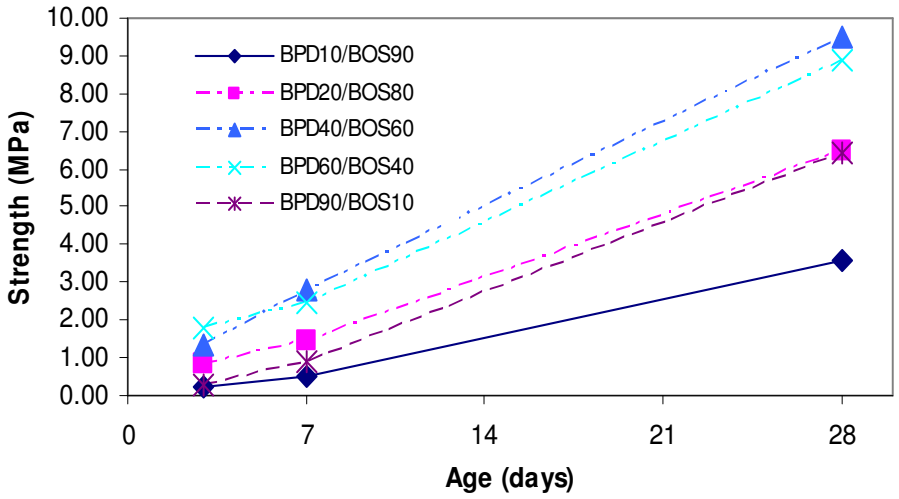

Figure 29. Compressive strength development of pastes containing BPD and BOS.

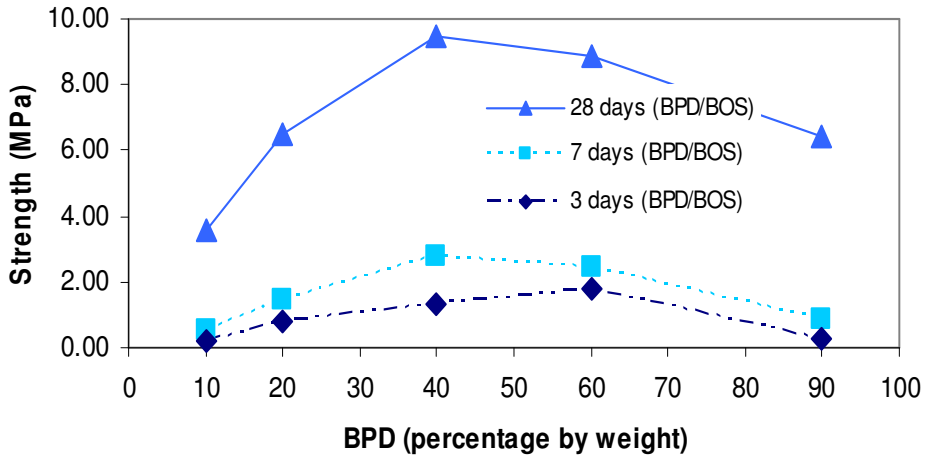

Figure 30. Compressive strength of BPD-BOS mixes versus BPD content at different ages.

Based on the highest compressive strength achieved at 28 days, the mix design was carried forward and paste mixes containing 5–30% PG and same ratio of BPD to BOS were made. The highest strength at 3, 7 and 28 days was for the mix containing 10% plasterboard gypsum (Figures 31 and 32). Increasing the amount of PG above 10% resulted in a decrease in compressive strength (Figure 32). Therefore, it was initially concluded that the mix PG10/BPD36/BOS54 was the optimum mixture in this combination.

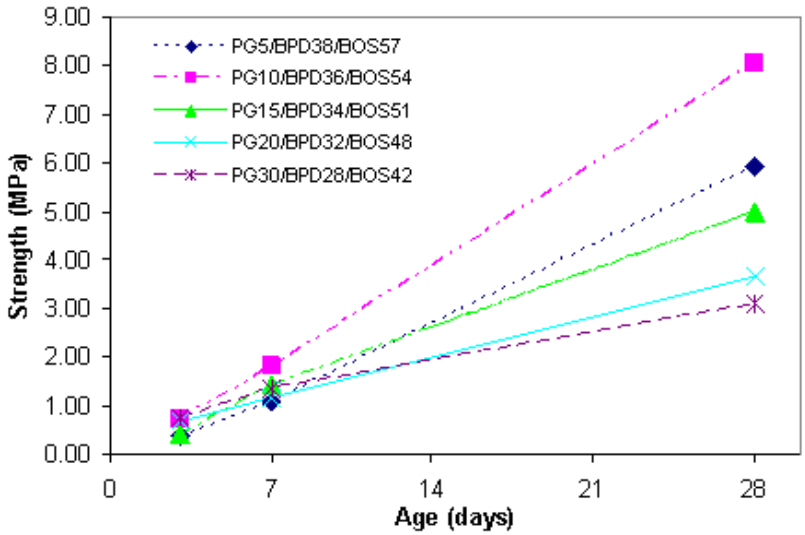

Figure 31. Compressive strength development of pastes containing PG, BPD and BOS.

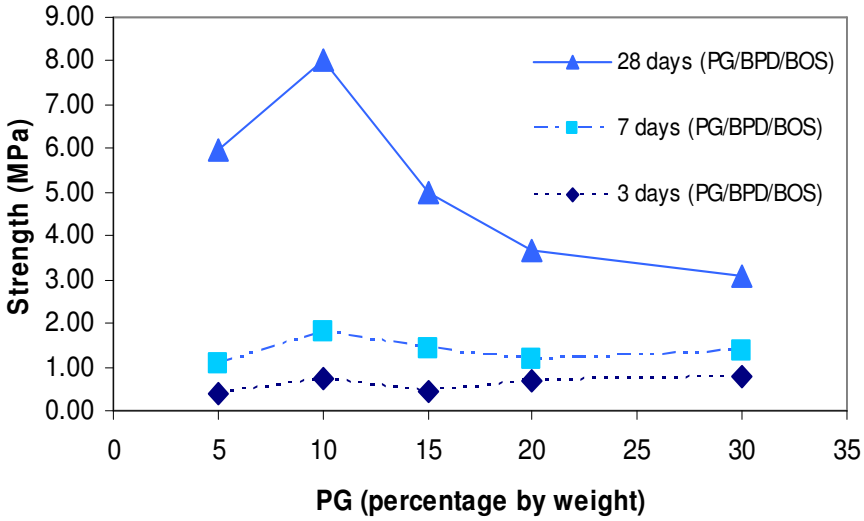

Figure 32. Compressive strength of PG-BPD-BOS mixes versus PG content.

(b) BPD-PG-BOS Mixture

The results for compressive strength of another combination of bypass dust, gypsum and slag (BPD-PG-BOS) are presented in Table 24. In this combination, the BPD was added to the optimum initial mixture of PG and BOS.

The strength development of PG-BOS and BPD-PG-BOS mixes is shown in Figures 33 and 34 respectively. In the first stage, the mixture of 20% PG and 80% BOS achieved the highest strength at all test ages. The catalyst effect of PG in the binary combination of PG-BOS was considerable, reducing the amount of BOS from 90% to 80% and combined with a corresponding increase in PG content from 10% to 20%, increasing the PG content by 10% resulted in a 16% increase in strength. In the ternary combination, the mix without BPD gained higher strength at 3 and 7 days, but the mix with 5% BPD achieved the highest strength at 28 days.

The effect of the amount of PG and BPD on binary and ternary combinations of PG-BOS and BPD-PG-BOS at different ages is shown in Figures 35 and 36 respectively. Figure 35 indicates the optimum percentage for PG in the binary combination is 20% and shows a dramatic decrease in strength when PG is increased from 20% to 60%.

The effect of BPD in the ternary system shown in Figure 36 is quite remarkable: the compressive strength fell by up to 50% as a result of increasing the BPD content from 5 to 20%. The strength improved slightly when the BPD content increased from 20% to 30%, and then remained the same for higher contents of BPD. The effect of BPD on the hydration and strength gain of ternary combinations is discussed in section 2.1.6.6.

According to the results for BPD-PG-BOS mixes, the highest compressive strength was for mix BPD5/PG19/BOS76. These results were subsequently modified to achieve the final optimum proportions.

Table 24. Compressive strength of BPD-PG-BOS mixes*

Mix code	Strength at days (MPa)†			Flow (mm)	Density (kg/m^3)
	3	7	28		
PG10/BOS90	0.34	1.17	8.8	170	2170
PG20/BOS80	0.95	2.3	10.26	158	2110
PG40/BOS60	0.76	1.63	6.4	110	2020
PG60/BOS40	0.75	1.17	4.04	90	1900
BPD0/PG20/BOS80	0.95	2.3	10.26	158	2110
BPD5/PG19/BOS76	0.31	1.43	10.5	175	2180
BPD10/PG18/BOS72	0.27	1.3	8.7	177	2140
BPD20/PG16/BOS64	0.29	1.25	5.8	160	2110
BPD30/PG14/BOS56	0.45	1.27	6.7	185	2090
BPD50/PG10/BOS40	0.83	2.02	6.9	171	2020

* Figures 34–38 are derived from this table.

† Highlighted cells indicate the highest or optimum compressive strength achieved in each group.

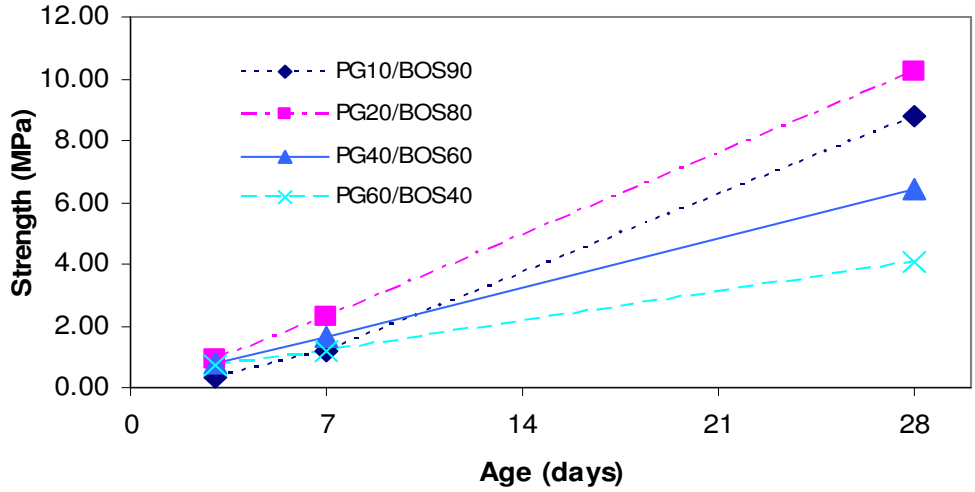

Figure 33. Compressive strength development of PG-BOS mixes.

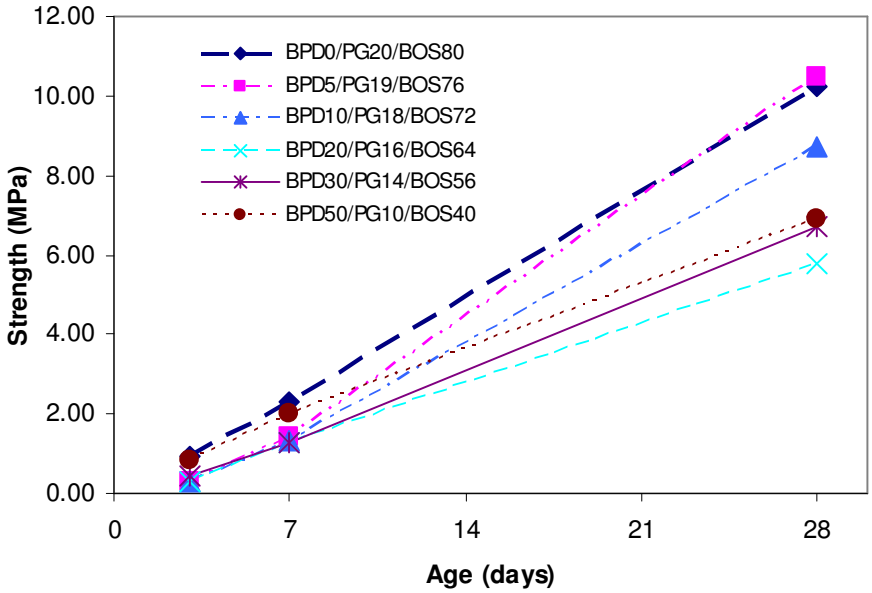

Figure 34. Compressive strength development of BPD-PG-BOS mixes.

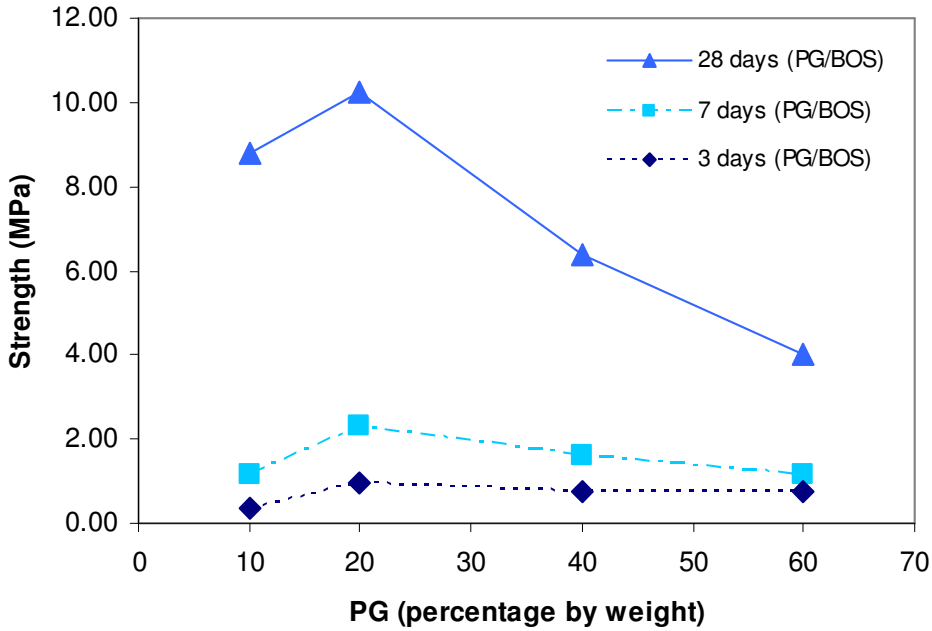

Figure 35. Compressive strength of PG-BOS mixes versus PG content .

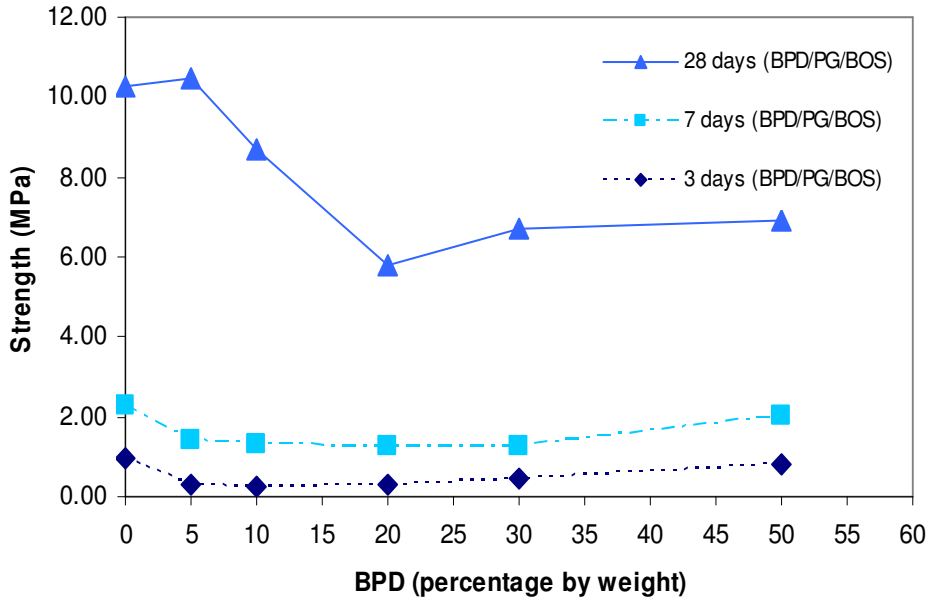

Figure 36. Compressive strength of BPD-PG-BOS mixes versus BPD content.

The role of PG in both binary and ternary systems is shown in Figure 37. In the ternary system, increasing the PG content up to 16% in the mix resulted in a reduction in compressive strength. However, a further increase in the amount of PG led to a considerable improvement in strength, with the maximum value of 10.5 MPa as the optimum in this particular combination (Table 24).

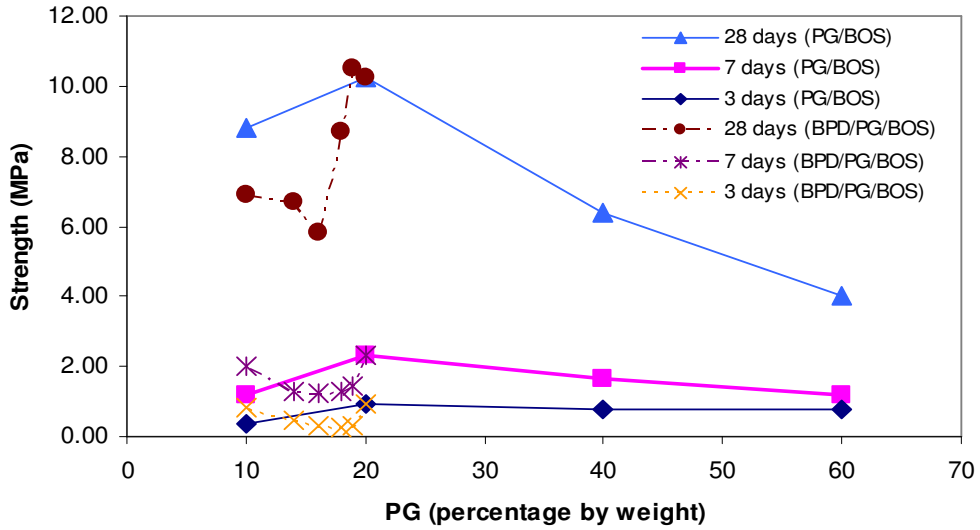

Figure 37. Compressive strength of PG-BOS and BPD-PG-BOS mixes versus PG content.

(c) BOS-PG-BPD Mixture

In order to investigate all possible combinations of PG, BPD and BOS mixtures, the combination of PG-BPD was also considered. The results for compressive strength testing are shown in Table 25.

Table 25. Compressive strength of PG-BPD mixes*

Mix code	Strength at days (MPa)†			Flow (mm)	Density (kg/m^3)
	3	7	28		
PG10/BPD90	3.1	5.45	12.55	103	1970
PG20/BPD80	2.25	3.65	8	105	1930
PG40/BPD60	1.42	2.2	4.69	108	1910
PG60/BPD40	0.94	1.3	2.5	108	1730

* Figures 39 and 40 are derived from this table.

† Highlighted cell indicates the highest or optimum compressive strength achieved in the group.

As shown in Figures 38 and 39, the higher the BPD content, the higher the compressive strength. This is due to the cementitious properties of BPD, which acts as the main binder in this combination. However, as BPD is not considered a pozzolanic material, further reaction between gypsum and BPD will not take place.

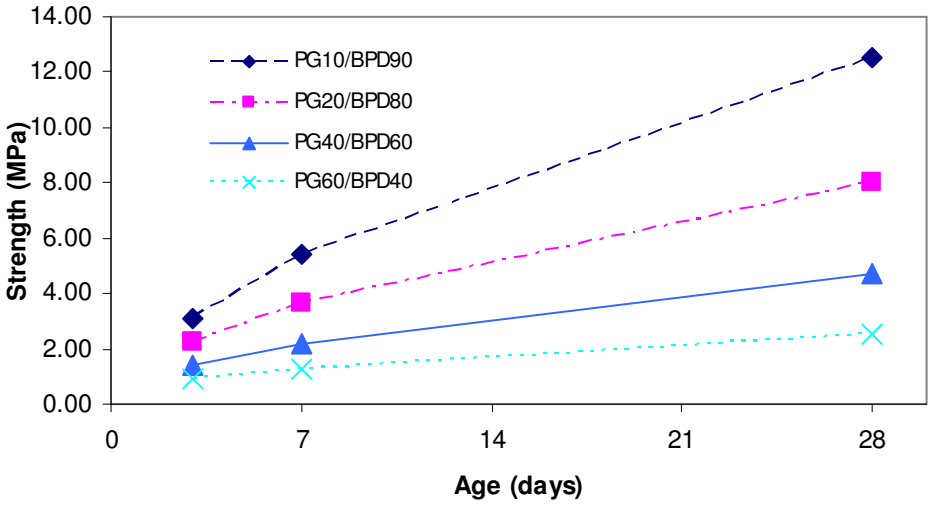

Figure 38. Compressive strength development of PG-BPD mixes.

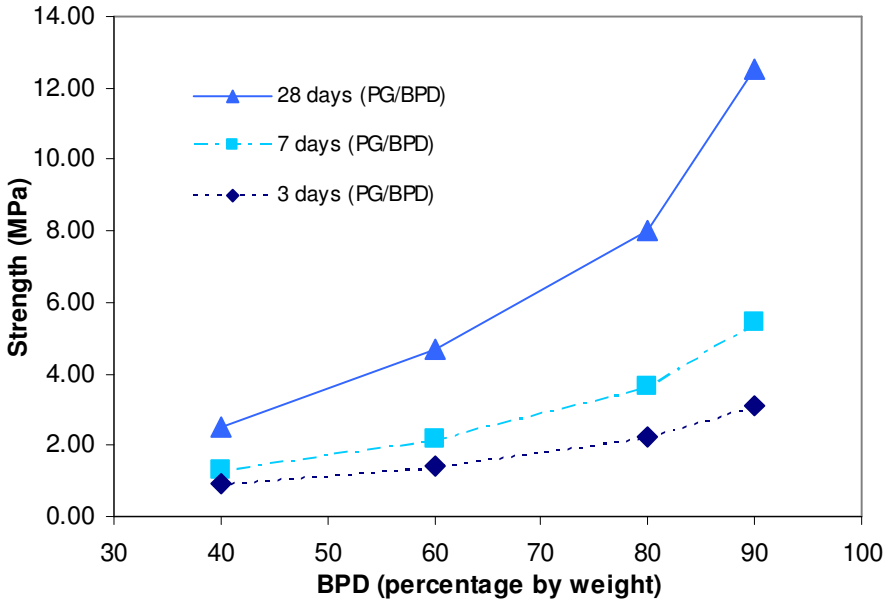

Figure 39. Compressive strength of PG-BPD mixes versus BPD content.

2.1.6.1.5. The Novel Binder

The results of further paste mixes to finalise the optimisation of the ternary system of BOS, PG and BPD are presented in Table 26. Figure 41 shows the strength development of the above mixes.

The mix incorporating 80% BOS, 15% PG and 5% BPD achieved the highest compressive strength. It shows the acceptable potential of BOS as this mix contained a high quantity of BOS. A close look at results reveals the effect of BPD in the mix incorporating 18% BPD, 2% PG and 80% BOS, which resulted in an almost similar strength. This result indicates that the activating effect of BPD and PG on BOS correlates to the ratio of PG to BPD. The mechanism and parameters affecting the hydration of slag in the ternary system are discussed in section 2.1.6.6.

It was concluded that the optimum proportions of the ternary combination of PG, BPD and BOS is 15% PG, 5% BPD and 80% BOS. This blended mixture is referred to in this report as "The Novel Binder "or 'Coventry Binder'.

Table 26. Fine tuning of mixtures of PG, BPD and BOS – compressive strength*

Mix code	Strength at days (MPa)†			Flow (mm)	Density (kg/m^3)
	3	7	28		
PG10/BPD90	3.1	5.45	12.55	103	1970
PG20/BPD80	2.25	3.65	8	105	1930
PG40/BPD60	1.42	2.2	4.69	108	1910
PG60/BPD40	0.94	1.3	2.5	108	1730

* Figure 41 is derived from this table.

† Highlighted cell indicates the highest or optimum compressive strength achieved in each group.

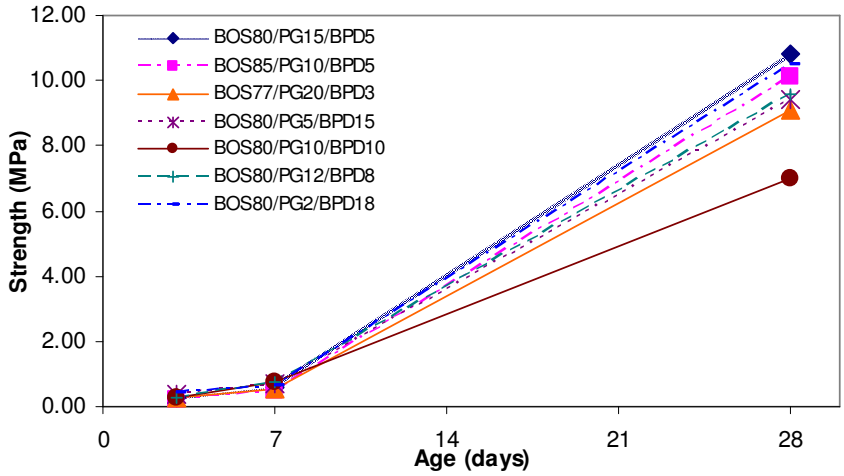

Figure 40. Fine tuning mixture of PG, BPD and BOS strength development – compressive strength.

Figure 41 summarises the results for the compressive strength of various combinations of PG, BPD and BOS against PG content. This summary shows that:

- optimisation of the ternary system depends on the alteration of components selected in each step of the optimisation process;
- optimisation is a not a linear task and various combinations of material will not result in the same compressive strength; and
- the results can be improved by slight changes in proportions of materials to include those mixes that are not necessarily considered by following the linear optimisation method.
- the drop in strength for mixes with 10% PG (i.e. the double points for 10% PG, in figure 41) corresponds to mixes with same PG content but different amount of BOS and BPD. (BOS85/PG10/BPD5 and BOS80/PG10/BPD10) as summarised in Table 26. This shows the significant effect of minor changes in the amount of pozzolan and activators on compressive strength of mixes.

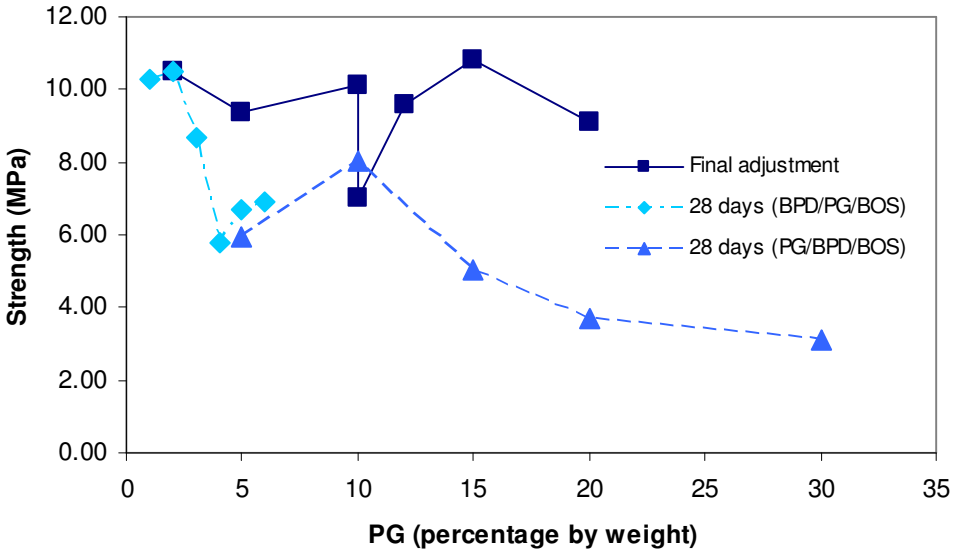

Figure 41. Compressive strength of various combinations of PG, BPD and BOS versus content.

2.1.6.1.6. Semi-Dry Mixture of PG-BPD-BOS and PG-BPD-BOS-ROSA

The effects of water content and compaction on two selected mixtures of materials were then investigated. Mixes were made using various water-to-binder ratios, and compacted using a metal tamper to achieve the maximum possible compaction. Results of compressive strength testing are presented in Table 27.

Table 27. Compressive strength of semi-dry mixtures of PG-BPD-BOS and PG-BPD-BOS-ROSA

Mix code	Strength at days (MPa)*			Flow (mm)	Density (kg/m^3)	L/S
	3	7	28			
PG15/BPD5/BOS80-0.3	0.32	1.5	11.2	175	2030	0.3
PG15/BPD5/BOS80-0.2	1.11	2.83	20.1	0	2380	0.2
PG15/BPD5/BOS80-0.15	2.1	6.5	25.9	0	2490	0.15
PG15/BPD5/BOS80-0.13	5.1	12.8	30.55	0	2540	0.13
PG15/BPD5/BOS30/ROSA50-0.3	0.36	1.1	19.1	125	1100	0.3
PG15/BPD5/BOS30/ROSA50-0.25	0.62	1.18	21.5	0	1920	0.25
PG15/BPD5/BOS30/ROSA50-0.23	0.82	2.58	24.9	0	1920	0.23
PG15/BPD5/BOS30/ROSA50-0.19	0.98	2.6	26.6	0	1830	0.19
PG15/BPD5/BOS30/ROSA50-0.15	0.87	2.49	25.9	0	1880	0.15

* Highlighted cells indicate the highest or optimum compressive strength achieved in each group.

These results highlight the dramatic improvement in compressive strength of mixes which have low water content. It is generally accepted that a reduction in the amount of water will result in less pores and improved paste pore structure. In addition, less water in the system will affect the setting time of the mixture as the hydration product can fill the gaps between unreacted materials more quickly.

The highest achieved strength in this set of mixes was 30.55 MPa (Table 27), which is almost comparable with ordinary Portland cement. Figures 42 and 43 show the strength development of the mixes at different ages.

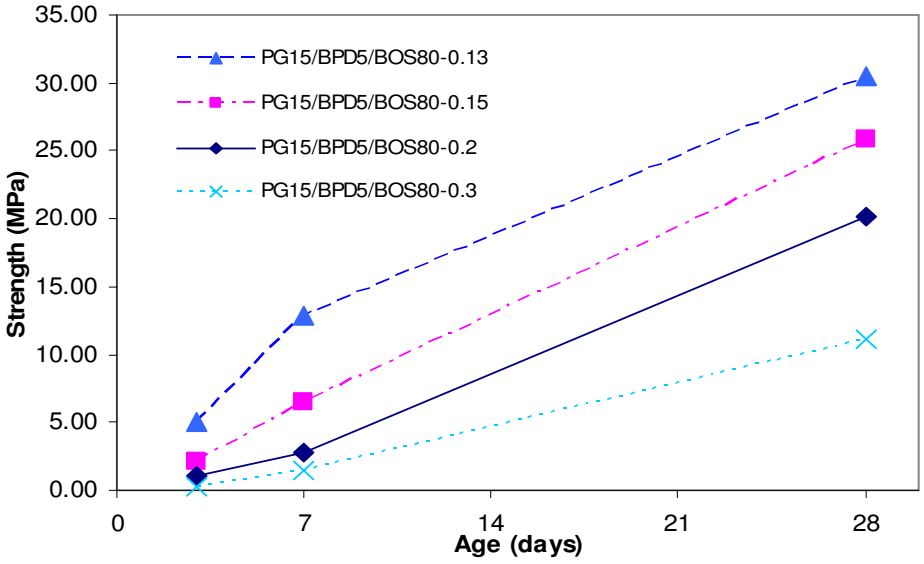

Figure 42. Compressive strength development of semi-dry PG-BPD-BOS with various L/S ratios.

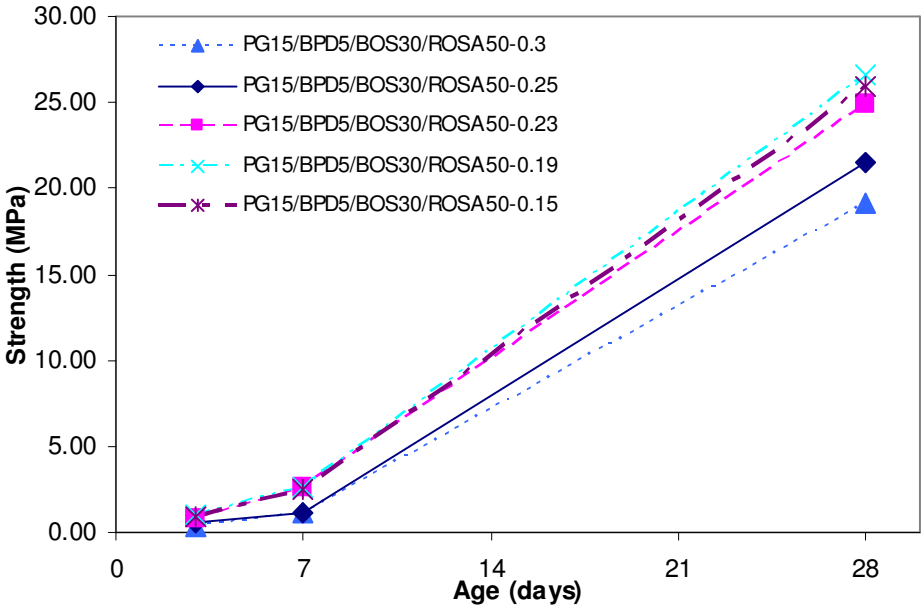

Figure 43. Compressive strength development of semi-dry PG-BPD-BOS-ROSA with various L/S ratios.

The mixture containing ROSA also showed satisfactory compressive strength (Figure 44). However, the water demand in the mix incorporating ROSA is higher than the mix without it.

The effect of water content on the compaction of semi-dry mixes together with compressive strength is shown in Figure 45.

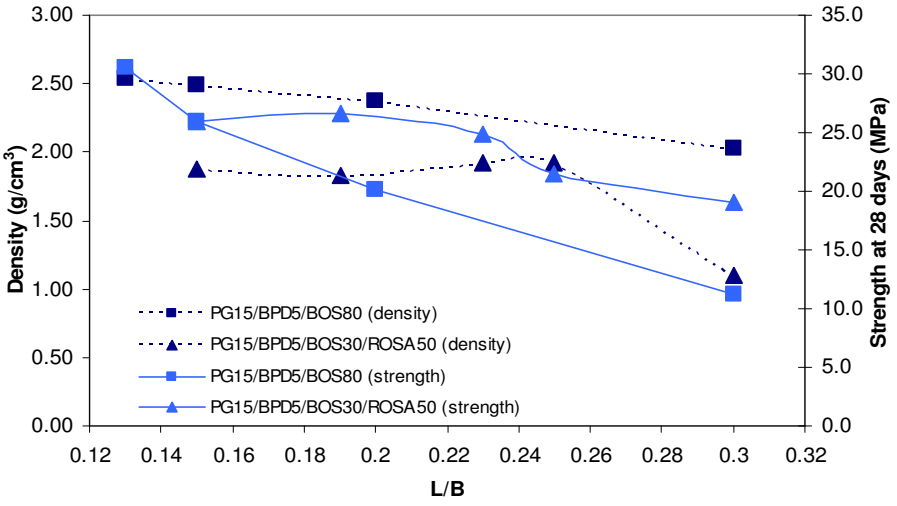

Figure 44. Effect of L/B ratios on density and compressive strength of semi-dry pastes.

The highest compressive strength was found for the mix with 15%PG, 5% BPD and 80% BOS, and a water/binder (L/B) ratio of 0.13 (Figure 44). The increase in the density of this paste mix from 2 with an L/B ratio of 0.3 to 2.6 at an L/B of 0.13 (i.e. reduced water content) is important and emphasises the direct relationship of compressive strength with the density of the mix; in other words, the higher the compaction of the mix, the higher the compressive strength.

A close look at the results of density and compressive strength of the mix employing ROSA reveals the effect of water content on the compactibility of this mixture. Reducing the L/B ratio from 0.25 to 0.15 resulted in a lower density although the compressive strength rose slightly (Figure 44). From laboratory experience, mixes containing ROSA demand more water. Therefore, compaction of such mixes at very low water to binder ratio will not give a satisfactory finished surface that can be easily disturbed after compaction.

These results suggested that a semi-dry mixture of PG-BPD-BOS would be a strong choice for the site trials. Further combinations were investigated in this reserach but these resulted in less compressive strength that this semi-dry mixture. Section 2.1.6.2 describes the results of investigations into the use of the blend PG15/BOS80/BPD5 (Coventry Binder) in roller-compacted concrete.

2.1.6.1.7. Effec tof Lime and MKD on BOS, PG and ROSA Mixtures

The effect of commercial hydrated lime and waste MKD from a lime kiln on the hydration of BOS and ROSA was investigated in binary and ternary mixtures of lime, BOS, ROSA and PG.

(a) Lime or MKD with BOS

A limited range of binary mixtures of hydrated lime or MKD with BOS were tested for compressive strength (Tables 27 and 28).

Table 27. Compressive strength of lime-BOS mixtures

Mix code	Strength at days (MPa)*			Flow (mm)	Density (kg/m3)
	3	7	28		
Lime10/BOS90	0.04	0.17	0.49	>250	2120
Lime30/BOS70	0.24	0.33	1.06	167	1936
Lime50/BOS50	0.39	0.6	1.38	124	1832
Lime70/BOS30	0.58	0.76	1.18	89	1712

* Highlighted cell indicates the highest or optimum compressive strength achieved in the group.

Table 28. Compressive strength of MKD-BOS mixtures

Mix code	Strength at days (MPa)*			Flow (mm)	Density (kg/m3)
	3	7	28		
MKD10/BOS90	0.05	0.17	0.55	>250	2000

Table 28. (continued)

Mix code	Strength at days (MPa)*			Flow (mm)	Density (kg/m3)
	3	7	28		
MKD30/BOS70	0.07	0.18	0.63	172	2080
MKD50/BOS50	0.16	0.25	0.59	132	1984
MKD70/BOS30	0.22	0.27	0.49	93	1944

* Highlighted cell indicates the highest or optimum compressive strength achieved in the group.

The optimum amount of hydrated lime in the binary mixture of BOS-lime was 50%, resulting in a strength of 1.38 MPa (Table 27). At 28 days, 0.63 MPa was the highest strength for MKD-BOS binary mixtures which corresponded to 30% MKD (Table 28). Commercial hydrated lime, which is mainly calcium hydroxide, was thus more effective at activating the BOS than MKD, which consists primarily of calcium carbonate and calcium hydroxide.

Compressive strength development of lime-BOS and MKD-BOS mixes is shown in Figures 44 and 45. Although the mix incorporating 70% hydrated lime showed the highest strength at 7 days, the mixture of 50% lime and 50% BOS achieved the optimum strength in the binary system at 28 days (Figure 44). The same trend was observed in the binary system of MKD-BOS where the mix incorporating 30% MKD and 70% BOS achieved the highest compressive strength (Figure 45). This is due to the long-term pozzolanic reaction of BOS with calcium hydroxide in MKD and hydrated lime. The higher early strength of these mixes is due to formation of calcium carbonate once the calcium hydroxide present had been exposed to atmospheric carbon dioxide.

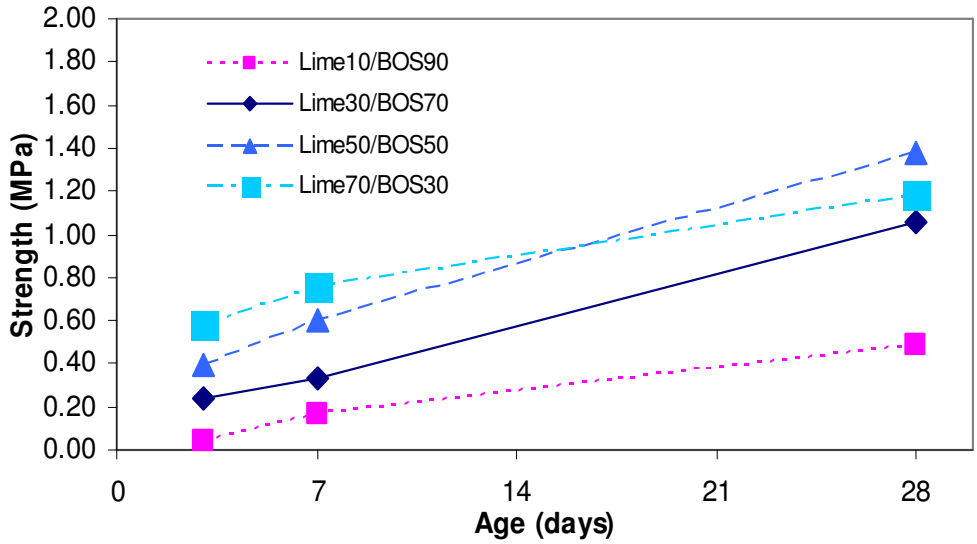

Figure 44. Compressive strength development of lime-BOS mixtures.

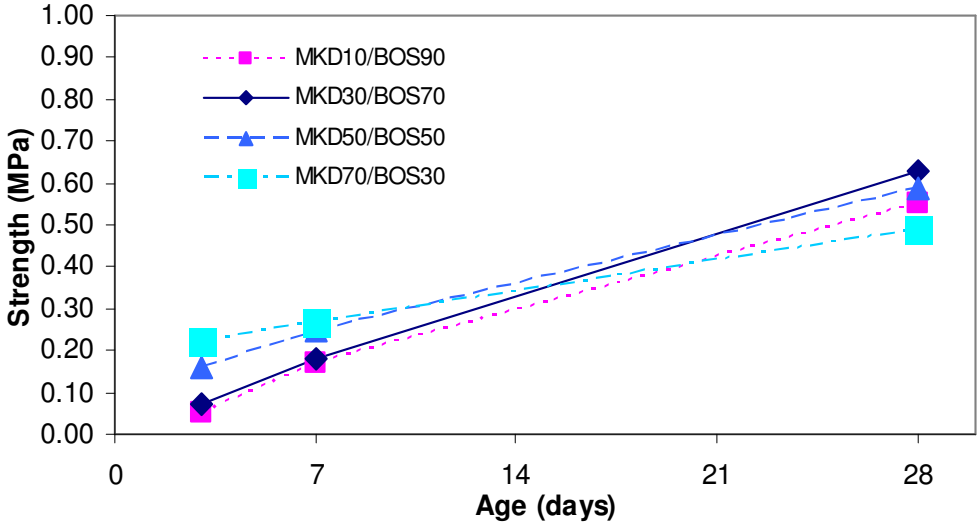

Figure 45. Compressive strength development of MKD-BOS mixtures.

Figure 46 uses data from Tables 27 and 28 to present a comparison of the binary systems BPD-BOS and the lime/MKD-BOS mixes. BPD was more efficient at reacting with BOS to form a cementitious gel. This is partly because of the cementitious properties of BPD itself (phases such as C_3S and C_2S present in the BPD are mainly responsible for this phenomenon).

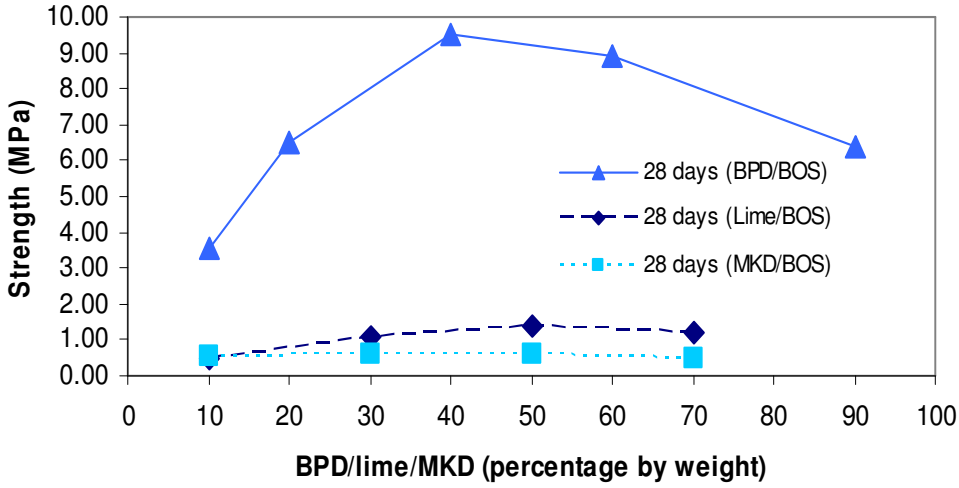

Figure 46. Comparison of the compressive strength of lime/MKD/BPD-BOS mixtures versus lime/MKD/BPD content.

(b) Lime or MKD with ROSA

Tables 29 and 30 present the compressive strength of mixtures incorporating ROSA. The optimum amount of hydrated lime in lime-ROSA and MKD-ROSA mixtures was 50%, corresponding to the strength of 3.23 and 2.84 MPa respectively. Hydrated lime was more efficient in activating ROSA, although the compressive strength in both mixes was almost similar.

Table 29. Compressive strength of lime-ROSA mixtures

Mix code	Strength at days (MPa)*			Flow (mm)	Density (kg/m3)
	3	7	28		
Lime10/ROSA90	0.21	0.49	1.12	130	1552
Lime30/ROSA70	0.31	0.5	2.68	114	1576
Lime50/ROSA50	0.24	0.45	3.23	95	1592
Lime70/ROSA30	0.48	0.71	2.21	87	1598

* Highlighted cell indicates the highest or optimum compressive strength achieved in the group.

Table 30. Compressive strength of MKD-ROSA mixtures

Mix code	Strength at days (MPa)*			Flow (mm)	Density (kg/m3)
	3	7	28		
MKD10/ROSA90	0.26	0.46	0.9	142	1512
MKD30/ROSA70	0.21	0.41	1.58	124	1592
MKD50/ROSA50	0.16	0.32	2.84	98	1616
MKD70/ROSA30	0.09	0.21	2.7	94	1620

* Highlighted cell indicates the highest or optimum compressive strength achieved in the group.

Figures 47 and 48 show the strength development of lime-ROSA and MKD-ROSA mixes respectively. In the mix incorporating 90% ROSA and 10% lime, the amount of activator was insufficient to release the pozzolanic potential of ROSA. In contrast, in the mix employing 50% lime, the rate of strength gain increased at 7 days and it showed the highest strength in this binary system (Figure 47).

In MKD-ROSA mixtures, the strength of the mixes incorporating 50% and 70% MKD showed almost similar compressive strength (Figure 47). This phenomenon could be because, within an optimum range, the presence of more calcium hydroxide leads to more activation of pozzolanic materials.

Figure 49 used data from Tables 34 and 35 to present a comparison of binary mixtures of BPD-ROSA with the lime/MKD-ROSA mixtures. The mixture incorporating BPD achieved much a higher compressive strength compared with those made with hydrated lime and MKD. This result is similar to those achieved with binary combinations of BPD-BOS. As mentioned previously, this could be due to cementitious compounds present in BPD resulting in formation of more cementitious matrix within 28 days.

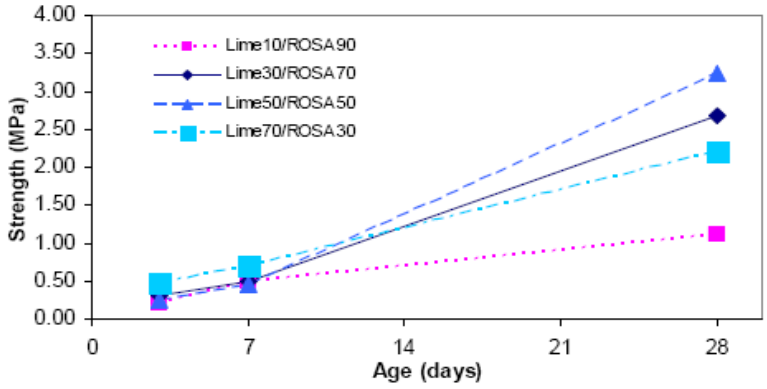

Figure 47. Compressive strength development of lime-ROSA mixtures.

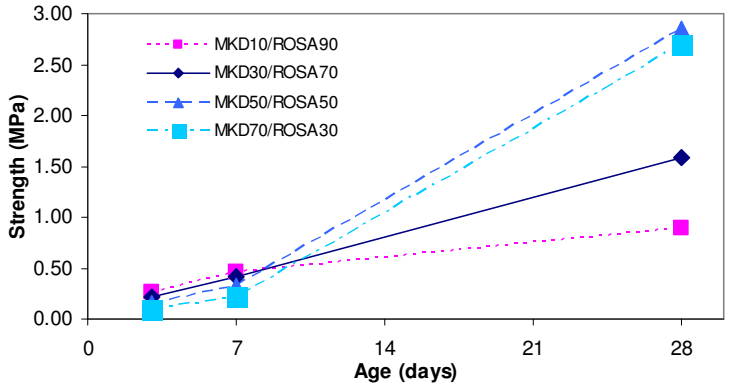

Figure 48. Compressive strength development of MKD-ROSA mixtures.

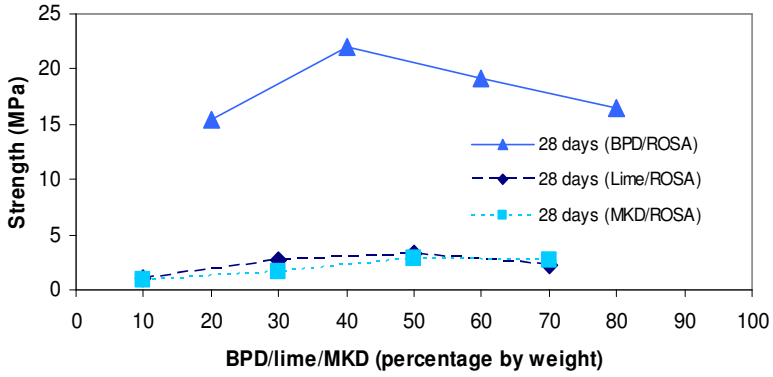

Figure 49. Comparison of the compressive strength of lime/MKD/BPD-ROSA mixtures versus lime/MKD/BPD content.

(c) Lime and MKD to Replace BPD

In order to compare the effect of hydrated and MKD waste lime in mixtures containing PG using the optimum proportions of PG-BOS-BPD and PG-BOS-ROSA-BPD obtained previously, the BPD content was replaced by commercial hydrated lime and MKD. In addition, two ternary mixes incorporating ROSA, PG and lime/MKD were made to investigate the effect of lime on the activation of ROSA in presence of PG. Table 31 presents the results of compressive strength testing of these mixes.

Table 31. Compressive strength of PG-BOS-ROSA mixture

Mix code	Strength at days (MPa)*			Flow (mm)	Density (kg/m^3)
	3	7	28		
BOS80/PG15/Lime5	0.18	0.52	1.7	114	2168
BOS80/PG15/MKD5	0.12	0.31	1.02	152	1976
BOS30/ROSA50/PG15/Lime5	0.64	2.54	10.56	108	1888
BOS30/ROSA50/PG15/MKD5	0.16	0.22	0.79	118	1832
ROSA75/PG15/MKD10	0.42	0.97	9.51	110	1632
ROSA65/PG15/MKD20	0.68	1.05	12.3	94	1752

* Highlighted cell indicates the highest or optimum compressive strength achieved in the group.

The replacement of BPD with hydrated lime or MKD resulted in very low strength (1.7 MPa) compared with when BPD was used (10.8 MPa) (Table 24). In addition, the mix containing MKD showed less strength than the mix containing hydrated lime. A similar trend was observed in mixes made with ROSA when BPD was replaced by lime or MKD (Figure 50).

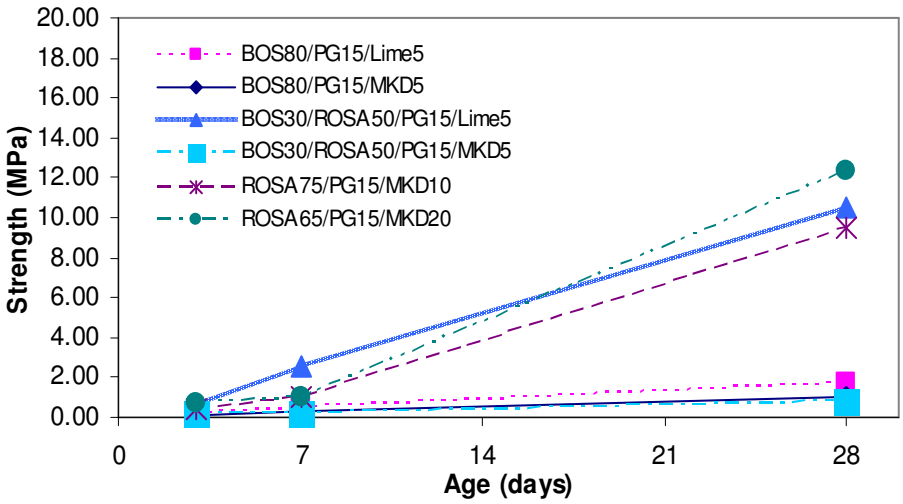

Figure 50. Compressive strength development of MKD/lime, BOS, ROSA and PG mixtures.

However, the ternary mixture of ROSA-PG-MKD showed that, with the same amount of PG, replacing BOS and lime with ROSA and MKD results in similar compressive strength. In other words, the efficiency of 30% BOS and 5% lime is about the same as 25% ROSA and 5% MKD. This implies that more calcium hydroxide is needed to activate the same amount of BOS compared with ROSA in order to achieve the same compressive strength.

Figures 51 and 52 show the comparison of the replacement of BPD with hydrated lime and MKD in the BOS-PG-BPD and BOS-ROSA-PG-BPD mixtures respectively. Replacement of BPD with hydrated lime or MKD in the ternary system BOS-PG-BPD resulted in less compressive strength (Figure 51). The comparison also revealed that the lime and BKD do not have a similar efficiency in terms of activation of BOS; lime is less efficient than BKD resulting in a lower compressive strength.

The efficiency of hydrated lime in the BOS-ROSA-PG mixture was higher than MKD, but they both suffer from a lack of efficiency compared with BPD. The compressive strength fell by about 50% when BPD was replaced with hydrated lime (Figure 52). The mix incorporating MKD as a replacement for BPD showed the lowest compressive strength of 0.79 MPa after 28 days (Table 36).

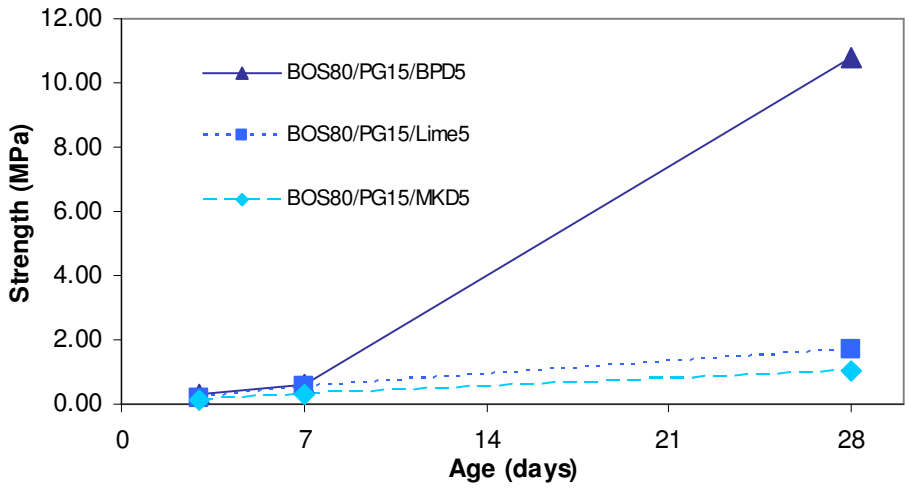

Figure 51. Comparison of the replacement of BPD with lime and MKD in BOS-PG-BPD mixtures.

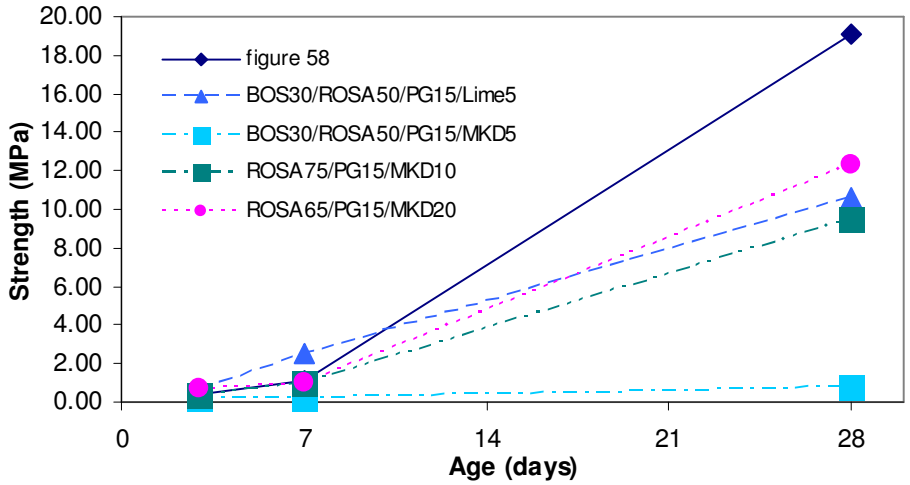

Figure 52. Comparison of the replacement of BPD with lime and MKD in BOS-ROSA-PG-BPD mixtures.

2.1.6.1.8. Long-Term Compressive Strength of BOS, PG, BPD And ROSA Mixtures

Table 32 presents the results of compressive strength of paste mixtures containing PG, BOS, ROSA and BPD up to 90 days. The strength results of this group of paste mixtures up to 28 days are discussed in section 2.1.6.1.5. In some mixtures, the compressive strength increased by up to 60% after 90 days moist curing. This demonstrates the intrinsic potential of BOS and ROSA to form a hydrated cementitious matrix in presence of sufficient alkali.

Table 32. Long-term compressive strength of PG, BOS, ROSA and BPD paste mixtures

Mix code	L/S	Strength at days (MPa)				Flow (mm)	Density (kg/m^3)
		3	7	28	90		
BOS80/PG15/BPD5	0.3	0.28	0.59	10.8	16.52	162	2540
BOS85/PG10/BPD5	0.3	0.21	0.46	10.1	15.7	162	2550
BOS77/PG20/BPD3	0.3	0.26	0.54	9.1	13.64	158	2370
BOS80/PG5/BPD15	0.3	0.35	0.68	9.4	16.1	140	2630
BOS80/PG10/BPD10	0.3	0.29	0.78	7	12.2	148	2570
BOS80/PG12/BPD8	0.3	0.28	0.76	9.6	11.8	154	2580
BOS80/PG2/BPD18	0.3	0.41	0.65	10.5	16.1	124	2700
BOS80/PG15/BPD5(semi-dry)	0.13	5.1	12.8	30.55	38.35	Semi -dry	2540
BOS30/ROSA50/PG15 /BPD5(semi-dry)	0.19	0.98	2.6	26.6	42.1	Semi -dry	1830

As shown in Figure 53, the compressive strength of the paste mixes developed rapidly up to 28 days and then at a slower pace up to 90 days. In paste mixtures with a L/S ratio of 0.3, the highest strength was obtained with the mix incorporating 80% BOS, 15% PG and 5% BPD at both 28 and 90 days. But for semi-dry mixes, the mix incorporating ROSA showed a higher strength gain after 90 days. This result revealed the superior performance of combining ROSA and BOS, which is caused by faster reaction of ROSA to form pozzolanic calcium silicate hydrate (CSH) gel. It can also be postulated that the mix made without ROSA could reach the same level of strength after a longer period of curing. The rate of strength gain in all PG-BOS-BPD mixtures was almost similar (55% from 28 days to 90 days age).

To evaluate the effect of longer periods of curing on the compressive strength of paste mixtures, a group of PG-CKD-BOS mixtures was tested at a curing age of 360 days under the standard curing conditions (Table 33).

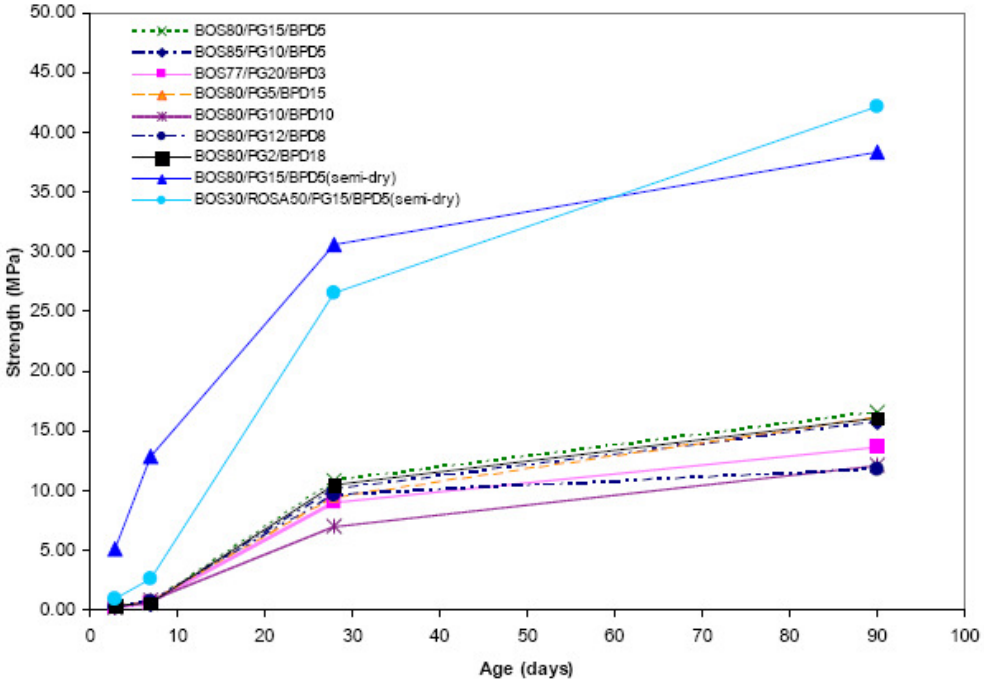

Figure 53 Long-term compressive strength development of PG, BOS, ROSA and BPD mixtures.

Table 33. Long-term compressive strength of PG-CKD-BOS mixtures

Mix code	L/S	Strength at days (MPa)				Flow (mm)	Density (kg/m^3)
		3	7	28	360		
PG15/CKD5/BOS80-0.2	0.2	0.43	1.5	7.68	31.4	78	1970

Table 33. (Continued)

Mix code	L/S	Strength at days (MPa)				Flow (mm)	Density (kg/m^3)
		3	7	28	360		
PG15/CKD5/BOS80-0.25	0.25	0.37	1.1	5.65	30.27	145	2060
PG15/CKD5/BOS80-0.3	0.3	0.22	0.87	4.15	23.07	191	1890
PG15/CKD5/BOS80-0.4	0.4	0.15	0.39	2.49	12.15	High	1790

There was a four- to five-fold increase in the strength of paste mixtures at 360 days compared with the 28-day test results. This reveals the considerable potential of BOS to form a strong cementitious matrix as well as the slow reacting nature of this pozzolanic material even in presence of activators such as gypsum and alkalis.

The effect of L/S ratio on long-term compressive strength of PG-CKD-BOS mixes is shown in Figure 54. The rate of strength gain increased when the L/S ratio decreased from 0.4 to 0.2; in other words, the lower the water content in the mix, the higher pace of strength gain in the paste mixtures. This could be due to less voids forming in the cementitious structure of the samples available to be filled by the increasing amount of pozzolanic product in the longer period of curing. The highest strength in this group of mixes was for the mix made with a L/S ratio of 0.2.

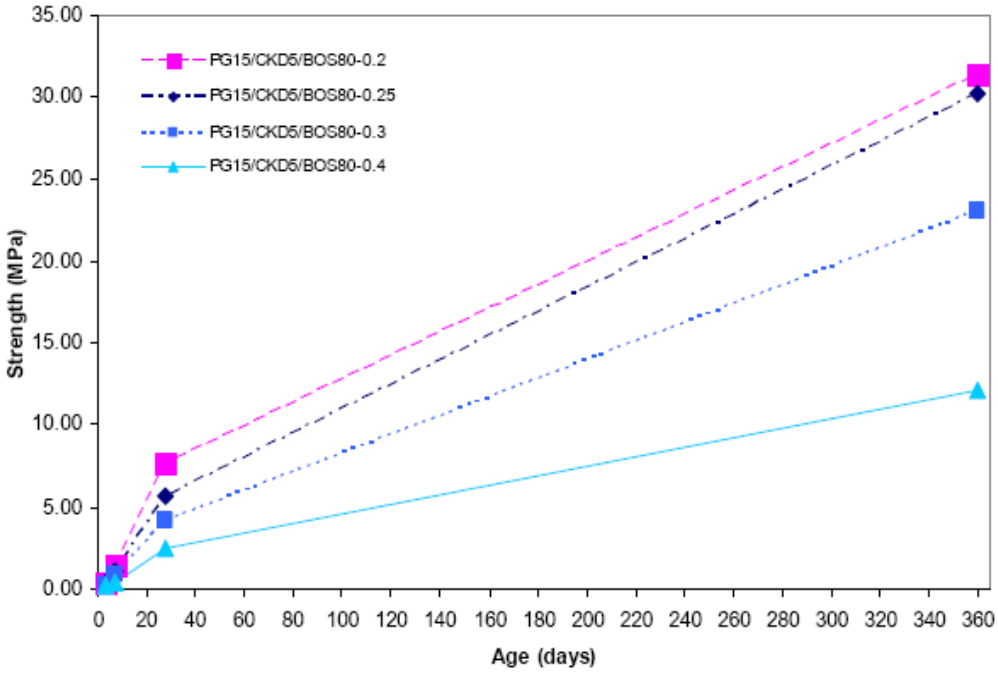

Figure 54. Long-term compressive strength development of PG-CKD-BOS paste mixtures (50 mm cubes).

2.1.6.2. Concrete Mixes

Concrete mixes were developed according to the optimised proportions obtained from paste mixtures described above. The effect of workability was investigated by employing two different types of superplasticisers.

As shown with the semi-dry paste mixtures, water content plays a major role in the strength of pastes and concretes. It was therefore proposed to use the minimum amount of water in the concrete mixes. The low proportion of water resulted in concrete with a very low or even zero slump.

The compressive strength of concrete is linked directly with the level of compaction. Therefore, concrete with zero slump should be compacted in different ways from conventional methods in which a vibrating table is used. These types of concretes are known as roller-compacted concrete (RCC) and usually contain low proportions of cement.

Due to the use of slow-reacting cementitious novel binder materials in this project, the 'binder content' was kept at a normal amount of 380 kg/m^3. Compaction for 150-mm cube moulds was carried out using a hammer drill and attached plate. The results of compressive strength testing of the various concrete mixes are presented in Table 34 (all results have been converted to the strength for 150-mm standard cubes).

Figure 55 shows the strength development of concrete mixes made using proportions obtained from candidate paste mixes incorporating PG, BPD and BOS. Using recycled aggregate (RA) resulted in considerably less compressive strength compared with those mixes made with natural aggregates and the same water content.

This suggests that the weakest link in the concrete that developed was the interface between the cementitious matrix and the aggregate. As the binder was made of slow-reacting pozzolanic materials (mainly BOS), the bond between the aggregate and the paste was not strong enough to resist the tension.

The amount and type of aggregate plays a major role in the ultimate compressive strength of a concrete mix. The recycled aggregate used contained some asphalt and fine clay or silt, which had a detrimental affect on the matrix aggregate interface, thereby reducing the ultimate strength of the concrete. To cope with the problem of concrete with low strength, increasing the workability of mixes using superplasticiser (SP) was considered.

Using superplasticiser to increase the flow of the concrete had a beneficial effect on compressive strength (Tables 34 and 35).

Two types of superplasticiser – sulphonate base and polymer base – were used in this study. The sulphonate chains of conventional superplasticisers carry a high anionic charge and are immediately adsorbed onto the surface of the cement particles, rendering them negatively charged. However, the adsorbed sulphonate chains are overlapped rapidly by crystals developed during the hydration of the cement; the consequence is early loss of the superplasticising action. In contrast, the new generation polymer superplasticisers have anionic carboxylic groups and long polyethylene chains. After the addition of the superplasticiser to concrete, its anionic main chain is adsorbed onto the positively charged surface of the cement particles whereas the side chains induce a steric repulsion effect between the cement particles. This repulsive force means that maximum dispersibility is attained and agglomeration can be avoided.

In this research the polymer superplasticiser (PSP) was found to be more efficient than ordinary superplasticiser (SP) in increasing the flow of the mix, but appeared to have a negative effect on the compressive strength of the concrete (Figures 53 and 54). This might be

due to the retarding effect of this type of superplasticiser on the blended binder. Moreover, it would impose an extra cost when using this type of concrete made with waste materials.

Table 34. Compressive strength of PG/BPD/BOS concrete mixes developed

Mix code	Strength at days (MPa)*			Slump (mm)	Density (kg/m^3)	L/B
	3	7	28			
PG15/BPD5/BOS80 (SP)	1.19	1.67	7.65	10	2380	0.4
PG15/BPD34/BOS51	1.45	1.99	7.29	10	2300	0.4
PG15/BPD5/BOS80 (PSP)	0.76	1.08	6.6	180	2400	0.4
PG15/BPD5/BOS80 (RA-PSP)	1.02	1.89	5.67	20	2310	0.4
PG15/BPD5/BOS80 (PPG-PSP)	0.29	0.8	3.06	160	2400	0.4
PG15/BPD5/BOS80 (RA-PPG-PSP)	0.01	0.52	1.83	40	2270	0.4
PG15/BPD5/BOS80 (RA-RCC)	0.96	2.02	10.8	0	2390	0.25

* Highlighted cell indicates the highest or optimum compressive strength achieved in the group.
SP = superplasticiser
PSP = polymer superplasticiser
RA = recycled aggregate
PPG = processed plasterboard gypsum
RCC = roller-compacted concrete

Table 35. Compressive strength of PG/BPD/BOS/ROSA concrete mixes developed

Mix code	Strength at days (MPa)*			Slump (mm)	Density (kg/m3)	L/B
	3	7	28			
PG15/BPD5/BOS60/ROSA20	0.61	1.03	5.49	0	2310	0.4
PG10/BPD5/BOS32/ROSA53 (SP)	0.79	1.62	10.98	120	2440	0.4
PG15/BPD5/BOS30/ROSA50 (RA-PSP)	0.58	1.28	9.27	30	2250	0.4
PG15/BPD5/BOS30/ROSA50 (RA-RCC)	1.23	2.2	12.3	0	2310	0.3

* Highlighted cell indicates the highest or optimum compressive strength achieved in the group.
SP = superplasticiser
PSP = polymer superplasticiser
RA = recycled aggregate
RCC = roller-compacted concrete

Use of roller-compacted concrete with a minimum amount of water was therefore proposed. Mixes with RCC gave the highest compressive strength; although the compressive strength at early ages was not high, an acceptable compressive strength was achieved in the long run. This mix was chosen for the site trial to be used as sub-base layer in the car park area (see section 3).

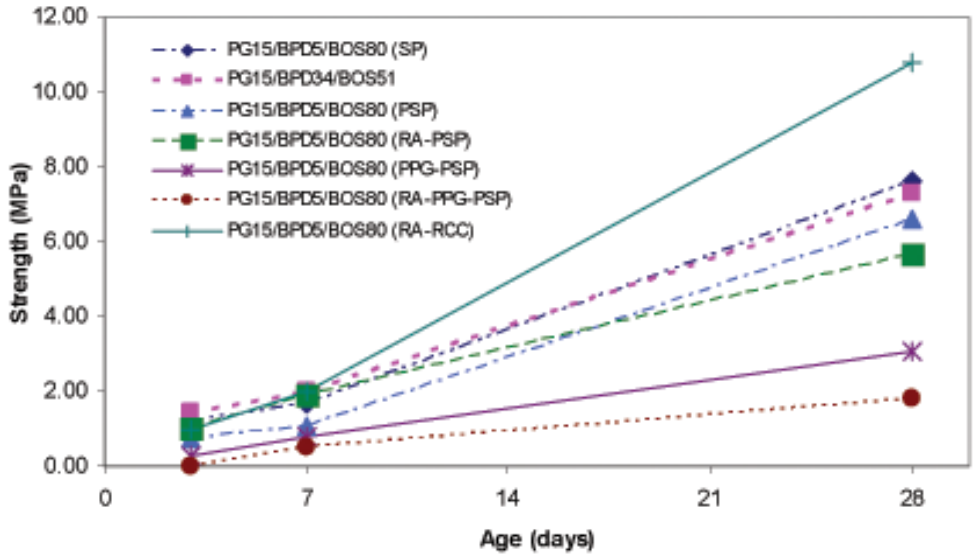

Figure 55. Compressive strength development of concrete mixes of PG-BPD-BOS.

Figure 56 shows the results obtained for concrete mixes made with binder incorporating ROSA. The compressive strength development of concrete using plasterboard gypsum, BOS, ROSA and BPD shows clearly the slow-reacting nature of this type of binder. However, the ultimate compressive strength of the mix was acceptable and it was considered as an option for the site trial. But as described in section 3.1.6, the highest compressive strength of semi-dry paste was for the mixture of 15% PG, 5% BPD and 80% BOS (Table 27)

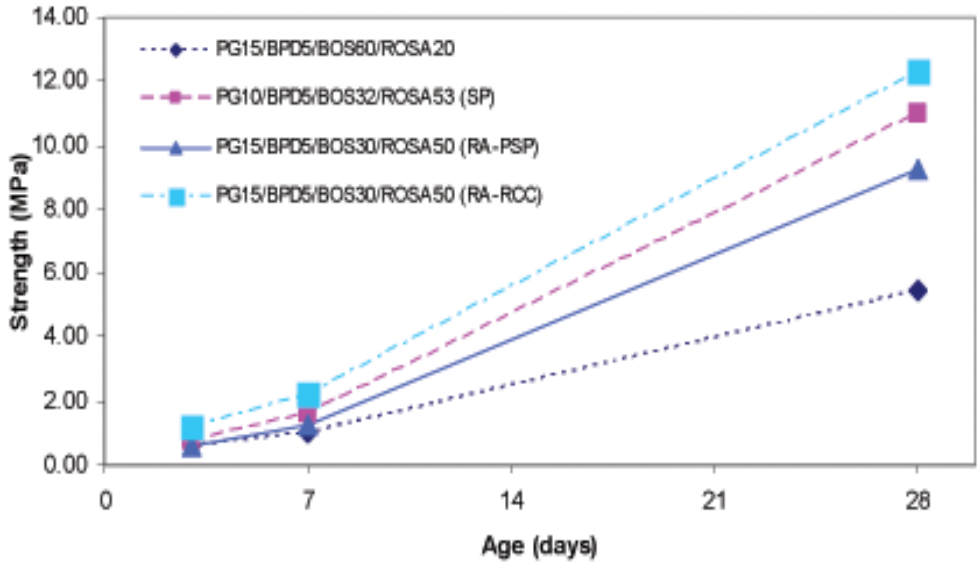

Figure 56. Compressive strength development of concrete mixes of PG-BPD-BOS-ROSA.

In addition, limitations in materials preparation meant that the mixture with fewer different materials was preferred. This mixture is referred to as the Coventry Binder.

2.1.6.3. Soil Stabilisation

The recommendations of the Transport Research Laboratory (TRL) Road Note 31 [18] for strength requirements of cement and lime stabilised sub-base and base materials are summarised in Table 36. The seven-day strength of stabilised soil using 50% by weight of the Coventry Binder is within the recommended range of strength for a sub-base layer. Furthermore, the seven-day strength of stabilised soil using 60% by weight of Binder-B is within the recommended range of strength for sub-base and base layers.

Table 36. Recommended strength of cement and lime stabilised sub-base and base materials [18]

Type	Soil unconfined compressive cube strength at 7 days (MPa)
Stabilised base (CB 1)	3.0–6.0
Stabilised base (CB 2)	1.5–3.0
Stabilised sub-base	0.75–1.5

Tables 37 and 38 present the compressive strength results of two different soils (Soil-A and Soil-B) stabilised with two types of novel binders (Binder-A and Binder-B).

Soil-A is sandy clay and Soil-B is silty sand (see section 2.1.4.2). Binder-A is mix PG15/BPD5/BOS80 (The Novel Binder or Coventry Binder) and Binder-B is mix PG15/BPD5/BOS50/ROSA30.

Table 37. Compressive strength of stabilised Soil-A with various amounts of Coventry Binder and Binder-B

Mix code	Strength at days (MPa)*		Dry density (kg/m3)
	7	28	
Unstabilised Soil-A	0.19	0.11	1820
Soil-A 80/Binder-A 20	0.67	1.56	1900
Soil-A 60/Binder-A 40	0.82	1.86	1940
Soil-A 50/Binder-A 50	1.14	3.75	1970
Soil-A 40/Binder-A 60	1.22	4.45	2010
Soil-A 40/Binder-B 60	2.16	10.80	1890

* Highlighted cell indicates the highest or optimum compressive strength achieved in the group.

Table 38. Compressive strength of stabilised Soil-B using various amounts of Coventry Binder*

Mix code	Strength at days (MPa)*		Dry density (kg/m3)
	7	28	
Unstabilised Soil-B	0.21	0.13	1800
Soil-B 80/Binder-A 20	1.07	2.80	1900

Mix code	Strength at days (MPa)*		Dry density (kg/m3)
	7	28	
Soil-B 60/Binder-A 40	1.21	3.40	1950
Soil-B 50/Binder-A 50	1.43	5.98	1990

* Highlighted cell indicates the highest or optimum compressive strength achieved in the group.

Figures 57 and 58 show the strength development of the two stabilised soils at 7 and 28 days. The stabilised soil with 60% of binder incorporating ROSA (Binder-B) showed the highest strength (Figure 57), revealing the potential of ROSA for use in soil stabilisation. The mix with 50% by weight of Binder-A performed satisfactorily according to TRL recommendations. Comparison with the compressive strength of stabilised soil with no binder reveals the beneficial effect of the novel blended binders in stabilising these two types of soil.

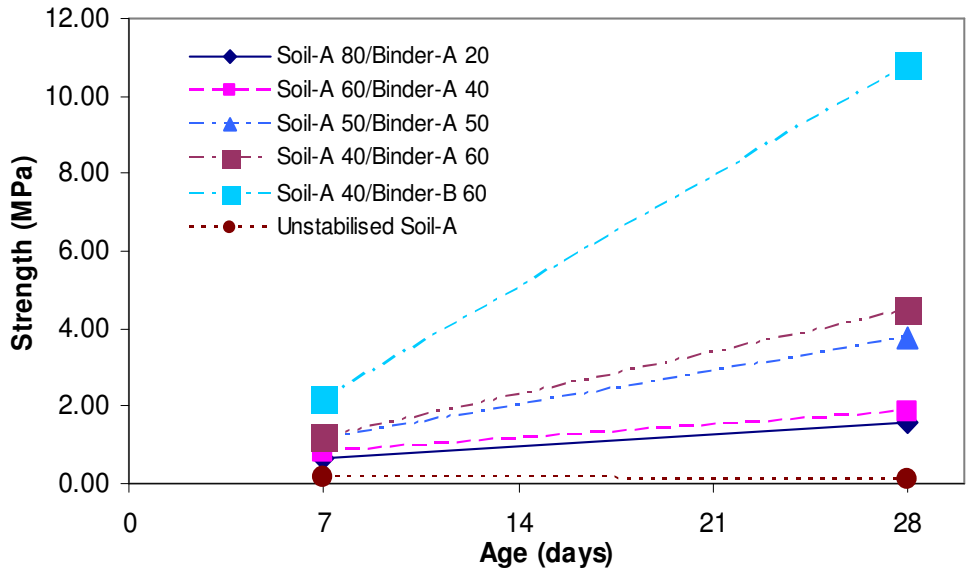

Figure 57. Compressive strength development of Stabilised Soil-A blended with Binder-A and Binder-B.

Binder-A (Coventry Binder) performed relatively better with Soil-B (Figure 57) than with Soil-A (Figure 58). Soil-A was taken from one of the trial sites (see section 3.3) long before the trial was due to begin out. But this soil was not available later and another source of soil (Soil-B) was provided from the same site for the site trial tests.

The effect of binder content is shown in Figures 59–61. Increasing the amount of binder mixed with the soil resulted in a higher compressive strength. The pattern was found to be similar for both soils. It can be postulated that the relationship between compressive strength and binder content is linear (Figures 59 and 60), although more investigation is needed to establish the precise relationship.

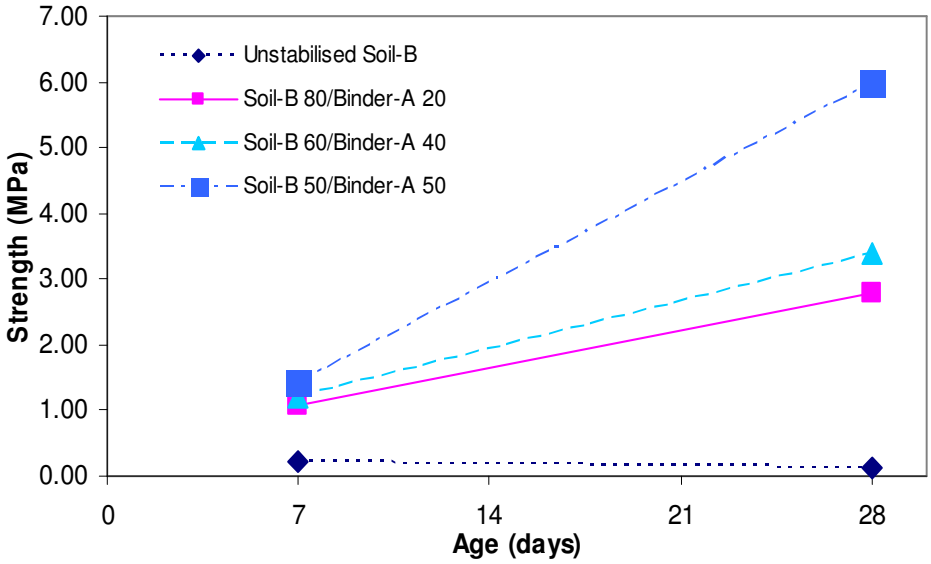

Figure 58. Compressive strength development of Stabilised Soil-B blended with Binder-A.

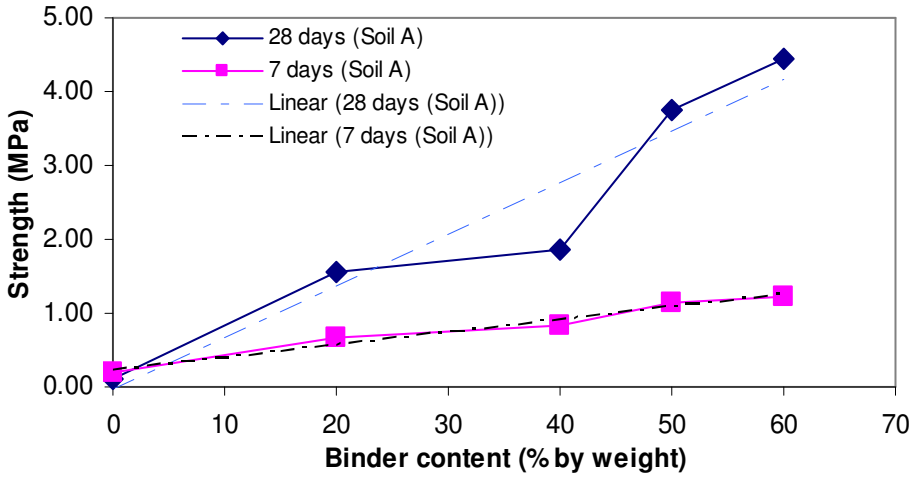

Figure 59. Compressive strength of Stabilised Soil-A versus binder content.

2.1.6.4. Hydrogen Sulphide Release

Under the anaerobic conditions in landfills, the gypsum in plasterboard can react with biodegradable waste (such as the paper backing of the plasterboard itself) to produce toxic hydrogen sulphide gas. By binding the sulphate content of the plasterboard into a low permeability matrix, the reaction with the paper leading to the release of hydrogen sulphide will not proceed.

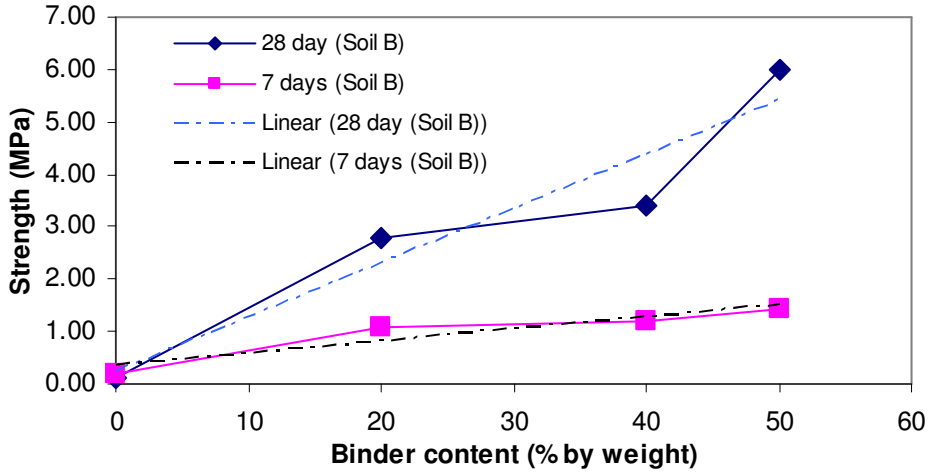

Figure 60. Compressive strength of Stabilised Soil-B versus binder content.

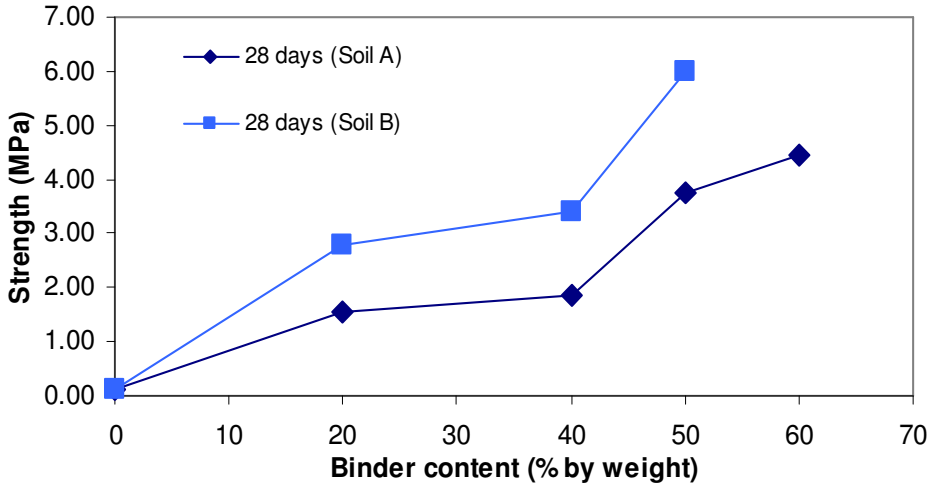

Figure 61. Comparison of compressive strength of Soil-A and Soil-B with blended mixture of PG-BPD-BOS (Binder-A).

During the life of a road, the surface layer and drainage systems will keep the foundation dry but end-of-life conditions also need to be considered. The ability to use plasterboard without paper removal is a key aspect of this work.

In order to confirm that hydrogen sulphide (H_2S) was not emitted from the developed blended powder, paste samples were prepared using the original blended powder with 10 and 20% (by weight) extra paper added to the mix. Specimens were kept in airtight plastic bottles to trap any hydrogen sulphide released (Figure 62). Samples were stored at 20° C in a similar manner to other paste specimens.

Figure 62. Plastic bottles containing paste specimens for H2S check.

The bottles were removed from the curing propagator after 28 days. The following methods were used to determine any H_2S released.

2.1.6.4.1. *Infrared spectrometry*

In this method, gas was extracted from the bottle using a gas-tight syringe and injected into a pre-vacuumed infrared (IR) gas cell. The spectrum obtained was then analysed according the standard pattern for hydrogen sulphide (Figure 63).

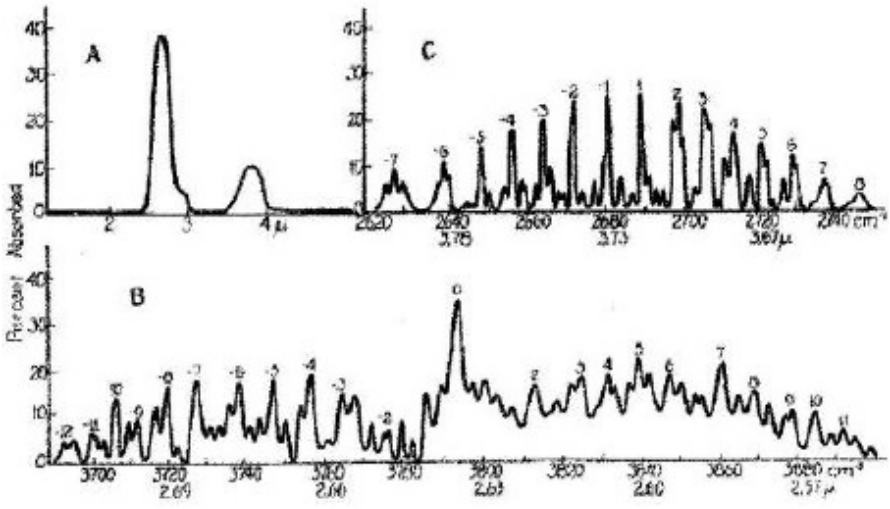

Figure 63. Different parts (A, B and C) of the infrared spectrum for H2S [19].

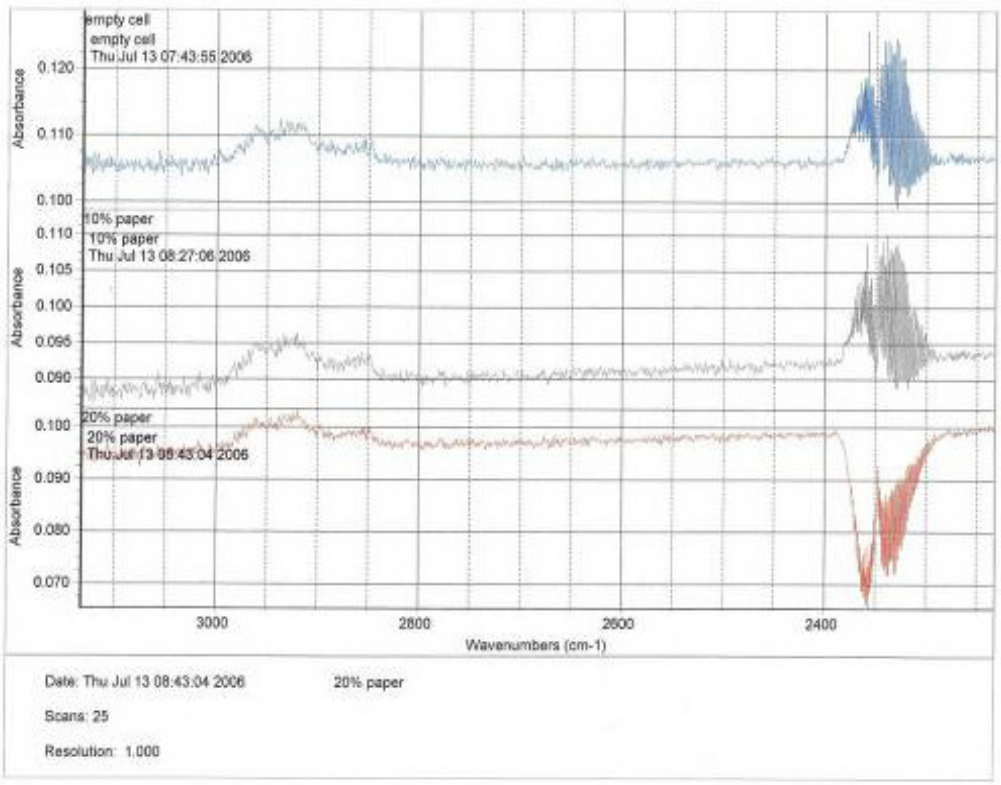

Figure 64. IR spectra of gas extracted from paste samples with 10 and 20% paper.

Figure 64 shows the IR spectra of the gas extracted from specimens containing 10 and 20% paper. No distinctive difference can be seen between the spectrum obtained with an empty cell and the one containing extracted gas.

The accuracy of this method depends on the level of vacuum of the empty cell and the method of injecting gas into the cell. It appeared that, although high pressure vacuum was applied to empty any gas from the IR cell, it still contained some gases such as carbon dioxide (CO_2) or carbon monoxide (CO).

In order to validate more effectively, pure hydrogen sulphide gas was injected into the IR cell. Figure 65 shows a magnified part of the spectrum for pure H_2S. The magnified parts of the spectra for the samples with 10 and 20% paper shown in Figures 66 and 67 were compared with the spectrum for pure H_2S, but no similarity was found between the pattern of gas injected and pure hydrogen sulphide. The initial conclusion from this investigation was that no hydrogen sulphide was released from the paste specimens.

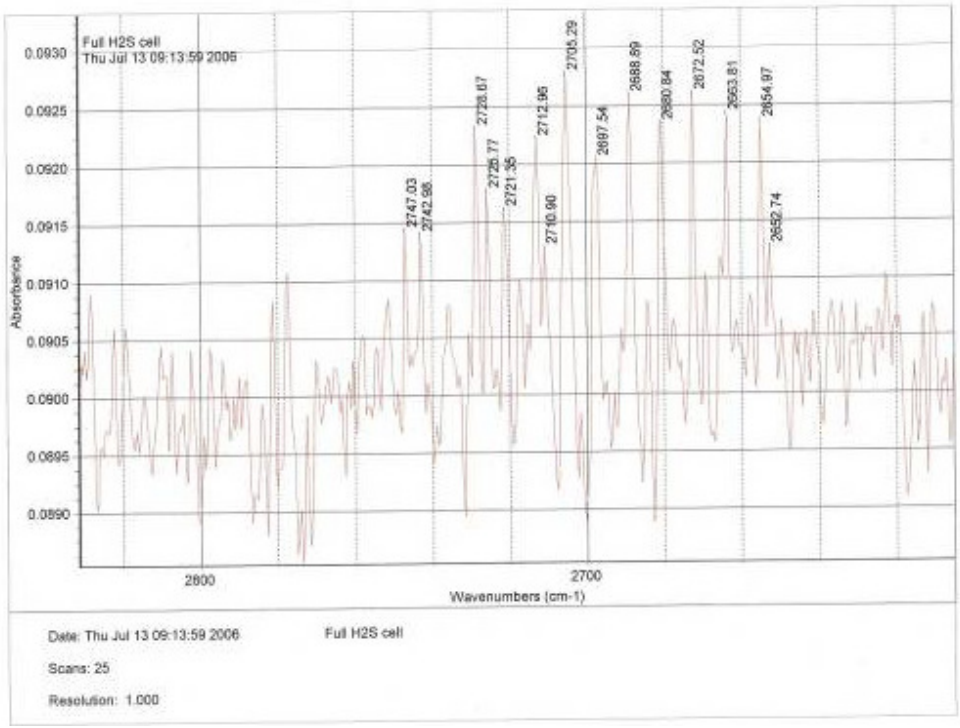

Figure 65. Magnified IR spectrum of pure hydrogen sulphide (wavelength 2600–2800 cm-1).

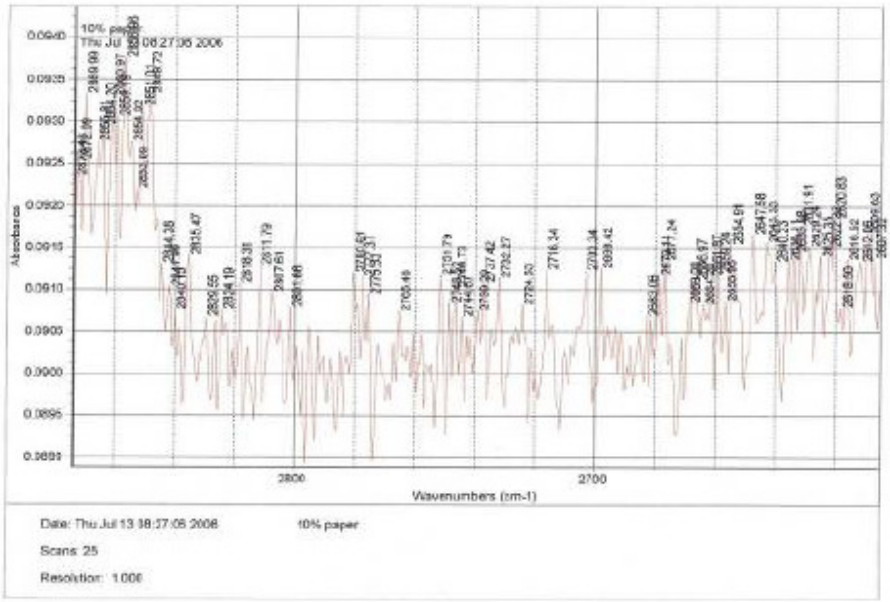

Figure 66. Magnified IR spectrum of sample with 10% paper (wavelength 2600–2800 cm-1).

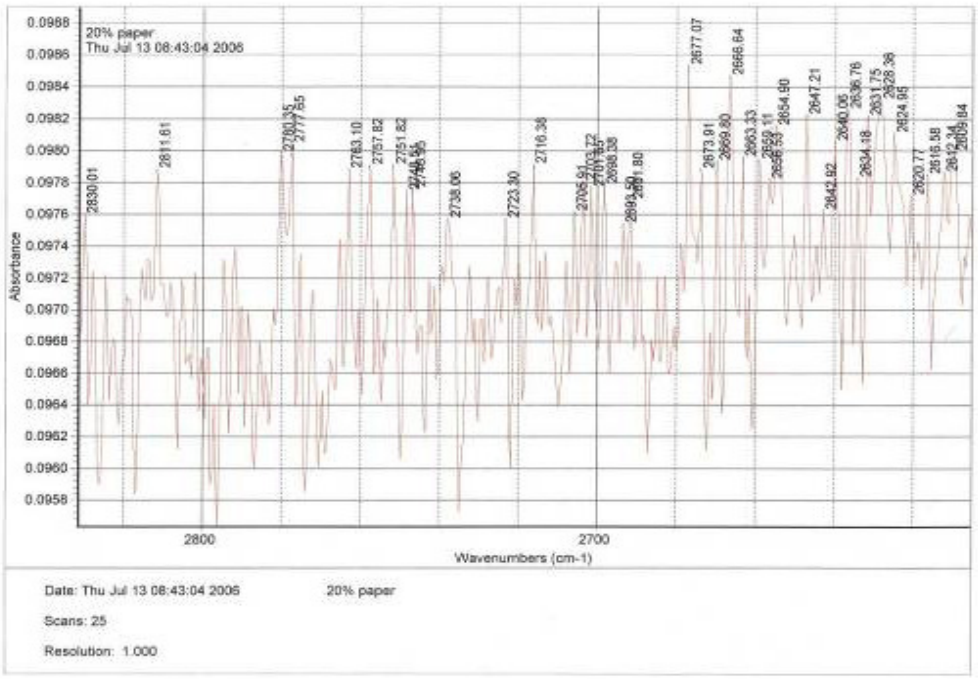

Figure 67. Magnified IR spectrum of sample with 20% paper (wavelength 2600–2800 cm-1).

2.1.6.4.2 XRF Analysis

In another approach, XRF analysis was carried out on a sample of original blended powder and paste samples prepared with 5, 10 and 20% extra paper at 1, 14 and 28 days after casting.

It was proposed that monitoring the comparative amounts of sulphate in the original blended powder and in paste samples over a period of time would give an indication of any loss or conversion of sulphur to other compounds such as hydrogen sulphide.

The results of XRF analysis of samples containing different percentage of paper are presented in Table 39. These indicate that the amount of sulphate (measured as SO_3) did not change considerably between samples tested at different ages. The variation in sulphate content was within ±4% and did not follow any distinctive pattern. However, comparison between samples with less than 0.5% by weight paper and those containing 5, 10 and 20% by weight paper indicated that the higher the amount of paper, the higher the amount of sulphate. This might be due to the presence of sulphate in the paper itself.

The results with samples containing 10 and 20% paper indicated that no conversion of sulphate to hydrogen sulphide gas had occurred by 28 days. Since most chemical reactions take place in presence of water, it can be postulated that hydrogen sulphide gas is more likely to be emitted when the samples are fresh, i.e. during early ages of paste mixtures. This implies that conversion of sulphate to hydrogen sulphide is more unlikely when the rate of reaction falls during the later stages of hydration.

Table 39. XRF analysis of mixtures containing various percentage of paper

Mix	Percentage											
	SiO_2	TiO_2	Al_2O_3	Fe_2O_3	MnO	MgO	CaO	Na_2O	K_2O	P_2O_5	SO_3	**LOI**
Paste <0.5% paper (1 day)	11.12	0.32	2.16	18.89	2.78	6.95	41.12	-0.01	0.36	1.09	8.97	7.14
Paste <0.5% paper (14 days)	11.02	0.33	1.98	19.13	2.88	6.9	41.12	-0.02	0.34	1.17	8.92	7.47
Paste <0.5% paper (28 days)	11.05	0.31	2.17	18.37	2.67	6.82	39.88	0	0.46	1.03	9.91	8.31
Paste + 5% paper (14 days)	10.77	0.31	2.27	18.35	2.66	7.2	40.26	-0.04	0.55	1.03	10.24	7.35
Paste + 10% paper (14 days)	10.99	0.32	2.3	18.74	2.74	7.41	40.12	-0.04	0.56	1.06	9.79	6.63
Paste + 20% paper (1 day)	10.74	0.34	2.27	18.62	2.61	7.17	39.21	-0.02	0.75	1.08	10.45	6.82
Paste + 20% paper (14 days)	10.91	0.31	2.3	18.43	2.68	7.27	40.21	-0.02	0.72	1.04	10.37	6.17
Paste + 20% paper (28 days)	10.62	0.3	2.28	17.8	2.6	7.04	39.58	-0.01	0.78	1	10.81	7.69
Binder powder	11.46	0.34	2.26	19.59	2.87	7.19	42.34	-0.02	0.63	1.12	9.68	2.08

2.1.6.4.3. H2S detection tubes

To confirm the presence or absence of hydrogen sulphide from the paste mixture containing paper, a very accurate and sensitive device was used to detect the hydrogen sulphide gas. Figures 68 and 69 show the H2S detection tube and the pump kit respectively. This device indicates the presence of trace amounts of hydrogen sulphide (accuracy 0.2–5 ppm) by a change in colour of chemicals in the tube.

Figure 68. Drager Accuro H2S detection tube.

Figure 69. Drager Accuro pump kit and H2S detection tube.

Paste samples containing 5, 10, 15, 20 and 50% extra paper was tested at 1, 14 and 28 days curing (Figure 70). No change in colour was observed during testing of different samples (Figure 71). This indicated the absence of hydrogen sulphide in the airtight containers and confirmed that hydrogen sulphide was not formed even when the binder contained a large amount of paper (50%).

Figure 70. Testing the paste samples using the H2S detection tube

Figure 71. Comparison between new and used H2S detection tube for mix containing 50% paper.

2.1.6.5. High Pressure Through-Flow Test

Paste and concrete specimens of blended powder were made using a cylindrical mould for a high pressure through-flow test. This test was performed to:

- confirm the long-term stability of the mixes; and
- check the potential for leaching to the environment.

Figure 72 shows the modified Hoek cell in which distilled water is eluted through a column of proposed material under a pressure gradient [20, 21].

Figure 72. Hoek cells used for high pressure through-flow test.

Figure 73 shows paste samples prepared for the high pressure through-flow test. Samples were cut from the cylindrical specimens and made with the two binders and two L/B ratios of 0.13 and 0.15. Paste and concrete samples from the site trials (see section 3) were also tested and compared with OPC paste. Sample solutions were collected from the specimens tested in the Hoek cell and analysed using an inductively coupled plasma (ICP) spectrometer in the chemistry department at Coventry University (Table 40).

Figure 73. Paste specimens prepared for high pressure through-flow test.

Table 40. ICP analysis of high pressure through-flow test samples (ppm) at Department of Chemistry, Coventry University

Element	BOS80/PG15 /BPD5 (0.15, Lab.)	BOS80/PG15 /BPD5 (0.13, Lab.)	BOS30/ROSA50 /PG15/BPD5 (0.19, Lab)	BOS80/PG15/BPD5 (0.13, Site)	BOS80/PG15/BPD5 (0.13, Site core)	RCC (Site)	OPC paste (0.3)
Na	182.8	178.9	172.9	16.75	706.7	116.4	43.3
Mg	<1	<1	<1	<1	<1	<1	0
Al	0	0	0	0	0	0	0
Ba	0	0	0	0	0	0	0
Ca	1101	1021	1558	1373	1664	403.8	154
K	3195	3611	2042	604.7	2155	1326	35.1
Cr	0	0	0	0	0	0	0
Ni	0	0	0	0	0	0	0
Pb	0	0	0	0	0	0	0
S	449.1	460.7	375.5	214.5	840.3	116.2	14.5
Si	78.7	51.62	35.53	2.96	1.64	9.94	0
Sr	0	0	0	0	0	0	0
P	<1	<1	<1	2.01	1.99	<1	<0.2

Table 41. Repeated ICP analysis of high pressure through-flow test samples (ppm) at Department of Geology, Leicester University

Element	BOS80/PG15 /BPD5 (0.15, Lab.)	BOS80/PG15 /BPD5 (0.13, Lab.)	BOS30/ROSA50 /PG15/BPD5 (0.19, Lab)	BOS80/PG15 /BPD5 (0.13, Site)	BOS80/PG15/BPD5 (0.13, Site core)	RCC (Site)
Na	264.78	286.47	201.85	27.49	775.66	143.55

Table 41. (Continued)

Element	BOS80/PG15 /BPD5 (0.15, Lab.)	BOS80/PG15 /BPD5 (0.13, Lab.)	BOS30/ROSA50 /PG15/BPD5 (0.19, Lab)	BOS80/PG15 /BPD5 (0.13, Site)	BOS80/PG15/BPD5 (0.13, Site core)	RCC (Site)
Mg	0.02	0	30.64	0.02	0.03	0
Al	0	0	0.04	0	0.02	1.04
Ba	0	0	0	0	0	0
Ca	1065.8	1524.2	1630.25	1328.35	1518.23	239.5
K	4684.37	5181.02	2033.01	551.9	1742.45	1132.91
Cr	0	0	0	0	0	0
Ni	0	0	0	0	0	0
Pb	0	0	0	0	0	0
S	762.04	722.42	667.98	363.83	1320.33	198.75
Si	66.6	47.67	28.6	0	0	7.07
Fe	0	0	0.09	0	0.01	0
Sr	0	0	0	0	0	0
P	0	<1	0	0	2.07	1.87

The results indicated that no heavy metal elements had leached from the samples. The major ions dissolved in water were sodium, potassium, calcium, silicon and sulphur – all considered to typically exist in soil and rocks.

Comparison between samples made with the blended binder and with OPC indicated that the level of sulphur (as sulphate) and calcium leached from the samples made with the novel binders under high pressure water was more than from those made using OPC. This could be due to the lower hydration rate and reduced cementitious matrix available to bind the sulphates and calcium ions formed in samples made with novel cement. However, the conditions under which the high pressure through-flow test is carried out are much more accelerated than normal ground conditions. Thus, dissolution of a high level of sulphate ions is not expected using these novel binders.

Table 40 also shows that the amount of sulphate and calcium dissolved from the RCC mix used in the site trial was less than from the semi-dry paste mixes. This is because less cementitious material was used to make the concrete mix. However, the levels of sulphate and calcium dissolved from site core samples were much higher than those from samples made in the laboratory or taken during the site trial.

The high amount of potassium found in all the samples was not expected due to the low amount of potassium oxide (K_2O) in the binder used. To validate the ICP results, the analysis was repeated using an independent ICP machine at Leicester University's geology department (Table 41). The concentration of elements in this second set of results was in the same order as from the analysis carried out using the ICP machine at Coventry University. Slight changes in the concentration of ions might have been due to precipitation or internal reactions in the solutions during storage of the samples. The concentration of potassium remained high in all samples.

To determine the source of potassium in the binder, chemical analysis of the raw materials was repeated using XRF. The chemical compositions of BOS and PG found were similar to previous analyses, but the BPD used to make the Coventry Binder contained more potassium than the previous batch of BPD (Table 1 in section 2.1.3). This illustrates the variation in the chemical composition of BPD from one batch to another. As the potassium in BPD is in the soluble form of K_2O, the high concentrations of potassium in the solutions from the high pressure through-flow test probably arise from the BPD used in the blended binder.

The coefficient of permeability of laboratory and site paste and concrete samples was also measured in the high pressure through-flow test (Table 42). The semi-dry site paste [BOS80/PG15/BPD5 (0.13, Site)] had the highest permeability compared with the laboratory samples; this was due to the lower moisture content when compacting the sub-base layer in the site trial. However, the coefficient was only 10 times greater than that for OPC and, in real ground conditions, the effect will be less than with the high-pressure water conditions in the test. The permeability of concrete varies over four orders of magnitude, so a factor of 10 difference is not as significant for permeability as it would be for strength. The measured permeability of RCC used in the Lowdham Grange site trial (see section 3.2) was less than OPC paste, possibly due to the presence of aggregates in the concrete. Aggregates generally have a lower permeability than cement matrices, so the presence of large volume of aggregates in the RCC concrete resulted in a lower permeability than the OPC paste.

Table 42. Coefficient of permeability to water of laboratory and site samples

Mix	Coefficient of permeability to water (m/s)
BOS80/PG15/BPD5 (0.15, Lab.)	3.98E-11
BOS80/PG15/BPD5 (0.13, Lab.)	1.64E-10
BOS30/ROSA50/PG15/BPD5 (0.19, Lab)	1.29E-10
BOS80/PG15/BPD5 (0.13, Site)	4.11E-09
BOS80/PG15/BPD5 (0.13, Core)	3.57E-09
RCC (Site)	6.91E-11
OPC paste (0.3)	6.03E-10

2.1.6.6. X-Ray Diffraction of Paste Mixtures and Hydration Mechanism

The changes in mineralogy of BOS80/PG15-BPD5 (0.13) semi-dry paste mixture at different ages were investigated using X-ray diffraction (XRD). Figure 74 shows the XRD patterns of paste mixtures after 1, 3, 7, 28 and 180 days curing at 20° C and 98% RH.

Gypsum was the dominant crystalline phase, an observation related to the presence of plasterboard gypsum in the mixture. The initial setting and early age strength of the paste is associated with the formation of ettringite as a result of the reaction of sulphate from gypsum with aluminium and calcium dissolved from the BOS. The peak associated with ettringite was more evident after 3 days, corresponding to the lower strength of the paste than at 7 and 28 days. At the later ages, more ettringite was found in the mixture and higher strength was achieved.

The long-term strength of the mixture is related mainly to the formation of CSH within the cementitious matrix around slag particles, which it was not possible to determine using XRD due its amorphous structure. At 180 days, the presence of a strong peak of ettringite indicated the stability of this phase in the long-term curing of the samples in a moist condition.

Alkali-activated slag mixes are sensitive to carbonation [5] and this phenomenon was observed in XRD patterns of paste mixes at 180 days (Figures 74 and 75). The peak associated with calcite was identified at 28 and 180 days, indicating the formation of a considerable amount of calcium carbonate within the matrix. According to Bakharev [22], the main reasons for rapid carbonation of alkali-activated slag are the absence of portlandite as a hydration product (it normally acts as a carbonation buffer in cement systems) and the low pH of the pore solution. In OPC pastes, a near-surface layer of precipitated calcium carbonate acts as a seal and reduces the diffusion speed of CO2 into the cementitious matrix. Furthermore, the low Ca/Si ratio of CSH could accelerate carbonation. The carbonation rate in hydrated slag and sulphate mixes is controlled only by the carbonation of CSH and ettringite. Thus the higher content of hydrates can reduce the rate of carbonation. This phenomenon was also observed in this investigation. The peak associated with calcite remained at the same intensity in samples at 28 and 180 days. The presence of a very low intensity peak of portlandite was in the line with the findings of Bakharev [22].

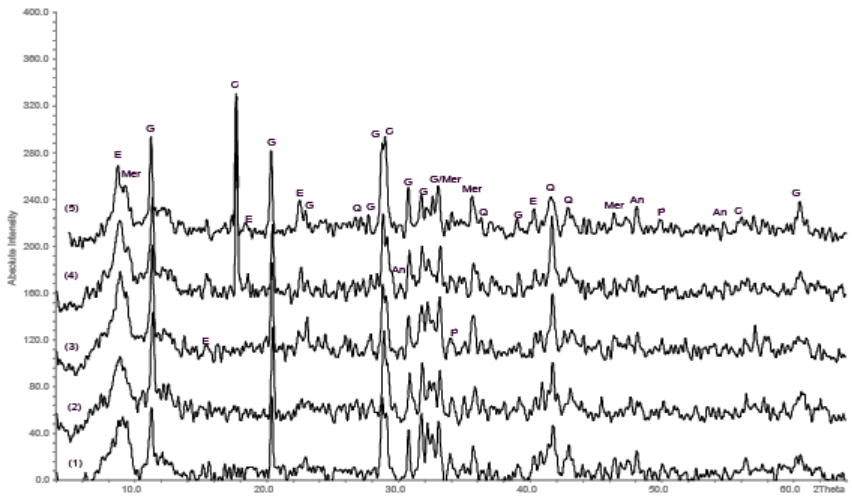

Figure 74. XRD of PG-BOS-BPD(0.13) semi-dry pastes at different ages: (1) 1 day; (2) 3 days; (3) 7 days; (4) 28 days; and (5) 180 days (An = anorthite, C = calcite, E = ettringite, G = gypsum, Mer = merwinite, P = Portlandite, Q = quartz).

The phases related to slag (merwinite) were identified within the matrix, indicating the presence of unhydrated slag particles within the mixture (Figure 74). As the slag is a slow-reacting material, it may be that only a low percentage of the total slag fraction reacts at 28 and even 180 days.

Figure 75 shows the expanded XRD patterns of Coventry Binder (PF-BOS-BPD) semi-dry paste at values of 2Theta (2θ) of 6–20°. The growth of ettringite with time was observed in peaks at 9.096, 15.79 and 17.83°, though the strongest intensity appeared at 9.096°. In addition, the strong peak of calcite at 17.073° indicated the intensity of carbonation on the hydrated matrix of the mixture.

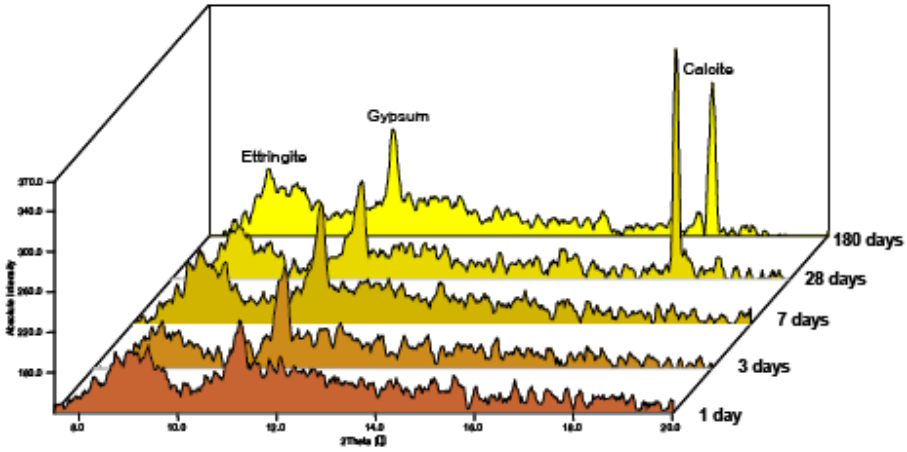

Figure 75. X-ray analysis of PG-BOS-BPD (0.13) semi-dry paste at different ages showing ettringite and calcite evolution.

Figure 76 shows the XRD patterns of stabilised soil samples containing 20, 40 and 60% Coventry Binder after 28 days curing at standard condition. The intensity of the peak associated with gypsum was lower in the sample containing 60% binder, possibly due to the advanced reaction of binder within the clay and the inclusion of sulphates from gypsum in hydration products.

The presence of a peak associated with ettringite confirmed that part of the gypsum was present in the sulphate-bearing component of ettringite. Quartz was the predominant phase in stabilised soil samples; it was the main constituent of the sandy clay used in this investigation. The presence of a kaolinite peak in the pattern also indicated the mixture of siliceous gravel/sand and clay in the soil.

The formation of calcite in samples containing more binder was due to the carbonation of hardened binder within the clay; the more binder used to stabilise the clay, the higher the intensity of calcite in the XRD pattern.

It was not possible to determine the formation of CSH cementitious gel in the matrix of stabilised soil using XRD. However, the lower intensity of quartz in the sample made with 60% binder could be due to the reaction between silica and alumina in clay constituents with alkalis in the binder to form cementitious gel. The presence of a trace of portlandite confirmed the contribution of calcium hydroxide from BPD in the hydration reactions.

Figure 77 shows the hydration scheme of slag in the presence of gypsum and alkalis based on the results obtained in this project and previous experience. The sequence of the hydration reactions at different stages after mixing the binder with water can be explained as follows.

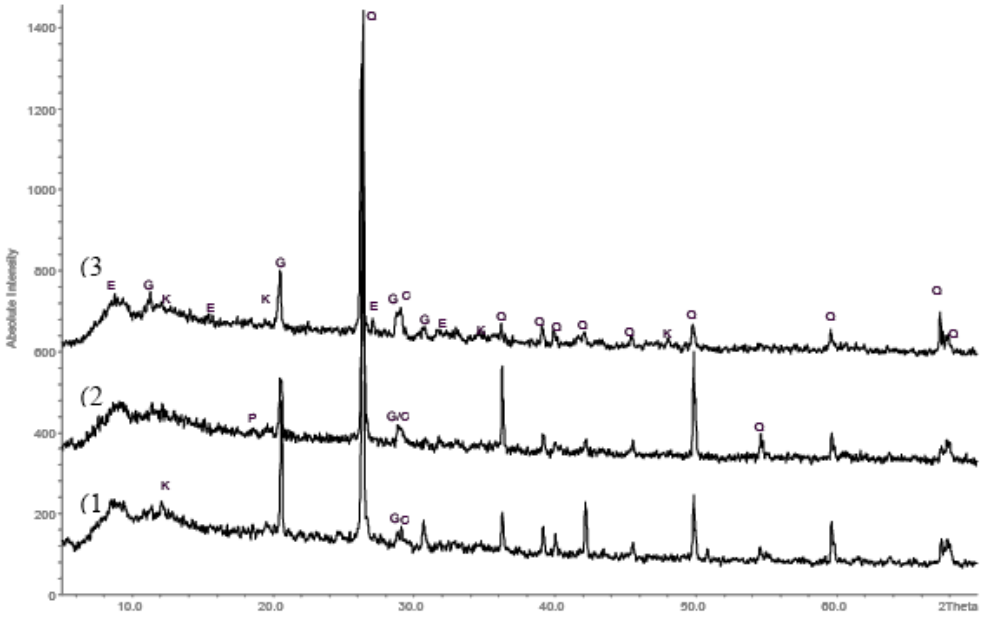

Figure 76. XRD of stabilised soil with different percentages of Coventry Binder: (1) 20%; (2) 40%; and (3) 60% (C = calcite, E = ettringite, G = gypsum, K = kaolinite, P = portlandite, Q = quartz).

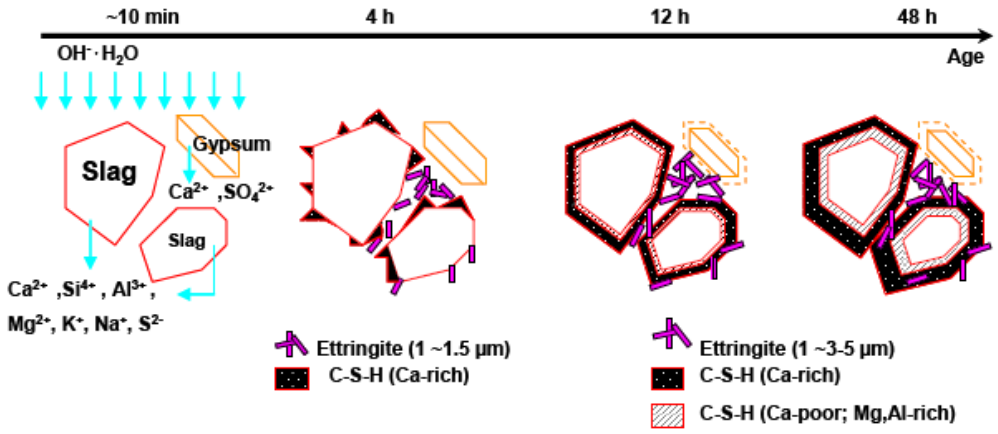

Figure 77. Hydration scheme for the hardening of alkali-sulphate activated slag.

Directly after mixing with water, ions of readily soluble alkali compounds and free lime from the cement BPD – as well as released ions from the slag and gypsum – enter solution. Ca^{2+}, Al^{3+}, Si^{4+}, Mg^{2+}, $SO4^{2-}$. Na^{+}, K^{+} and OH^{-} ions are available in the system after about 10 minutes of hydration [7]. The pH of the pore solution then increases to approximately 11.6. Alongside the rising calcium concentrations, the pH increases to 12.3 after 2 hours of hydration. A high saturation index was calculated for ettringite [23], with a maximum saturation index occurring between 2 and 4 hours. Scanning electron microscopy (SEM) micrographs of paste [24] showed ettringite needles (1–1.5 µm) loosely distributed in the hydrating structure and CSH formation beginning on the surface of slag grains after 4 hours (as shown schematically in Figure 77).

As a result of hydrate precipitation, Ca^{2+}, $A^{l3}+$, Si^{4+} and OH^{-} ions are partly removed from the pore solution. The sulphate content of the pore solution increases in order to balance the positive charges on the alkali metal (Group I: Na^{+}, K^{+}) and alkaline earth (Group II: Ca^{2+}, Mg^{2+}) ions created by the removal of the hydroxide ions. The hydration reactions accelerate the corrosion of the slag to reach an apparent chemical equilibrium between solid and liquid phases. The rising Group I, Group II and sulphate content indicates continuous hydration of the slag-gypsum-bypass dust paste. The additional positive ions are balanced with the sulphate ions in the pore solution, resulting in the pH of the pore solution remaining nearly constant at between 11.7 and 12.0 [24].

Richardson [25] reported finding two CSH reaction fronts around the hydrating slag grains; the inner layer showed a lower Ca/Si ratio (Ca/Si ~1.2) than the outer layer (Ca/Si ~1.4). However, it is possible that a homogenous Ca/Si ratio may be approached with progressing hydration time. The morphology of CSH observed by Richardson [25] was more foil-like than the fibrillar CSH of OPC with high Ca/Si ratios of ~1.8. Moreover, the low solubility of magnesium may cause the precipitation of magnesium-containing hydrates such as hydrotalcite. Thus, the inner hydrate layer could contain more aluminium and magnesium than the outer layer. Möser [26] showed an incorporation of magnesium and aluminium into the structure of the magnesium-calcium-silicate-aluminate-hydrate (M-C-S-A-H) identified as hydration products of slag. More recently Brews and Glasser [27] described the possibility of

magnesium silicate hydrate (MSH) gel formation as an additional product of hydrated blast furnace slag.

Two separate spatial equilibria arise as a result of the accumulation at the slag surface of dense CSH. Hence further hydration reactions are controlled by diffusion. This causes a very slow reaction rate, which declines with the increased thickness of the CSH layer around the slag. The formation of this layer means that only about 26% (by weight) of the total slag fraction can react at 60 days [7].

Several researchers have reported the sensitivity of alkali-sulphate activated slag mixtures to imprecise dosages of alkaline activators [28, 29]. The results presented in section 5.1.2 also showed that the compressive strength fell as the CKD/BPD content of the binary and ternary paste mixtures increased. The lower strength due to a high alkali metal content in the pore solution can be attributed to the location of the ettringite precipitation [30].

Ettringite forms hexagonal-prismatic crystals based on columns of cations of the composition $\{Ca_3[Al(OH)_6].12H_2O\}^{3+}$ [31] in which the $Al(OH)_6^{3-}$ octahedra are bound up with the edge-sharing CaO_8 polyhedra. This means that each aluminium ion, bound into the crystal, is connected to Ca^{2+} ions with which they share OH^- ions. The intervening channels contain the SO_4^{2-} tetrahedra and remaining water molecules. The water molecules are partly bound very close into the ettringite structure. Figure 78 shows a structural model of ettringite [31].

Ettringite appears in many different forms and shapes, although the causes of this are not yet fully explained. According to investigations by Chartschenko and colleagues [32, 33], the length–thickness ratio of ettringite crystals is extremely dependent on the pH value of the reaction solution (Figure 79). Long, fibre-shaped crystals are formed at pH values between 10 and 12, but extremely microcrystalline ettringite is present at pH values above 13.0.

Mehta [34] described two modifications of ettringite which differ in habit and size. The long lath-like crystals, which can be 10–100 μm long and several μm thick, formed at low hydroxyl ion concentrations (i.e. with low pH values in the pore solution) and were designated by Mehta as Type I. If a hydrated binder contains significant amounts of these large ettringite crystals, this would lead to high strength but not to expansion effects. Mehta therefore proposed that Type I ettringite is not expansive. The rod-like crystals, which are only 1–2 μm long and 0.1–0.2 μm thick or even smaller, form at the high hydroxyl ion concentrations present during hydration of OPC or high alkaline-activated slag; these were called Type II ettringite by Mehta. According to Mehta, fairly large amounts of this microcrystalline ettringite can cause expansion effects through water adsorption. The expansion-related properties of the novel blended binder used in this project are discussed in section 2.1.6.7 and can be associated with the formation of the microcrystalline form of ettringite within the cementitious matrix.

In alkali-sulphate activated slag systems with low alkali contents, ettringite is precipitated preferably in larger pores. Environmental SEM (ESEM) micrographs of alkali-sulphate activated slag paste with high alkali contents in the pore solution demonstrated a preferred growth of ettringite crystals on the surface of hydrated slag grains [35]. The addition of positive charges to the pore solution (Na^+, K^+, Ca^{2+}) leads to an increased sulphate concentration (negative charges) in order to obtain a charge-balanced pore solution.

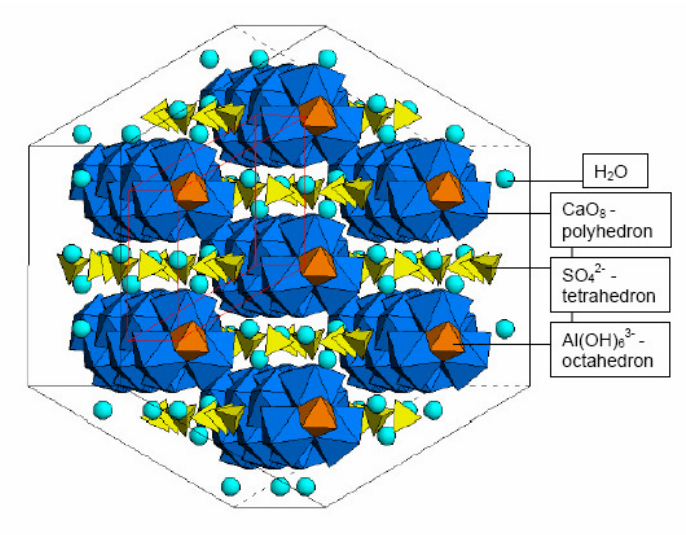

Figure 78. Structural model of ettringite [31].

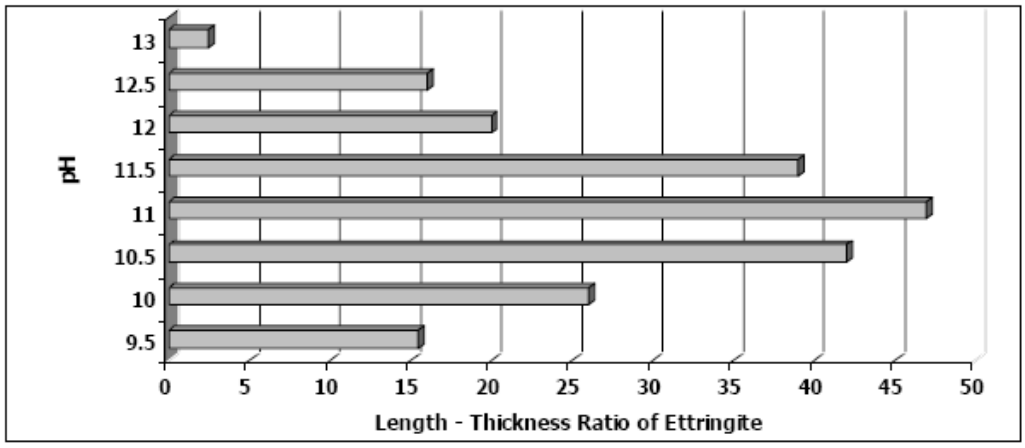

Figure 79. Change in length–thickness ratio of ettringite crystals [31].

A high local supersaturation for ettringite near the surface of the slag grains results from the enhanced content of sulphate and hydroxide in the pore fluid. The precipitation of ettringite impedes the migration of aluminium ions from slag grains into the pore solution and the concentration of aluminium ions is <0.1 mmol/l from the beginning. Taylor [31] described a similar mechanism for a high concentration of calcium in the pore solution. As a consequence, spatial isolation of the slag grains in conjunction with a coarsening of the pore structure leads to lower compressive strength.

The ettringite layer on the slag surface can be responsible for the lower reaction rates due to a lower diffusion rate of ions from the slag into the pore solution. Furthermore, the formation of microcrystalline ettringite at higher pH can result in a denser layer of ettringite around the slag grains, lowering the hydration rate of slag in the matrix.

2.1.6.7. Length Change of PG-BOS-BPD Paste and Mortar Mixtures

To provide information on the long-term durability and stability of the Coventry Binder, the length change of paste and mortar samples made using the novel binder was measured according to ASTM C151 [36]. The length change was also compared with a control OPC mortar sample.

Prism samples of 25×25×285 mm were made using gang prism moulds with steel inserts fitted at both ends of each sample. Figure 80 shows the apparatus used to determine the length change of hardened paste and mortars (ASTM C490) [37]. The length change of samples was measured at 3, 7, 14 and 28 days, with the results reported as the percentage change.

The maximum allowed expansion or shrinkage of any mix depends on the type of binder application. For example, for in expansion due to alkali-silica reactivity (ASR), ASTM C1260 [38] and ASTM C227 [39] indicate a 26-week test limit of 0.1%. BS 812-123: 1999 [40], which is also related to ASR expansion, sets the limit of 0.1% at 52 weeks. BS 2028: 1968 [41] recommended the maximum shrinkage of 500×10-6 to 600×10-6 (relative length change) for pre-cast construction blocks used for general applications.

Figure 80. Apparatus for determination of length change.

Details of the paste (P) and mortar (M) mixes investigated are given in Table 43. Mortars were made using a sand to binder ratio of 2.7 with different L/S ratios. The semi-dry paste investigated was similar to the mix used in the site trial, i.e. Coventry Binder (COV). Samples were cured at 20° C and 98% RH, though the paste and mortar mixes made with the Coventry Binder were also placed at 40° C to investigate the effect of curing temperature on the expansion of this novel blended binder.

Table 43 Mix proportions of paste and mortars for length change test

Mix code	Binder (%)	Sand (%)	L/S	Temperature (° C)
COVP-20-0.13	100	–	0.13	20
COVM-20-0.13	27	73	0.13	20
COVM-20-0.3	27	73	0.3	20
COVM-20-0.5	27	73	0.5	20
OPCM-20-0.5	27	73	0.5	20
COVP-40-0.13	100	–	0.13	40
COVM-40-0.13	27	73	0.13	40

Figure 81 shows the results of the length change test for paste and mortar mixes made using Coventry Binder and OPC. The greatest expansion was observed in the paste mix (COVP-20-0.13) that had the lowest L/S ratio of 0.13.

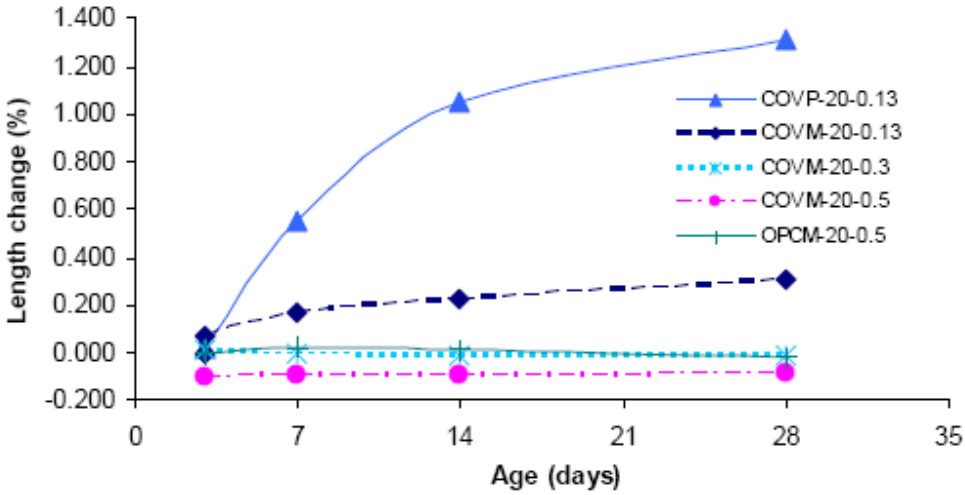

Figure 81. Length change of paste and mortar mixes at different ages.

Incorporating aggregate in the mixture resulted in less expansion, mainly because less binder was used in the mix and the constraining effect of fine and coarse aggregate in the system. The expansion of mortar samples made with a similar water to binder ratio was only about 15% of that of the semi-dry paste. In addition, the lower L/S ratio led to greater expansion in the mortar samples.

A possible explanation for the lower expansion in samples made with a higher water to binder ratio could be the increased available space within the pore structure of the cementitious matrix that can be filled up by expansive hydration products as time progresses. Mortar samples made with a L/S ratio of 0.5 showed shrinkage from an early age of curing

due to the evaporation of excess water immediately after casting. The length of the control OPC samples remained nearly the same, with slight shrinkage at 28 days. This was as reported by Neville [5].

The observed expansions for paste and mortar mixes made with Coventry Binder using a L/S ratio of 0.13 exceeded the recommended limit of expansion in BS 812-123: 1999 [40] for destructive ASR in concrete. It also exceeded the ASTM C227 [39] six-month test limit of 0.1% at only 7 days. This demonstrated the expansive nature of the Coventry Binder, which might be considered an advantage for use in certain applications in which expansive cements are needed. In addition, no limit was suggested for cements used for backfilling or road foundations. Such an expansion can to, some extent, be restrained with steel reinforcement providing a protective layer is present to prevent corrosion of the steel due the chloride effect in a sulphate-bearing environment. The reason for the expansion of the novel blended binder is not yet clear, though formation of ettringite as a part of cementitious matrix and also the higher MgO content of BOS (as discussed above) might be responsible for progressive expansion of the hardened paste and mortars. The lower binder content in mortar and concrete mixtures results from less ettringite being formed within the matrix; less expansion was therefore observed in those samples.

With respect to the effect of temperature on the expansion of paste and mortars made using the Coventry Binder, Figure 82 shows the results of length change in samples cured at 20° and 40° C for 28 days. The expansion of paste and mortar mixes cured at higher temperature was lower than those cured at a standard temperature of 20° C and at a similar humidity (98% RH).

The expansion of the mortar sample made with the Coventry Binder cured at 40° C (COVM-40-0.13) remained almost constant and did not exceed the limit of 0.1% at 28 days. In addition, the expansion of the paste mixture cured at 40° C was about 30% of those cured at 20° C.

The lower expansion of paste and mortar mixes cured at the higher temperature might be due to faster hydration of slag at elevated temperatures, resulting in higher strength. This can provide more constraints within the cementitious matrix and therefore less expansion is observed. This implies that the Coventry Binder can be used in pre-cast concrete manufacture in which elevated and high pressure curing is used to produce concrete paving blocks. However, further investigations are needed to evaluate the effect of steam and high pressure curing on this novel blended binder.

Figure 83 shows an overall comparison of the length change of the paste and mortar samples at 28 days. Among all the samples investigated, the semi-dry paste sample made using Coventry Binder with a L/S ratio of 0.13 showed the greatest expansion after 28 days curing at 20° C and 98% RH. The semi-dry paste sample cured at 40° C showed almost similar expansion to the mortar sample cured at 20° C with the same L/S ratio.

This highlights the significant effect of curing temperature on the long-term performance of the novel Coventry Binder. The lowest expansion in the semi-dry paste and mortar samples (L/S 0.13) was observed in the mortar sample that was cured at 40° C for 28 days. Mortar samples made with higher L/S ratios did not show any expansion up to 28 days, though shrinkage was observed similar to that obtained with the control OPC mortar at 20° C. Moreover, the higher the water content in the mixture, the greater is the drying shrinkage in the mortar samples.

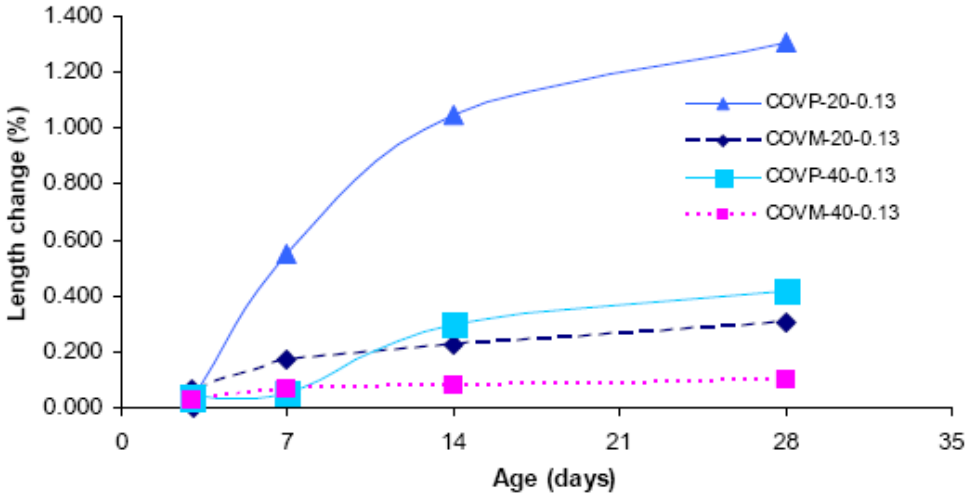

Figure 82.Effect of temperature on length change of paste and mortar mixes.

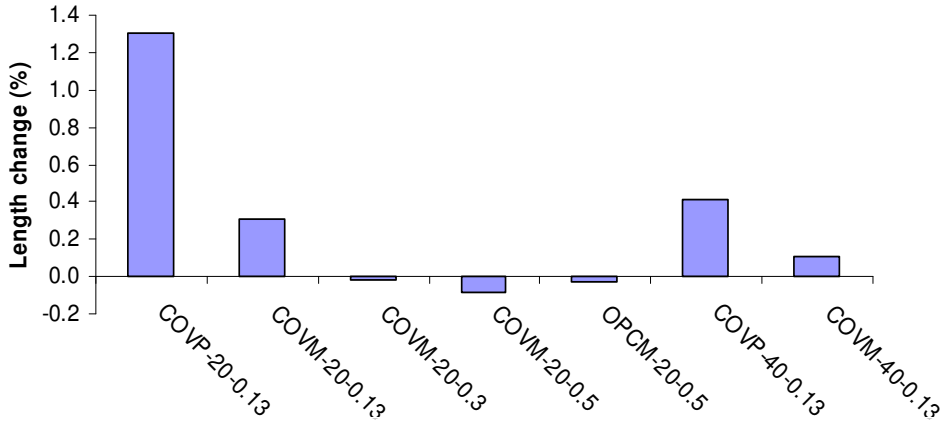

Figure 83. Comparison of length change of paste and mortar mixes at 28 days.

3. SITE TRIALS

Discussions with Skanska resulted in the selection of two construction sites to carry out the site trials:

- A car park at the Lowdham Grange prison construction site in Nottingham was selected to evaluate the use of roller-compacted concrete (RCC) as the sub-base layer using Coventry Binder.

- An area at the King's Mill Hospital construction site in Nottinghamshire was allocated to make a 22-metre access road using Coventry Binder stabilised soil and semi-dry paste (grout) as the sub-base and base course respectively.

The site trials were carried in July 2006 and the constructed layers evaluated until February 2007.

3.1. Material preparations

The final optimised proportions of the ternary mixture of PG, BPD and BOS as described in section 2.1.6 were chosen for the site trials.

In order to fulfil the requirements for concrete, stabilised soil and paste for the site trial, over 100 tonnes of blended powder was prepared at Ryder Point Processing in Matlock in Derbyshire (www.thebgs.co.uk/foundation-web/RyderPoint.html). The blended powder consisted of 80% ground BOS, 15% ground PG and 5% BPD supplied as blended powder.

The BOS was dried before grinding. Both the BOS and PG passed through a 500 µm mesh installed on the ball mill. The ground materials were then blended with BPD according to the designed proportions and bagged in 20-kg bags (Figure 84) and 1000-kg sling bags (Figures 85 and 86). The bags were shrink-wrapped before delivery.

Although the plasterboard supplied by Lafarge contained paper, the ground PG was sieved before blending and the major part of paper was removed. The BPD was expected to be in form of a fine powder, but it was found to contain big lumps of condensed material. To produce a fine blended powder, the lumps were removed as much as possible before blending the BPD with the other materials.

Pre-blending the material facilitates its use in ready-mix plants or with other types of mixing methods. The pre-blended powder was easy to use, like ordinary cement, with no further work or preparation required.

Figure 84. Blended powder delivered to the ready-mix plant in 20-kg bags.

Figure 85. Blended powder delivered to the King's Mill Hospital site in 1000-kg sling bags.

Figure 86. 1000-kg bags of blended powder ready to use (King's Mill Hospital site).

3.2. Lowdham Grange Site

A 6×17 m car park area at the Lowdham Grange prison construction site was allocated by Skanska for the sub-base trial for which the RCC designed in the laboratory experiments was used (see section 2.1.6.2).

Before work began the area was cordoned off using a pedestrian barrier. It was stripped of the existing hardcore to expose the sub-grade, which was hard clay, similar to that in the rest of the site. The sub-grade was trimmed to level, compacted and inspected by all parties (the contractor, WRAP and the technical group from Coventry University).

Figure 87 shows the layout of the construction layers designed for the site trial. This design was similar to that of the existing layers of constructed car park area in order to provide comparable data for the conventional sub-bases and the RCC layer.

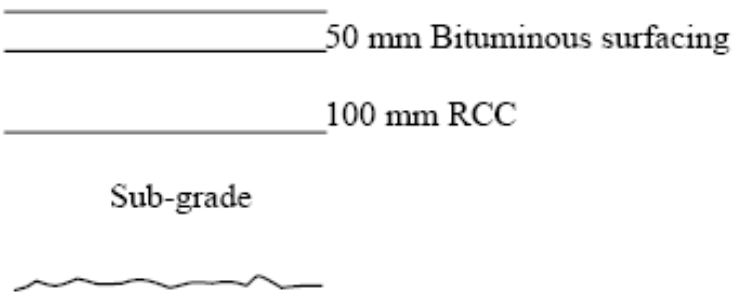

Figure 87. Layout of trial construction layers at Lowdham Grange site.

3.2.1. Ready-Mix Concrete

The RCC mix was prepared at a Lafarge ready-mix concrete plant at Lockington in Leicestershire (Figure 88). The concrete mix design used is presented in Table 44. The volume of the concrete required to construct the sub-base layer (in a loose condition) including wastage was estimated to be 16 m^3. It was therefore batched in three loads delivered by three truck mixers.

Table 44. Mix proportions of concrete mix used at the Lowdham Grange site trial

	Mix proportions (kg/m3)				
Mix code	Blended novel binder	Water	Recycled aggregate	W/B	Slump (mm)
PG15/BPD5/BOS80 (RA-RCC)	400	100	1900	0.25	0

The moisture of the aggregates was measured in the laboratory and also by an automatic sensor installed in the aggregate stock of the ready-mix plant. All necessary adjustments to the proportions of the concrete mix were carried out before the materials were loaded into the truck mixers.

Figure 88. Lafarge ready-mix concrete batching plant.

Aggregates and part of the water content were loaded first into the truck mixer (Figure 89) to allow the aggregates to absorb enough water and reach SSD condition.

Figure 89. Loading aggregates and water into the truck mixer.

After mixing the aggregates and water thoroughly for about five minutes, the blended binder was loaded manually into the truck mixer. It had been planned to load the blended binder into the truck mixer using an auger system but a scheduling problem meant that the binder had to be loaded by hand (Figures 90 and 91).

Figure 90. Loading blended binder into the truck mixer.

Figure 91. Loading blended binder bags into the truck mixer.

The mixture of aggregates, water and blended binder was mixed thoroughly in the truck mixer for about 10 minutes before being delivered to the site.

The same procedure was carried out to load all three truck mixers (two 5-m^3 trucks and one 6-m^3 truck) used to batch the 16 m^3 of concrete.

3.2.2. Placing Concrete and Compaction

A layer of 160 mm of concrete was placed over the sub-grade layer using the truck mixer chute (Figure 92) before being spread and levelled manually (Figure 93). As the concrete was delivered in three truck loads, placing and compaction of the RCC layer was carried out in three segments of the allocated area. As a result, a slightly different moisture content and compaction level was expected for different sections. However, the workability of the mixes on-site was observed to be very consistent. The hot weather on the day was allowed for in all measurements.

The placed concrete layer was then compacted using a 3-tonne vibrating roller in accordance with the compaction requirements of the Specification for Highways Works [42] to form a 100-mm RCC layer as shown in Figures 94 and 95.

Figure 92. Placing concrete using the truck mixer chute.

Figure 93. Placing and spreading the last batch of concrete.

Figure 94. Spreading the concrete using a mechanical excavator.

Figure 95. Concrete compaction using a 3-tonne vibrating roller.

The completed layer of RRC is shown in Figure 96. The surface of the concrete was sprayed with a bituminous emulsion layer to prevent evaporation of water up to 28 days curing.

Figure 96. Completed 100-mm layer of RCC at the Lowdham Grange site.

3.2.3.Concrete Sampling

To evaluate the level of compaction of concrete in the site trial and compare it with laboratory experiments, 150-mm cubes samples were prepared from each batch of concrete delivered to the site. Concrete samples were compacted using a hammer drill and attached plate in three layers (Figure 97). These samples were kept under standard curing conditions in the laboratory; the results of compressive strength testing are presented in section 3.4.

Figure 97.Sampling of concrete using 150-mm cubes and hammer drill.

3.3. King's Mill Hospital Site

A 22-m length of the site access road (4 m wide) was allocated by Skanska within the stores area of the King's Mill Hospital construction site.

The trial included two major works undertaken to evaluate the feasibility and performance of the Coventry Binder for use in soil stabilisation and also as a binder itself. The construction layers of the 22 metres of temporary access road were designed to compare conventional cement stabilised soil and bituminous base course layers with Coventry Binder stabilised soil and semi-dry compacted paste (grout). Figure 98 shows the layout of the designed layers for each section of the trial access road.

Table 45 presents the proportions of materials used for soil stabilisation and the semi-dry paste. The volume of stabilised soil needed for the site trial was estimated at 72 m^3 (in a loose condition) including wastage. For the semi-dry paste, the volume of material needed was

estimated to be 6 m^3 (in a loose condition) and including wastage. As shown in Figure 98, half the temporary access road was designed to be constructed using a conventional base course of the same thickness as the semi-dry compacted paste. Finally, the surface of the whole road was paved using 50 mm bituminous wearing surface.

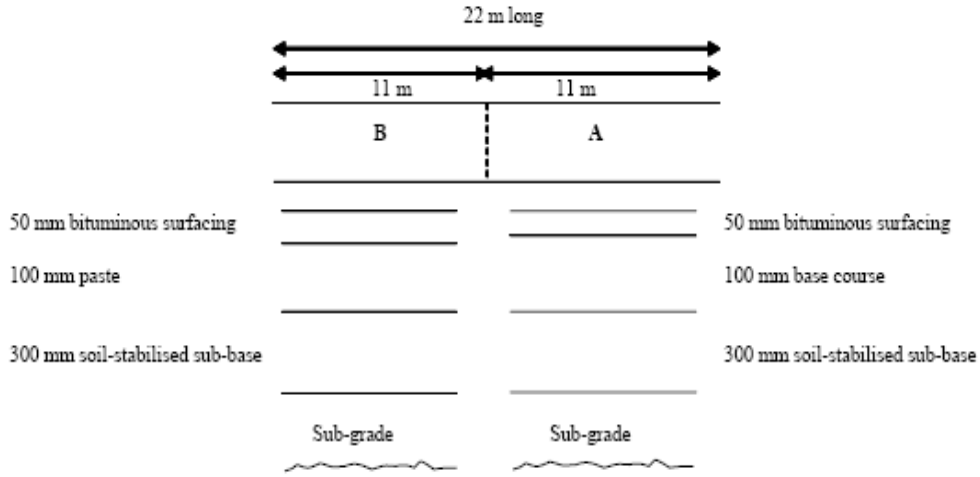

Figure 98. Layout of the trial construction layers at the King's Mill Hospital site.

Table 45. Mix proportions of stabilised soil and semi-dry compacted paste (grout) mixes used

Mix code	Soil (%)	Binder (%)	Moisture content (%)
Stabilised soil (Soil50/Binder50)	50	50	14.2
Semi-dry paste (PG15/BPD5/BOS80-0.13)	–	100	13

3.3.1. Site Preparation

The area identified in the stores area of the north field compound was stripped of existing hardcore to expose the sub-grade, which was sandy and similar to that in the rest of the north field. The area was trimmed to level, compacted and inspected by all parties (the contractor, WRAP and the technical group from Coventry University). Figures 99 and 100 show the preparation of the trial area using Skanska's heavy excavator.

Figure 99. Preparation of the trial area using an excavator.

Figure 100. Trimming and levelling the trial area to expose the sub-grade.

3.3.2. Soil stabilisation

A 300-mm layer of soil stabilised using Coventry Binder was placed on the prepared area. First, the soil was spread and levelled using a JCB machine (Figures 101 and 102). As the allocated area sloped, all efforts were made to spread the soil with the same thickness along the road (Figure 103).

Figure 101. Spreading and levelling the soil in the trial area.

Figure 102. Levelling the spread soil using the JCB.

Figure 103. Controlling the accuracy of the thickness of spread soil.

The blended powder was then spread over the area using a volumetric method. To achieve the required amount of binder per cubic metre of the compacted soil, 150 mm of the blended powder was spread over the trial area manually and using the JCB. Figures 104 and 105 show the placing and levelling of the powder on top of the level soil.

Figure 104. Placing and spreading the powder on top of levelled soil.

Figure 105.Levelled layer of powder on top of the soil.

The mixture of soil and powder was blended using a rotavating blending machine as shown in Figures 106–108. The powerful and heavy blade of the machine provided a homogeneous blend of soil and binder along the road.

Figure 106. Blending the mixture of soil and binder using the rotavator (rotavator moving into position).

Figure 107. Rotavator in blending position.

Figure 108. Inspecting the blended soil and powder before adding extra water.

As the natural moisture of the soil used was not enough to provide the optimum compaction of stabilised soil, extra water was added to the mixture using a mobile sprinkler (Figure 109.). Then the mixture was blended again using the rotavating blender and levelled using the JCB. Visual control of the water content was challenging due to the hot weather and rapid evaporation. But despite this, the moisture content and compaction of the stabilised soil was satisfactory.

Figure 109. Watering the mixture of soil and the binder using the sprinkler.

The blended soil and powder with sufficient moisture was levelled using the JCB and compacted using a 10-tonne vibrating roller. Figure 110 shows the levelled, stabilised soil and Figure 111 the compaction being carried out. The finished surface is shown in Figure 112. To protect the layer from rain and evaporation, a bituminous emulsion layer was sprayed on top of the finished surface.

Figure 110. Levelled blended soil and powder ready for compaction.

Figure 111. Compacting the blended soil and the binder using the 10-tonne roller.

Figure 112. Finished surface of the stabilised soil.

3.3.2.1 Sampling

Sampling of the stabilised soil was performed in order to evaluate the moisture, level of compaction and compressive strength of the blended soil and binder. The results (see Tables 42 and 43) were compared with laboratory results for quality control purposes.

Two sets of 100 and 150 mm cubes were prepared using the standard method. For the 100-mm cubes, stabilised soil was compacted in three layers using a standard proctor rammer (25 drops). For 150-mm cubes, the blended soil and binder was compacted in five layers by 51 drops of the standard proctor rammer (Figure 113).

Figure 113. Sampling the stabilised soil.

3.3.3. Semi-Dry Compacted Paste

A layer of 100-mm semi-dry compacted paste using PG15/BPD5/BOS80 (Coventry Binder) was laid on top of the stabilised soil for half the length of the access road in order to compare it with the conventional base course laid on the other half of the trial road. Figure 114 shows the sprayed surface of the stabilised soil prior to constructing the paste layer.

Figure 114. Sprayed surface of stabilised soil before constructing the paste layer.

As the water content of the semi-dry paste was limited to 13%, a volumetric mixer was used to mix the blended binder with water (Figure 115). The mixer contained a vessel to accommodate the binder and a 1600-litre tank of water. The binder was passed to a screw by means of a belt conveyer where the water was added, and was mixed in the extending arm.

The semi-dry paste (grout) was spread through the extended arm of the volumetric mixer and then levelled using the JCB machine. The only challenge was measuring the amount of water because the mixer was not equipped with any means of measuring the amount of water added to the mixture. Therefore, the required amount of water was adjusted based on visual inspection and past experience. Figures 115 and 116 show the mixing and spreading of the semi-dry paste.

Figure 115. Loading the mixer with blended powder.

Figure 116. Spreading and levelling the semi-dry paste.

After levelling the semi-dry paste, the layer was compacted using a 3-tonne vibrating roller. Figures 117 and 118 show the compacted and finished surfaces of the layer respectively.

Figure 117. Compacting the semi-dry paste layer using a 3-tonne roller.

Figure 118. Finished surface of the compacted semi-dry paste.

The surface of the compacted semi-dry paste was sprayed with bituminous emulsion for curing purposes.

The other half of the trial road was later laid using a 100-mm base course and then the whole length of the road was paved with 50 mm of bituminous surfacing.

3.3.3.1. Sampling

Sampling the semi-dry paste was performed in order to evaluate the level of compaction, moisture content and compressive strength. Two sets of 100 and 50 mm cubes were prepared using the standard method [43, 44]. For 100-mm cubes, semi-dry paste was compacted in three layers using a standard Proctor rammer (25 drops). For 50-mm cubes, paste was compacted using a small tamper in three layers (Figure 119).

3.4. Site Trial Evaluation

The site trial evaluation was conducted at 14, 28, 90 and 180 days after placing the semi-dry paste and RCC in order to monitor the performance of the different base and sub-base layers prepared using Coventry Binder.

The strength of the semi-dry paste and RCC layers was evaluated using in-situ core drilling. In addition, a visual inspection for any kind of damage such as large deflections or settlement was carried out and the state of the site was monitored by taking photographs of different sections.

The following sections detail the results of the site trial evaluation for the King's Mill Hospital and Lowdham Grange sites.

Figure 119. Sampling the semi-dry paste using 100 and 50 mm cubes.

3.4.1. King's Mill Hospital site

The evaluation of the stabilised sub-grade and semi-dry sub-base at the King's Mill Hospital site was conducted in stages.

First, the moisture and compaction level of the stabilised soil using novel binder was measured using a nuclear density gauge. Table 46 shows the in-situ density and moisture content at four different points of the trial pavement.

The maximum dry density achieved in the laboratory was 2030 kg/m^3 and the optimum moisture content was about 13.9%. The stabilised soil layer was compacted at a slightly lower moisture content of 8.9% (Table 47). Although the amount of water added to the soil while mixed with the binder on-site was gauged by the look and feel of the mix, the results show that the variation in moisture content was within an acceptable range.

Table 46. In-situ density and moisture content of stabilised sub-grade

Location	Depth of test (mm)	Moisture (%)	Dry density (kg/m3)	Compaction (%)
5 m from lowest	125	8.9	1790	88
10 m from lowest	125	8.9	1755	87
15 m from lowest	125	10.3	1789	88
20 m from lowest	125	8.9	1793	88

The compressive strength of the stabilised soil was evaluated by measuring the strength of cube samples taken on the day of the site trial; 100-mm cube specimens were taken from middle and end sections of the trial road. Table 47 summarises the results of compressive strength and density together with the in-situ test results.

Table 47. Compressive strength of stabilised sub-grade together with in-situ density and moisture

	Laboratory tests					In-situ tests	
	Strength at days (MPa)			Moisture (%)	Dry density (kg/m^3)	Moisture (%)	Dry density (kg/m^3)
Mix code	3	7	28				
Unstabilised Soil-B (Lab.)	0.08	0.21	0.13	13.4	1835.1	–	–
Soil-B 50/Binder 50 (Lab.)	0.94	1.43	5.98	13.9	2030.15	–	–
Soil 50/Binder 50 (Site-Mid)	0.78	1.11	5.8	8.02	2033.06	8.9	1755
Soil 50/Binder 50 (Site-End)	0.96	1.15	5.1	7.9	2027.55	8.9	1793

The compressive strengths of the cube specimens from the site trial were close to the results obtained with laboratory samples (Table 47). Despite the stabilised sub-grade being compacted with a lower moisture content than the optimum moisture content defined in laboratory tests, satisfactory compressive strength results were achieved from the site samples. Figure 120 shows the strength development of the site sample and laboratory-designed stabilised soil. The rate of the strength gain in laboratory and site mixes was almost similar. The slight difference in the strength of the site specimens taken from the middle and end sections of the trial road could be due to a variation in moisture content at different locations.

With respect to the density of the stabilised sub-grade, the in-situ density measured after 1 day was less than the maximum dry density achieved in the laboratory. This was due to the lower moisture content (8.9%) used to compact the soil. Control of the moisture content was not precise on the day of site trial because of the hot weather and, as mentioned above, the suitable moisture content was defined by eye based on previous experience.

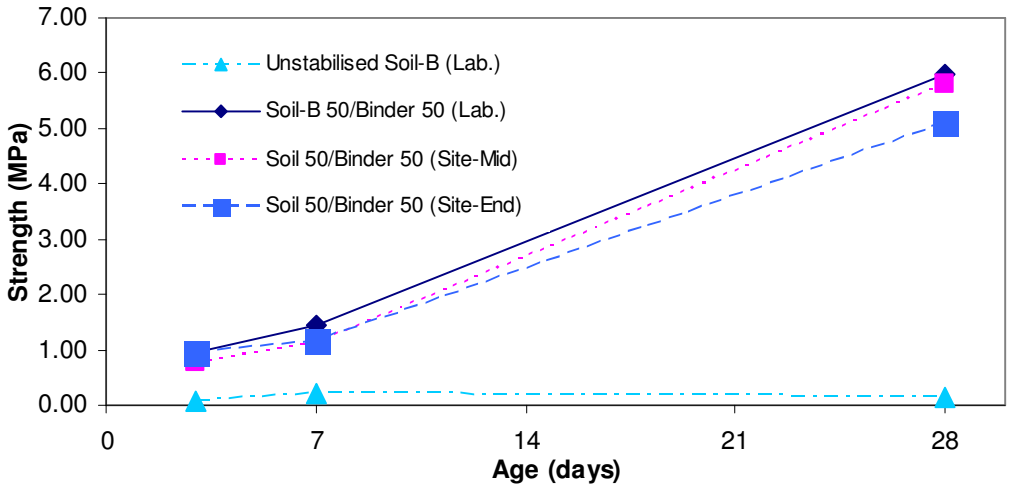

Figure 120. Compressive strength development of stabilised sub-grade at the King's Mill Hospital site.

A general view of trial road is shown in Figure 121. The lower part of the trial road, which was constructed with a semi-dry paste sub-base layer, has been subject to frequent loads from heavy trucks and occasionally from heavy excavators. There was no sign of cracking or large deflections of the surface of the road, as shown in the close-up view of the road surface in Figure 122. In addition, a close inspection of the road found no sign of cracking at the interface of that part of the road made with bituminous sub-base and that made with semi-dry paste.

These observations demonstrated that the performance of both layers under heavy site traffic was similar after three months. Further inspections conducted at six months also found no evidence of cracks or large displacements in the part of the road constructed with a sub-base layer made with Coventry Binder. This confirmed the adequacy of the long-term performance of Coventry Binder when used in the construction of road foundations.

Figure 121. General visual evaluation of trial road at the King's Mill Hospital site.

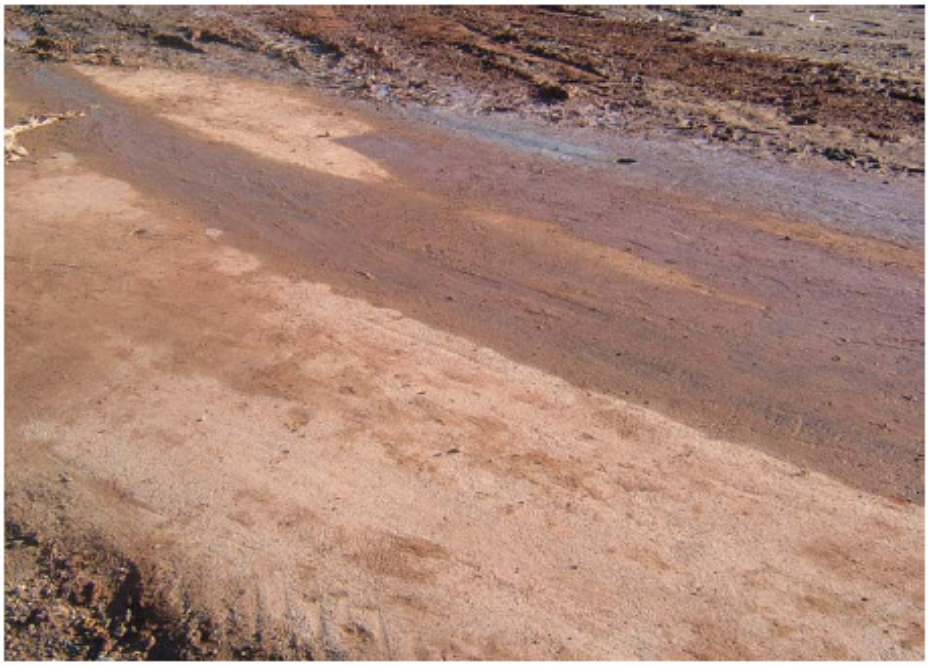

Figure 122. Close-up of the trial road at the King's Mill Hospital site.

In order to evaluate the compressive strength of the semi-dry paste layer, 100-mm core samples were drilled from the lower, middle and upper sections of the trial road. Figure 123 shows the apparatus used to drill the cores.

Figure 123.Coring machine used to drill the cores at the King's Mill Hospital site.

Figure 124 shows the drilled core from the lower section of trial road. The bituminous layer on top of the semi-dry paste was 50-mm wearing course laid 14 days after the semi-dry paste was placed. A 50-mm core sample was also taken in order to measure the permeability of the semi-dry paste.

Figure 124. Core sample taken from the lower part of trial road at the King's Mill Hospital site.

A group of core samples drilled from different locations in the trial road is shown in Figure 125. The sample on the left-hand side was taken from upper part of the trial road, which was laid using a bituminous sub-base layer.

Figure 125. Core samples taken from different locations in the trial road at the King's Mill Hospital site.

Table 48 gives the compressive strengths of the site samples and cores. The compressive strength of site samples measured on the day of the trial indicated that the strength of site trial semi-dry paste layer was 26% lower than that achieved in the laboratory mixes. This was due to the lower moisture content used in the site trial layer. However, the strength of the site cores taken at 14, 28, 90 and 180 days showed satisfactory performance for the placed semi-dry paste. The strength of the site cores was almost similar to that of the designed laboratory mixes at 28 days. Moreover, the long-term compressive strength of the site cores at 90 and 180 days was about 50% higher than the 28-day laboratory strength.

The strength development of the semi-dry site pastes in comparison with the laboratory mix is shown in Figure 126. The rate of strength gain in the site core samples declined at later ages in line with the laboratory results discussed in section 2.1.6.1.7. The strength continued to increase even at later ages. This was because the presence of the bituminous layer prevented the evaporation of moisture from the base layer and its drying out.

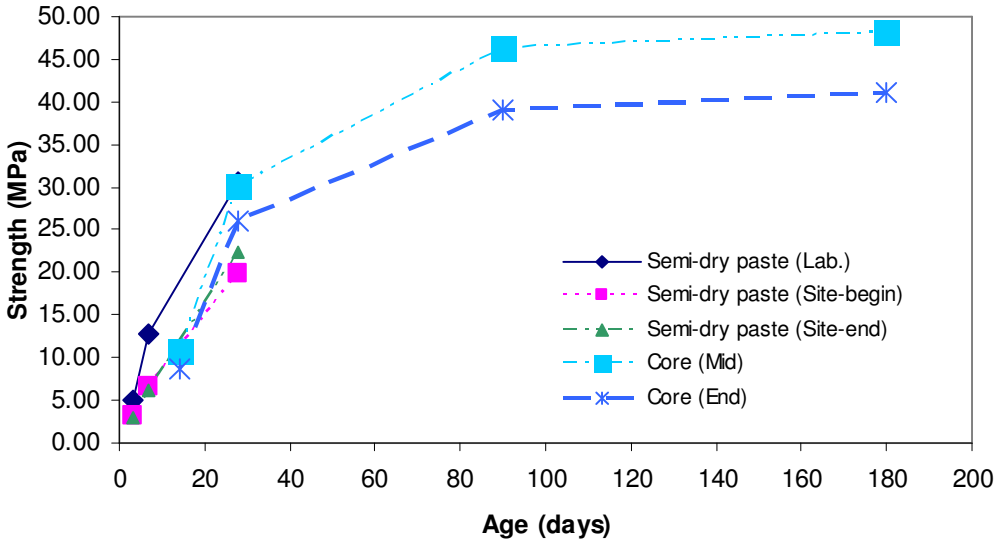

Figure 126. Compressive strength development of semi-dry site paste at the King's Mill Hospital site.

Table 48 Compressive strength of laboratory and site semi-dry paste layer

	Laboratory tests					In situ tests				
	Strength at days (MPa)			Moisture	Density	Strength at days (MPa)				Density
Mix code	3	7	28	(%)	(kg/m^3)	14	28	90	180	(kg/m^3)
Semi-dry paste (Lab.)	5.1	12.8	30.55	13	2540	–	–	–	–	–
Semi-dry paste (Site-Begin)	3.2	6.64	19.9	8.55	2487	–	–	–	–	–
Semi-dry paste (Site-End)	2.95	6.2	22.4	7.76	2492	–	–	–	–	–
Core (mid)	–	–	–	–	–	10.75	30.1	46.41	48.2	2381
Core (end)	–	–	–	–	–	8.64	26.1	38.98	41.1	2011

Table 49. Compressive strength of laboratory and site RCC layer

	Laboratory tests				In situ tests				
	Strength at days (MPa)			Density	Strength at days (MPa)				Density
Mix code	3	7	28	(kg/m^3)	14	28	90	180	(kg/m^3)
RCC (Lab.)	0.96	2.02	10.8	2390	–	–	–	–	–
RCC (Site-Truck 1)	0.7	1.2	5.47	2350	–	–	–	–	–
RCC (Site-Truck 2)	0.68	1.29	4.7	2232	–	–	–	–	–

RCC (Site-Truck 3)	0.99	1.42	7.1	2293	–	–	–	–	–
Core (Location 1)	–	–	–	–	Soft	8.7	13.41	16.4	2257
Core (Location 2)	–	–	–	–	Soft	10.11	15.43	17.3	2226

3.4.2. Lowdham Grange Site

Figure 127 shows a general view of the trial car park at the Lowdham Grange site. The car park was not covered with wearing surface as the strength of RCC layer was not sufficient when tested after 14 days. However, the area of the site trial was sprayed with a bitumen protective layer at 28 days and used for site access and storage. At 28 days and 90 days, the RCC layer was quite hard and even the leftover concrete at the sides of the area could not be removed easily. Although the surface of the RCC layer had irregularities due to the placing of the concrete in three segments, no signs of major deflection were observed in the trial car park.

Two core samples were drilled from the middle and end sections of the car park at 28, 90 and 180 days (Figure 128). The samples represented two different segments of the trial car park and corresponded to two different truck mixers delivering the concrete to the site. Cores taken from the site were cut at both ends using a lathe and tested for compressive strength. Figure 129 shows the prepared concrete core samples prior to compressive strength testing. Results for the site cores together with those from cube samples taken on the day of the site trial are presented in Table 49.

Figure 127. General view of trial car park site at Lowdham Grange.

Figure 128. Core sample taken from middle and end part of the trial car park at the Lowdham Grange site .

Figure 129. RCC core samples taken from different locations of the trial car park at the Lowdham Grange site.

The results obtained with the concrete cubes samples from each truck indicated that the compressive strength was much lower than the laboratory strength of 10.8 MPa. However, the cube samples were compacted using a vibrating table attached to a hammer drill and therefore, due to the size of the aggregates and the nature of the roller-compacted concrete, compaction was different in each set of moulds. As a result, these samples were less compacted than the RCC layer which was laid and compacted using a 3-tonne vibrating roller.

Although the strength of the concrete at the early age of 14 days was not enough to be cored (Table 49), a satisfactory strength was obtained at 28 days. Moreover, the long-term compressive strength of the concrete at 90 and 180 days demonstrated the excellent performance of this type of binder when used in roller-compacted concrete. This is due the energy of the compaction applied by the heavy vibrating roller to achieve a fully compacted layer of concrete.

Figure 130 shows the strength development of the site cubes and core samples. The slower rate of strength gain is obvious in the concrete samples and is similar to the paste mixtures at the King's Mill Hospital site trial. The rate of strength gain fell as time progressed. The slower rate of strength development from 90 to 180 days is associated with the slower hydration rate of slag in the mixes. The mechanism of the hydration of slag in the Coventry Binder is discussed in section 2.1.6.6. The formation of hydrated products around slag grains results in reduced diffusion of ions from the slag particles into the solution to allow the further formation of the CSH gel responsible for the compressive strength of the concrete.

The results indicated that an even higher compressive strength than the desired strength for the car park base layer was achievable using Coventry Binder. Moreover, it may be possible to improve the strength further with the use of chemical agents such as sodium silicate and sodium carbonate.

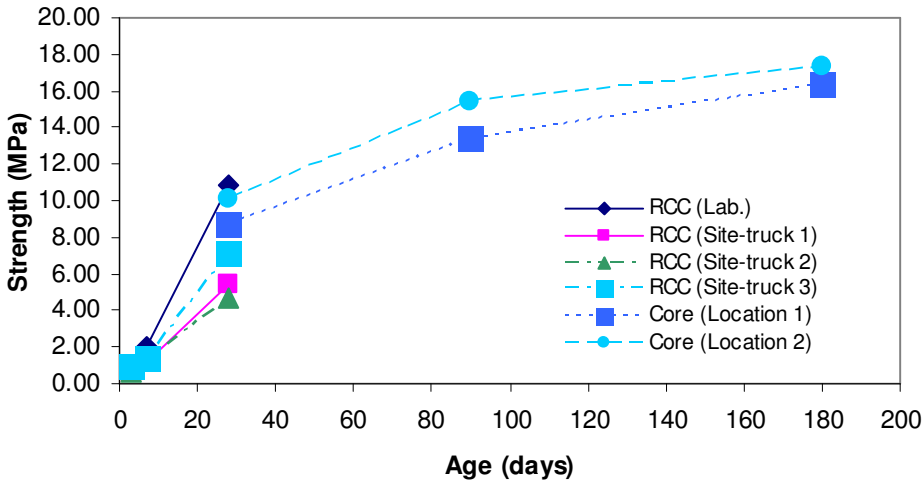

Figure 130. Compressive strength development of site RCC samples at the Lowdham Grange site.

4. OTHER APPLICATIONS FOR THE NOVEL BINDER

The positive results of these trials suggest that there may be wider applications for the novel binder beyond road construction, possibly:

- construction products, such as paving slabs, kerbs and blocks;
- trench reinstatement following utilities works;
- backfilling applications, such as cut and cover tunnels and stabilising mine shafts; and
- stabilising embankments.

Further work into these applications would reveal the huge potential for using recycled gypsum with other readily available pozzolanic wastes to make suitable binders as viable replacements for cement.

5. CONCLUSION

This study has demonstrated that plasterboard waste can be successfully used in low-medium strength concrete mixes for the foundations of minor roads and car parks. The laboratory based research and site trials have shown that:

- The optimum combination for the novel binder was a mix of 15% recycled gypsum from waste plasterboard, 5% bypass dust, and 80% basic oxygen slag, which gave a compressive strength of 11MPa at a water to binder ratio of 0.3.
- The novel binder could be used as a cementicious component to stabilise soil containing clay and/or sand.
- Semi-dry roller compacted paste using the novel binder with 13% water achieved the highest compressive strength of around 31MPa at 28 days age.
- The novel binder developed strength at a slower rate than ordinary Portland cement, so sufficient time must be allowed for the setting and curing.
- Due to the slow strength development of the binder, roller compacted concrete (RCC) seemed to be the perfect way to lay the road base layer with acceptable compressive strength of 10-12 MPa at age of 28 days.
- The same equipment used for mixing regular concrete was used for the novel binder site trials. There was no specialist equipment required for the research.

The research team at Coventry University have proved through successful laboratory testing and site trials that plasterboard waste can be a useful material in the construction industry. The novel binder is a blend entirely from by-product wastes and recycled materials and can be applied to numerous applications where cementitious properties are required.

This has demonstrated an innovative method of reuse for the construction industry that will minimise the volume of plasterboard waste sent to landfill, thus reducing disposal costs, whilst expanding the current markets for plasterboard waste.

6. REFERENCES

[1] Waste and Resources Action Programme (www.wrap.org.uk/construction/ plasterboard /background.html)

[2] AEA Technology Plc. 2006. Review of plasterboard material flows and barriers to greater use of recycled plasterboard. Technical report for WRAP. Available from: www.wrap.org.uk/construction/plasterboard/report_review.html [Accessed 19 April 2007].

[3] ACI Committee 229, ACI 229R,99, "Controlled low strength materials", American concrete Institute, Reapproved 2005.

[4] American Concrete Institute (ACI). Ground granulated blast furnace slag as cementitious constituent in concrete. In: ACI Manual of Concrete Practice Part 1: Materials and General Properties of Concrete, ACI 226.1R, 1989; pp. 1-16.

[5] Neville, A.M. Properties of Concrete; (4th and final edn.); Prentice Hall: London, 1995

[6] British Standards Institution (BSI). BS 4248: 2004. Supersulfated cement. BSI, London, 2004.

[7] Matschei, T.; Bellmann, F.; Stark, J. J. Adv. In Cem. Res. 2005, 17, 167-178

[8] Al-Jabri, K.S.; Taha, R.A.; Al-Hashmi, A.; Al-Harthy, A.S. *J. Const. Bld. Mat.* 2006, 20, 322-331.

[9] Al-Harthy, A.S.; Taha, R.; Al-Maamay, F. J. Const. Bld. Mat. 2003, 17, 353-360.

[10] Jones, M. ; McCarthy, A. Moving fly ash utilisation in concrete forward: a UK perspective. Presentation to International Ash Utilisation Symposium, Centre for Applied Energy Research, University of Kentucky, held 20–22 October 2003.

[11] British Standards Institution (BSI). BS EN 459-1: 2001. Building lime. Definitions, specifications and conformity criteria. BSI, London, 2001.

[12] British Standards Institution (BSI). BS 882: 1992. Specification for aggregates from natural sources for concrete. BSI, London. [Superseded by BS EN 12620: 2002. Aggregates for concrete], 2002.

[13] British Standards Institution (BSI). BS 1377-4: 1990. Methods of test for soils for civil engineering purposes. Compaction-related tests. BSI, London, 1990.

[14] British Standards Institution (BSI). BS 1881-125: 1986. Testing concrete. Methods for mixing and sampling fresh concrete in the laboratory. BSI, London, 1986.

[15] British Standards Institution (BSI). BS EN 12350-5: 2000. Testing fresh concrete. Flow table test. BSI, London, 2000.

[16] British Standards Institution (BSI). BS 4555-1: 1998. Methods of testing mortars, screeds and plasters. Physical testing. BSI, London. [Superseded by BS 4555: 2005. Mortar. Methods of test for mortar. Chemical analysis and physical testing], 2005.

[17] ASTM International. C230/C230M-03 Standard specification for flow table for use in tests of hydraulic cement. ASTM International, West Conshohocken (PA), 2003.

[18] Transport Research Laboratory. A guide to the structural design of bitumen surfaced road in tropical and sub tropical countries. Road Note No. 31. Department of Transport, London, 1993.

[19] Nielsen, H.H.; Barker, E.F. J. Phys. Rev. 1988, 37, 727-732.

[20] Technical literature on Hoek cell and drainage platens produced by Robertson Geologging, Conwy, Gwynedd LL31 9PX [www.geologging.com], 1994.

[21] Claisse, P.A.; Unsworth, H.P. The engineering of a cementitious barrier. In: Engineering Geology of Waste Disposal, Geological Society Engineering Geology Special Publication, 1995; No. 11, pp. 267-272. Geological Society, London.
[22] Bakharev, T. J. Cem. Con. Res. 2001, 31, 1277–1283.
[23] Warren, C.J.; Reardon, E.J. 1*J. Cem, Con. Res.* 1994, 24, 1515–1524.
[24] Odler, I.; Yan, P. *J. Adv. In Cem Res.* 1994, 6, 165–171.
[25] Richardson, I. G. J. Cem. Con. Res. 2000, 22, 97–113.
[26] Möser, B. Nano-Charakterisierung von Hydratphasen mittels Rasterelektronenmikroskopie. In: Proceedings of the 15th International Conference on Building Materials [Internationale Baustofftagung (Ibausil)], held Weimar 2003 (ed. H.B. Fisher), pp. 1-0589 to 1-0607. Finger-Institut für Baustoffkunde, Weimar.
[27] Brews, D.M.; Glasser, F.P. *J. Cem. Con. Res.* 2005, 35, 77–83.
[28] Stark, J.; Frohburg, U.; Mielke, I. Supersulfated cement with and without cement clinker. In: Proceedings of the International Symposium on Non-Traditional Cement and Concrete, held Brno (Czech Republic), (ed. V. Bílek and Z. Kerner), 2001; 25-138.
[29] Ottemann, J. J. Silikattechnik 1951, 2, 143–149.
[30] Scrivener, K.L.; Taylor, H.F.W. *J. Adv. In. Cem Res*. 1993, 5, 139-146.
[31] Taylor, H.F.W. Cement Chemistry (2nd. edn.), Reedwood Books, Trowbridge, 1997
[32] Chartschenko, I., Volke, K. and Stark, J. Untersuchungen über den Einfluß des pH-Wertes auf die Ettringitbildung. *Wissenschaftliche Zeitschrift der Hochschule für Architektur und Bauwesen Weimar*, 1993; 39(3), 171-176.
[33] Chartschenko, I. Theoretische Grundlagen zur Anwendung von Quellzementen in der Baupraxis. Habilitationsschrift [Professorial dissertation]. Weimar, Hochschule für Architektur und Bauwesen Weimar (HAB Weimar), 1995.
[34] Mehta, P.K. *J. Cem. Con. Res*. 1983, 13, 401-406.
[35] Puertas, F.; Fernandez, A.; Blanco-Varela, M.T. *J. Cem. Con. Res.* 2004, 34, 139-148.
[36] ASTM International. C151-05. Standard test method for autoclave expansion of hydraulic cement. ASTM International, West Conshohocken (PA), 2005
[37] ASTM International. C490-04. Standard practice for use of apparatus for the determination of length change of hardened cement paste, mortar and concrete. ASTM International, West Conshohocken (PA), 2004
[38] ASTM International. C1260-05a. Standard test method for potential alkali reactivity of aggregates (mortar-bar method). ASTM International, West Conshohocken (PA), 2005.
[39] ASTM International. C227- 03 Standard test method for potential alkali reactivity of cement-aggregate combinations (mortar-bar method). ASTM International, West Conshohocken (PA), 2003.
[40] British Standards Institution (BSI). BS 812-123: 1999. Testing aggregates. Method for determination of alkali-silica reactivity. Concrete prism method. BSI, London, 1999.
[41] British Standards Institution (BSI). BS 2028: 1968. Pre-cast concrete masonry units. Specification for pre-cast concrete masonry units. BSI, London, 1968.
[42] Highways Agency. Manual of Contract Documents for Highway Works: Volume 1 Specification for Highway Works. The Stationery Office, London, 2006.
[43] British Standards Institution (BSI). BS EN 12390-1: 2000. Testing fresh concrete. Sampling. BSI, London, 2000
[44] British Standards Institution (BSI). BS EN 12390-3: 2000. Testing fresh concrete. Vebe test. BSI, London, 2000.